




12-2015

Design of Digital Down Converter Chain for Software Defined Radio Systems on FPGA

Nagarjun Marappa
Western Michigan University

Follow this and additional works at: https://scholarworks.wmich.edu/masters_theses

 Part of the Computer Engineering Commons, and the Electrical and Computer Engineering Commons

Recommended Citation

Marappa, Nagarjun, "Design of Digital Down Converter Chain for Software Defined Radio Systems on FPGA" (2015). *Masters Theses*. 664.

https://scholarworks.wmich.edu/masters_theses/664

This Masters Thesis-Open Access is brought to you for free and open access by the Graduate College at ScholarWorks at WMU. It has been accepted for inclusion in Masters Theses by an authorized administrator of ScholarWorks at WMU. For more information, please contact wmu-scholarworks@wmich.edu.



DESIGN OF DIGITAL DOWN CONVERTER CHAIN FOR
SOFTWARE DEFINED RADIO SYSTEMS ON FPGA

by

Nagarjun Marappa

A thesis submitted to the Graduate College
in partial fulfillment of the requirements
for the Degree of Master of Science in Engineering (Computer)
Electrical and Computer Engineering
Western Michigan University
December 2015

Thesis Committee:

Bradley J. Bazuin, Ph.D., Chair
Janos L. Grantner, Ph.D.
Lina Sawalha, Ph.D.

DESIGN OF DIGITAL DOWN CONVERTER CHAIN FOR SOFTWARE DEFINED RADIO SYSTEMS ON FPGA

Nagarjun Marappa, M.S.E.

Western Michigan University, 2015

Modern communication systems have increasingly attempted to trade off the digital signal processing for analog circuitry. In performing this tradeoff, advanced algorithms have been implemented in both custom programmable hardware and in software; such systems are commonly called Software Defined Radios (SDR). Advanced software defined radios consist of highly configurable hardware and computers used as digital signal processing (DSP) platforms that provide the technology for realizing current and future generations of digital wireless communication infrastructure. Many sophisticated signal processing tasks are performed in SDR, including compression algorithms, channel estimation, equalization, forward error correction and protocol management. This research has focused on the custom and programmable hardware DSP devices which are commonly found prior to the baseband processor, performing critical tasks appearing after the analog to digital converter. The DSP techniques that are involved in this research are tuning, filtering and decimation of a received communication signal.

The research activity performed the fixed-point algorithmic simulation in MATLAB and the Xilinx VHDL implementation of integer precision complex mixing,

high rate filter decimation and two stage lower rate half-band filter decimation in order to develop a communication signal processor. In addition, a Xilinx based digital test data generator and output comparator design was developed to provide test data and analyze results in real time for the Xilinx communication signal processor developed.

Copyright by
Nagarjun Marappa
2015

ACKNOWLEDGMENTS

Firstly, I would like to express my deepest appreciation to my committee chair and my academic advisor Dr. Bradley J. Bazuin for his continuous support, guidance, motivation and immense knowledge. His guidance gleamed the way for my thesis. I could not have imagined a better mentor and advisor than him and I am indebted to him for sharing his expertise extended to me.

Besides my advisor, I would also like to thank the rest of my thesis committee members Dr. Janos L. Grantner and Dr. Lina Sawalha for their patience and encouragement. Their encouragement led to widen the area of my research in various prospective.

I also take this opportunity to thank my parents who stood by me at all times and gave me moral support in achieving and reaching to this point of my life. A special thanks to my all friends who supported me throughout my thesis, especially Lalith Narasimhan for his unceasing support and guidance.

I also place on record, my sense of gratitude to one and all, who directly or indirectly, have lent their hand in this venture.

Nagarjun Marappa

TABLE OF CONTENTS

ACKNOWLEDGMENTS	ii
LIST OF TABLES	vii
LIST OF FIGURES	viii
CHAPTER	
1. INTRODUCTION	1
1.1 Motivation.....	1
1.2 Research Objective	4
1.3 Structure of the Thesis	6
2. OVERVIEW	8
2.1 Background of Software Defined Radio.....	8
2.1.1 First Generation Software Defined Radios	9
2.1.2 Second Generation Software Defined Radio	10
2.2 Research Prototypes for SDR	12
2.3 Overview of Digital Down Converter Chain.....	13
3. THEORY OF CORDIC, CIC AND HALF-BAND FILTERS.....	18
3.1. CORDIC Processing.....	18
3.1.1 CORDIC Overview.....	18
3.1.2 CORDIC Algorithm.....	20

Table of Contents – Continued

CHAPTER		
	3.1.3 CORDIC Pre-Rotation.....	26
	3.1.3 CORDIC as NCO.....	29
	3.2 Filter Decimation for Down Converters	32
	3.2.1 Cascaded Integrator Comb Filter	32
	3.2.2 Half-Band Filters	42
	4. METHODOLOGY AND IMPLEMENTATION	49
	4.1 CORDIC Processing Unit.....	50
	4.1.1 Phase Accumulator	53
	4.1.2 Pre-Rotation	54
	4.1.3 CORDIC Engine	56
	4.1.4 MATLAB Implementation	58
	4.1.5 VHDL Implementation	60
	4.2 Cascaded Integrator Comb Filter.....	64
	4.2.1 MATLAB Implementation	65
	4.2.2 VHDL Implementation	69
	4.3 Half-Band Filters	71
	4.3.1 First Stage Half-Band Filter.....	72
	4.3.1.1 MATLAB Implementation	73

Table of Contents – Continued

CHAPTER		
	4.3.1.2 VHDL Implementation	77
	4.3.2 Second Stage Half-Band Filter	79
	4.3.2.1 MATLAB Implementation	83
	4.3.2.2 VHDL Implementation	86
	4.4 DDC Chain Gain Adjustment	90
	4.5 Xilinx Clocking and Clock Distribution	91
5. FPGA BASED DIGITAL PATTERN GENERATOR.....		94
5.1 Architecture of Digital Pattern Generator.....		95
5.2 Digital Pattern Generator Interface.....		95
5.2.1 Hardware Aspects		98
5.2.1.1 Wishbone - Zylon Processing Unit.....		98
5.2.1.2 Cellular RAM		102
5.2.1.3 FIFOs		102
5.2.1.3 Output FIFO.....		104
5.2.1.3 Input FIFO		108
5.2.1 Software Aspects		110
5.2.1.1 Generating Test Data		110
5.2.1.2 Copying Data to CRAM		111
5.2.1.3 ZPU Software		112

Table of Contents – Continued

CHAPTER	
6. RESULTS AND PERFORMANCE	115
6.1 Signal Processing Chain Verification	115
6.2 Pattern Generator Board Testing	126
6.2.1 Maximum Data Rate Achieved using ZPU	126
6.2.2 MATLAB limitations to Account for Hardware Transients...	128
6.3 Signal Processor Device Utilization Summary.....	129
6.4 Signal Processor Timing Verification.....	131
7. CONCLUSION AND FUTURE WORK	132
7.1 Conclusion	132
7.2 Future Work.....	133
7.3 Summary	134
REFERENCES	136
APPENDICES	
A - MATLAB Scripts	139
B - VHDL Implementation	153
C - Pattern Generator Code.....	177
D - ZPU Software	190

LIST OF TABLES

3-1 Technique used in CORDIC Pre-Rotation	28
3-2 Half-Band Computation Efficiency	47
4-1 Input Vector Quadrants	54
4-2 CORDIC Constants or Arc Tangent Radix Constants.....	57
4-3 CORDIC Processor Device Utilization Summary.....	63
4-4 CIC Filter Device Utilization Summary	71
4-5 Small (7-Tap) Half-Band Device Utilization Summary.....	79
4-6 Values on the Select Line of SRL16Es	88
4-7 Large (31-Tap) Half-Band Device Utilization Summary.....	90
5-1 Wishbone Slaves Memory Map	100
6-1 Signal Processor Device Utilization Summary	130

LIST OF FIGURES

1-1 Growth of Cellphone Users [3]	2
1-2 Multimedia Chipset for Mobile Devices [7].....	3
1-3 Thesis Hardware Setup.....	6
2-1 Ideal Software Defined Radio	9
2-2 First Generation SDR	10
2-3 Second Generation SDR.....	10
2-4 Digital Down Converter	14
2-5 Quadrature Mixing in Frequency Domain.....	15
2-6 Digital Down Converter Chain.....	16
3-1 CORDIC Micro-Rotations.....	20
3-2 Two-Dimensional Vector Rotation	21
3-3 Rotation through Iterative Micro-Rotations	23
3-4 Division using Shift Register.....	25
3-5 Region of Convergence for Inverse Tangent Function	26
3-6 Methodology for Pre-Rotation.....	29
3-7 FIR Implementation of Boxcar Filter	33
3-8 Boxcar Filter Frequency Response.....	36
3-9 Single Stage CIC Filter.....	37
3-10 Frequency Response of Integrator Comb (CIC) Filter	37
3-11 Spectrum of a Multistage CIC	39

List of Figures - Continued

3-12 Broadening Nulls at Successive Stages of CIC	39
3-13 Hogenauer Filter Structure of a Single Stage CIC Filter	40
3-14 Hogenauer Structure of a 3-stage CIC Filter	41
3-15 Zero-Phase Frequency Response	43
3-16 Half-Band Impulse Response	44
3-17 FIR Filter Structure	46
3-18 Symmetric FIR Filter Structure	46
3-19 First Stage Half-Band Filter	48
3-20 Second Stage Half-Band Filter	48
4-1 Architecture of Communication Signal Processing Board	51
4-2 CORDIC Processing Unit Core	52
4-3 CORDIC Phase Accumulator	54
4-4 Single Stage CORDIC using Shift Registers	56
4-5 CORDIC Implemented as NCO	59
4-6 Frequency Spectrum of the CORDIC Output (zoomed-in)	59
4-7 VHDL Implementation of a Single Stage CORDIC	60
4-8 CORDIC Pipelined Stages	61
4-9 CORDIC Initial Latency	62
4-10 CORDIC Output Truncation	62
4-11 Modelsim Simulation of CORDIC	63
4-12 3-Stage Pipelined CIC Filter	65

List of Figures - Continued

4-13 Frequency Spectrum of the CIC Filter	67
4-14 Spectral Droop in the Passband	68
4-15 Intermediate Outputs of CIC Filter Decimator	68
4-16 3-stage CIC Filter Decimator Output	69
4-17 RTL Schematic of Pipelined CIC Filter	69
4-18 CIC Filter Output on ModelSim Simulator	70
4-19 7-Tap Half-Band Filter Responses	72
4-20 Small Half-Band Filter Input and Output Spectrum.....	75
4-21 Small (7-Tap) Half-Band Filter Circuit Diagram	76
4-22 Strobe Logic for 7-Tap Half-Band Filter.....	77
4-23 31-Tap Half-Band Filter Response.....	80
4-24 2-Path Polyphase Filter Structure Decomposition.....	80
4-25 Large (31-Tap) Half-Band Filter Circuit Diagram	82
4-26 Large Half-Band Filter Input and Output Vectors.....	85
4-27 Large Half-Band Filter Input and Output Spectrum.....	85
4-28 17-bit Shift-Register of length 16 using SRL16Es.....	87
4-29 Timing analysis of large half-band filter structure	89
4-30 Spartan 6 Clock Distribution [27]	92
5-1 Nexys 3 Digital Pattern Generator and Output Comparator.....	96
5-2 Digilent Nexys 3 VHDC Connector [28]	96
5-3 Interfacing with Communication Signal Processor	98

List of Figures - Continued

5-4 Wishbone-ZPU Address Space	101
5-5 ZPU-Slave Communication.....	102
5-6 Output FIFO Status Register	104
5-7 Output FIFO State-Machine Flowchart.....	105
5-8 Output FIFO Write Process	106
5-9 Output of the Pattern Generator Board (ModelSim Simulator)	107
5-10 Output of the Pattern Generator Board (MSO-X 3034A)	108
5-11 Input FIFO Status Register	108
5-12 Input FIFO State-Machine Flowchart.....	109
5-13 Input FIFO Read Process.....	110
5-14 32-bit Binary Pattern in Little Endian Fashion.....	111
5-15 Writing Data to CRAM using Adept.....	112
5-16 ZPU Write and Comparison Scheme.....	113
6-1 CORDIC Time Domain Output.....	117
6-2 CORDIC Output Frequency Spectrum.....	117
6-3 Error between MATLAB and VHDL Implementation	118
6-4 MATLAB-ModelSim-Chipscope Somparisons	118
6-5 CIC Filter – Time Domain Comparison.....	119
6-6 Frequency Response of the CIC Filter Output	120
6-7 Error between MATLAB and VHDL implementation.....	120
6-8 First Stage Half-Band Filter – Time Domain Comparison.....	121

List of Figures - Continued

6-9 Output Spectrum of the First Half-Band Filter.....	122
6-10 Error between MATLAB and VHDL Implementation	122
6-11 Final Stage Half-Band Filter – Time Domain Comparison.....	123
6-12 Output Spectrum of the Final Stage half-Band Filter.....	124
6-13 Error between MATLAB and VHDL Implementation	124
6-14 MATLAB-ModelSim-Chipscope Comparisons.....	125
6-15 DDC Output using Chipscope-Pro Analyzer.....	125
6-16 Time Delay between 2 Successive FIFO Writes	127
6-17 FIFO Burst Write.....	128
6-18 Transient Response at the Output of the Final Stage Half-Band Filter	129
6-19 Signal Processor Timing Summary	131

Chapter 1

INTRODUCTION

1.1 Motivation

Long distance wireless communication has a century-old history, dating from the time when Guglielmo Marconi sent the telegraphic signals over a distance of approximately 1800 miles from Cornwall, across the Atlantic Ocean, to St. John Newfoundland in 1901 [1]. Since then, wireless communication has been one of the most important ways to transport voice and data using radio-frequencies (RF). Over the past century, wireless communication has progressed through the development and deployment of radios, radar, televisions, satellite and mobile telephone technologies.

The growth of the cellular radio and personal communication systems began to accelerate in the late 1970s. Since then, mobile phones have been a successful platform for local and long distance wireless communication and there has been a dramatic increase in the number of mobile phone users. It is predicted that the mobile phone usage will grow even further as shown in the Figure 1-1 [2]. Even more striking, according to recent statistics and on a global scale, there are more mobile phone subscriptions than people with access to electricity or access to safe drinking water [4].

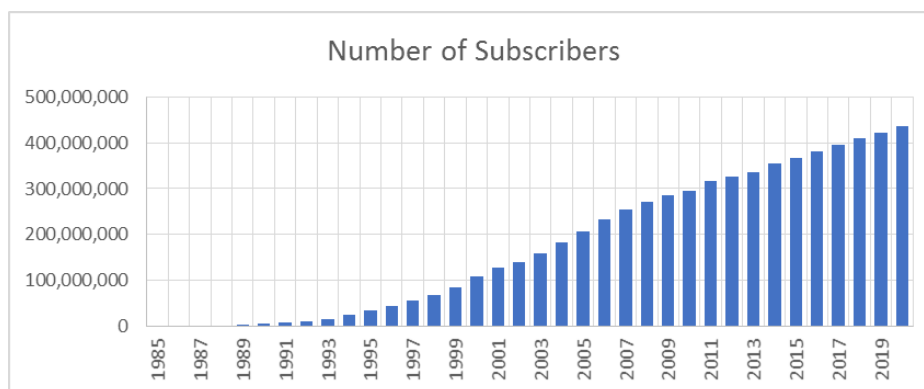


Figure 1-1 Growth of Cellphone Users [3]

This growth has directly influenced the consumers demand for convenience of high-speed ubiquitous communication. Hence, wireless functionality is becoming a fundamental requirement for many electronic products. Furthermore, the rapid growth in the Internet of Things (IoT) is further driving the proliferation of various wirelessly connected devices, such as smart-phones, tablets, wearable computing devices, security and surveillance systems, lighting control systems, remote keyless entry, smart homes and appliances, wireless sensor networks, automated highways and factories [5]. A variety of radio technology standards have been proposed, and have significantly evolved over the last decade in order to meet the needs of diverse applications ranging from, Private Area Networks (PANs) to Local Area Networks (LANs) and Wide-Area cellular Networks such as, Bluetooth, ZigBee, WiFi and the latest 4G-LTE systems [6].

In terms of hardware implementation, the wide range of radio technologies proposed involve a considerable amount of signal processing algorithms that have significant complexity. As a result, they generally requires one or more custom devices, such as Application Specific Integrated Circuits (ASICs) in order to achieve the high processing requirements, computation speeds and density needs by modern radio

standards for personal devices. Figure 1-2 illustrates an example of the current state of art system block diagram using a computer core and multimode ASICs as physical radios, where device functionality could be switched according to the selected mode of operation. The high cost of custom chip development implies the need for mass-market standards with significant volume in order to make a new concept viable. This in turn results in relatively long product development cycles. Also, the continuous increase in the number of competing standards and evolution occurring in the existing standards reduced the life span of products so dramatically that it is difficult to stay at the cutting edge of technology.

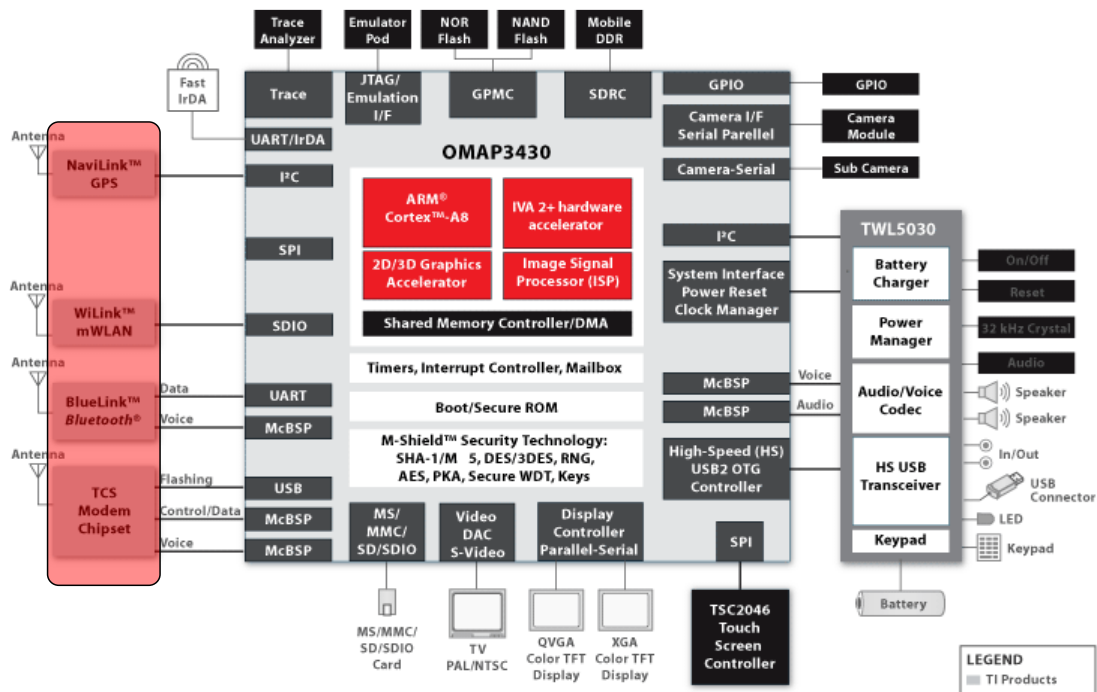


Figure 1-2 Multimedia Chipset for Mobile Devices [7]

The continued development of larger, faster, and more capable Field Programmable Gate Arrays (FPGAs) has supported increasingly more complex digital

signal processing implementations, including wireless communications. The large array of configurable logic blocks available within current FPGAs provides great flexibility and supports high speed processing. In combination, the rapid growth in the processing capabilities of FPGAs and DSPs has allowed Software Defined Radio (SDR) operations to be incorporated into prototype devices that can be readily transitioned into custom, high-volume wireless products capable of supporting a wide range of standards.

1.2 Research Objective

Many sophisticated signal processing tasks are performed in FPGAs or custom ASICs, including Digital Up/Down Conversion (DUC/DDC), interpolation and decimation filtering, channel estimation and equalization. Among the highest data rate and computationally complex signal processing tasks performed in SDR wireless communication system is DUC/DDC, also referred to as receiver tune-filter-decimation and transmitter interpolation-filter-tune signal processing. This research will focus on the processing performed in post analog-to-digital conversion, involving the DDC operations of tuning, filtering and decimation of a received communication signal.

The research activity performed and reported involves the fixed point integer arithmetic simulations of a narrow band Digital Down Converters (DDC) using MATLAB and the Register Transfer Level (RTL) implementation and verification on a Spartan 6 FPGA development board. The components of a DDC consist of a mixer and combinations lowpass filter decimators operating at the real-time sampling frequency of the communication system. To support such high-speed operation, distinct algorithmic techniques have been developed to perform the mixing and filtering required. For

complex mixing used for tuning, the COordinate Rotational Digital Computer (CORDIC) algorithm is implemented [8], while primary narrow-band filter decimation is performed using a Cascaded Integrator Comb (CIC) filter. Following this processing, two low rate half-band filter decimators were also implemented to enhance the passband and provide additional spectral shaping and stopband attenuation following the CIC filter.

In addition to the signal processing tasks, a second FPGA based development board has been designed, developed, and implemented as a digital pattern generator and output comparator to provide predefined periodic integer test data and allow comparison of periodic output results in real time from the communication signal processor development board. The pattern generator and result comparison FPGA contains a Zylins open source 32-bit softcore processor called the Zylins CPU (ZPU) that is used to command, control, transfer and compare the data inside the FPGA. The finite precision integer test signals and the theoretical results of the signal processor are stored in an on-board Pseudo Static Random Access Memory (PSRAM) from which the ZPU can source the pattern generator data and retrieve reference outputs to compare the collected processed result of the signal processing chain. The ZPUs software was written in C and compiled using the open source ZPU - GNU Compiler Collection (GCC) tools.

The project development and hardware test configuration is shown in Figure 1-3 where the project consists of two Digilent Nexys 3 development boards which have Spartan 6 (xc6slx16-3-csg324) FPGAs. One board is used as the pattern generator and result comparison board and the other is used as the target board (communication signal processor). These boards are connected through a high speed Very High Density Cable (VHDC) connector for sending and receiving the test signals.

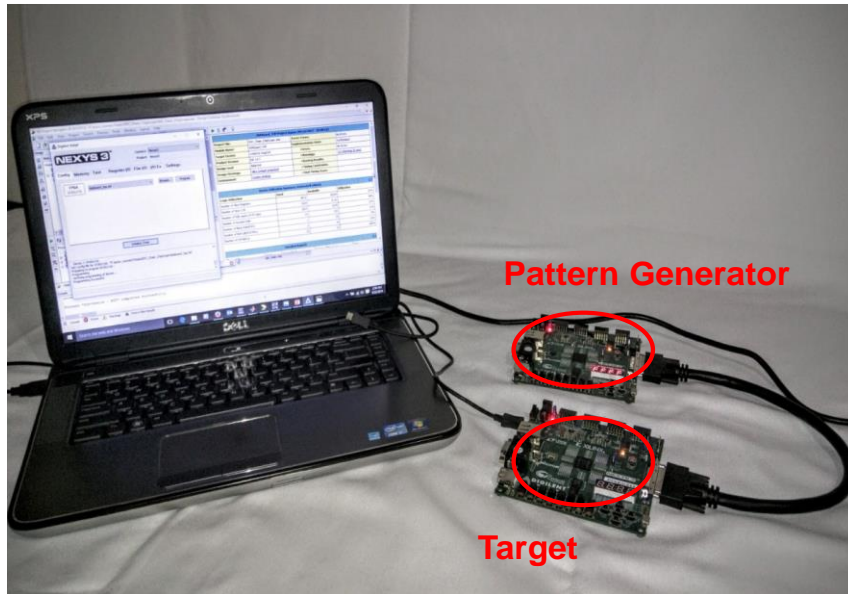


Figure 1-3 Thesis Hardware Setup

1.3 Structure of the Thesis

This thesis is organized as follows: Chapter 2 provides an overview of digitization and digital signal processing in wireless communication, its evolution, and a description of Software Defined Radio (SDR) system. It also discusses the different architectures proposed to implement Digital Down Conversion chains, both for narrow band and wide band receivers. Chapter 3 describes the architecture of the Digital Down Converter chain proposed in this thesis and discusses the mathematical model of the Digital Down Conversion chain. This chapter includes the description of CORDIC high rate integer precision mixing and both, high rate and lower rate filter decimator's. Chapter 4 discusses the design of the signal processing board and describes the hardware implementation details of the Digital Down Converter model presented in Chapter 3. This chapter also discusses the finite precision MATLAB simulations of all the individual

components of the Digital Down Conversion chain. Chapter 5 discusses the architectural design of the pattern generator and comparator using an embedded softcore processor on FPGA. The chapter includes a short description of the softcore processor used and also discusses the pattern and result finite integer test data generation process using MATLAB. Chapter 6 describes the results of the signal processing board implementation and validates the theoretical results with the experimental results for each individual components of the Digital Down Converter chain. The final chapter summarizes the work performed, suggests further design and development activities and concludes this thesis.

Chapter 2

OVERVIEW

2.1 Background of Software Defined Radio

Historically the term radio is defined as any device which is used to exchange information from point A to point B using electromagnetic waves of radio frequency. In traditional radio systems, almost all the physical layer functions were implemented on specialized analog and digital components [9]. These fixed hardware implementations were restricted to specific standards and protocols and offered minimum in terms of interoperability. These systems also had fixed identities that could not be altered without modifications to the underlying hardware. The end result being high initial development costs and longer development and release cycles.

In order to overcome these issues and achieve the flexibility of supporting multiple air interfaces and multiple modulation schemes, the concept of Software Defined Radio (SDR) came into existence [10]. The term software defined radio was first coined by Joseph Mitola in 1992 [11] and is defined as “a radio system where all or some of the physical layer functions are implemented in software” [12]. An ideal SDR is shown in the Figure 2-1. Here, the analog Radio Frequency (RF) spectrum is digitized as close to the antenna as possible so that all signal processing tasks are accomplished in digital domain. Digitizing at the antenna is currently not possible for the majority of high interest wireless signals as, Analog to Digital Converter (ADC) do not have sufficient sample

rates to support desired frequency bands and bandwidths and also lack the required sensitivity and dynamic range. Despite current limitations, SDR does still attempt to digitize the signal as early as possible in the receiver chain while converting to the analog domain as late as possible in the transmit chain.

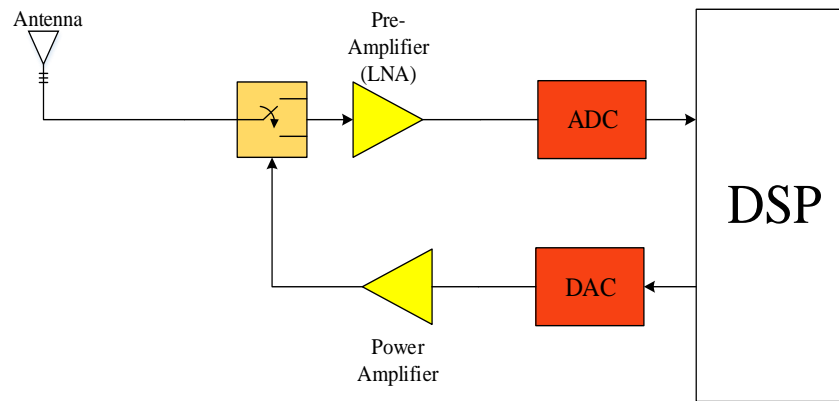


Figure 2-1 Ideal Software Defined Radio

2.1.1 First Generation Software Defined Radios

In the first generation software defined radio systems, technological limitations and cost considerations placed the ADCs and DACs at baseband. This meant only the baseband processing was in digital domain and the rest of the RF and IF stages were still in the analog domain. The architecture of a first generation SDR system is shown in the Figure 2-2

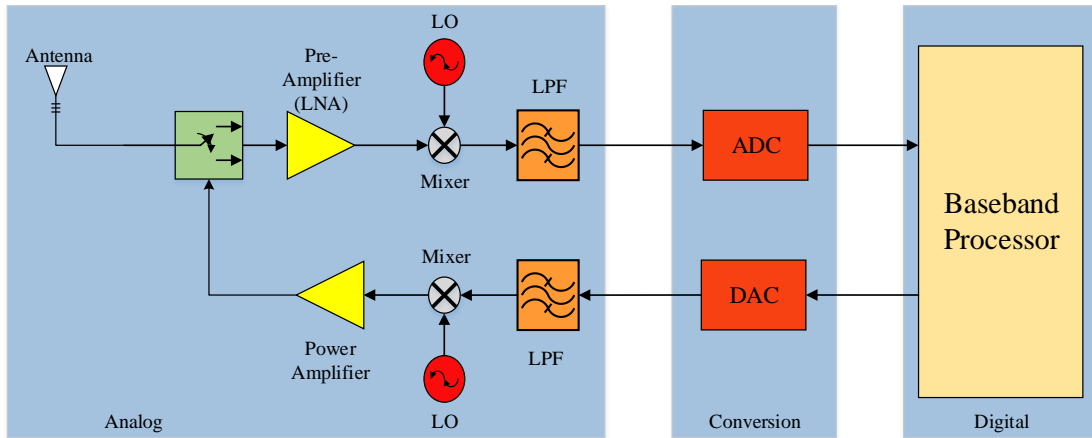


Figure 2-2 First Generation SDR

2.1.2 Second Generation Software Defined Radio

In the second generation SDR systems, advancements in ADC technology allowed them to be utilized at the IF stage rather than at baseband. An example of the second generation SDR is shown in the Figure 2-3.

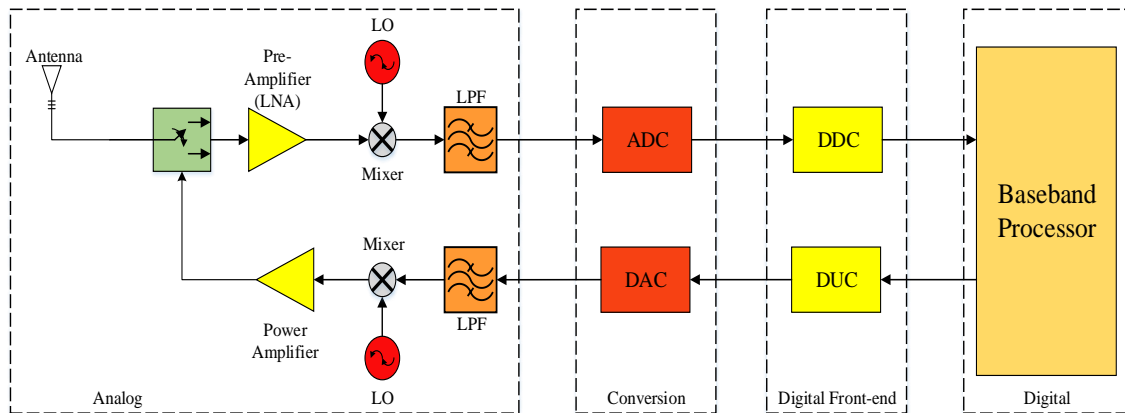


Figure 2-3 Second Generation SDR

A description of the key elements of the SDR system follows:

1. RF front-end

The RF front-end consists of Low Noise Amplifiers (LNA), mixers and filters. The RF signal received from the antenna is first amplified by the LNA and then mixed to either IF or baseband. Filtering is performed to remove the unwanted signals resulting from the mixing process and also to band limit the signal prior to the ADC. The reverse operation is performed at the transmit section of the FR frontend.

2. ADC and DAC

According to Nyquist-Shannon's theorem, "in order for a bandlimited baseband signal to be reconstructed fully, the sampling rate of an ADC should be greater than or equal to twice the bandwidth of a bandlimited signal" [13]. However, the ADCs and DACs in current generation radios are sampling broader spectral bands at much higher rate than narrowband signals of interest, typically in the range of several hundred MHz. This allows the SDRs to provide multimode support and operate on any signal within the wider bandwidth. The high sampling rate also facilitates relaxing the requirements of the antialiasing filter thereby reducing the complexity and the cost of RF components. Furthermore, since software defined radios are also used in mobile devices, it is important that these ADCs/DACs consume little power.

3. Digital Front-end

The digital front end is used to perform additional signal processing tasks that are required as a result of the over sampling at the ADC. The front end acts as an interface between the high bandwidth, high sample rate ADC and the low bandwidth, low sample rate requirements of the baseband. On the receive side, the front end consists of a digital

down converter chain and on the transmit side its inverse, the digital up converter chain.

The digital down converter first consist of a digital mixer to select the desired signal from the array of signals captured by the ADC. Filter-decimation in the DDC allows the bandwidth to be reduced to a range that is supported by the baseband processor, usually requiring much lower symbol rates. The digital up converter performs the opposite of all the operations described in the down converter.

4. Baseband processor

The baseband processor is responsible for modulation/demodulation, encoding/decoding, symbol and timing synchronization, timing recovery and a host of other signal processing tasks vital for the normal operation of the SDR. The baseband processor is usually implemented either on FPGA, General Purpose Processors (GPPs), Digital Signal Processors (DSPs) and Graphical Processing Units (GPUs) or a combination of multiple elements. The choice of the hardware element depends on the complexity of the signal processing required, the level of configurability and the cost of the overall system.

2.2 Research Prototypes for SDR

For current and future development, a number of research prototypes for SDR platforms have been developed in the past few years, including the WARP board from Rice University [14], the USRP platforms from Ettus Research [15], the GENI SDR platform form Rutgers University [16], and the SORA from Microsoft [17]. These state-of-the-art SDR platforms are more suitable for transceiver prototyping and reconfigurable

Access Points or Base Stations (BS) than consumer level devices due to the fact that they are expensive and consume a significant amount of power.

2.3 Overview of Digital Down Converter Chain

The evolution towards SDR has been driven in part by the evolution of the enabling technologies such as ADC/DAC and digital integrated circuit technology (ASICs, FPGAs, GPPs, DSPs and GPUs). However, today's GPPs and DSPs are not well suited for some computationally intensive processing and can be rather slow. Custom ASICs can have considerable development times and high initial costs. The advent of larger and faster FPGAs has opened up the field for digital signal processing implementation on FPGAs, where the large array of Configurable Logic Blocks (CLBs) within the FPGA gives great flexibility together with high speed for regular and structured algorithms. Once the FPGA is configured, it lacks the flexibility of a GPPs/DSPs but it can continuously perform computations with greater speed and efficiency and may be reconfigured. FPGAs are often used in communication systems where real time sample rate preprocessing with some degree of re-configurability is required. One such application is DDC and the mathematical inverse process DUC. DDC is a technique that takes a bandlimited high sample rate digitized signal, tunes the signal to a selected frequency, filters the tuned signal to a limited bandwidth and reduces the sample rate while still retaining all the signal information. DDCs are ubiquitously found in many devices such as cellular radios, radar systems, Wi-Fi radios, Bluetooth and ZigBee radios.

As mentioned before, the ADCs and DACs are operated at significantly higher rate in order to allow the SDRs to operate with wider bandwidths. But in many cases the signal of interest occupies only a small portion of that bandwidth. To filter the signal of interest at this high sample rate would require a prohibitively larger filter. As a result, special DSP techniques such as the combination of a complex mixer and CIC decimators or polyphase channelizers are used to tune to the desired bandwidth and reduce the sample rate of the received signal, to the rate which can be processed by concurrent processing elements efficiently.

A typical narrow band Digital Down Converter chain consists of an oscillator, a complex mixer, a CIC filter decimator and a spectral reshaping filter as shown in Figure 2-4. The first stage of the DDC is to down convert the stream of data from RF spectrum to baseband. This is accomplished through the process of multiplication or mixing with the complex sinusoidal waveform of the same frequency identical to the frequency of the signal of interest.

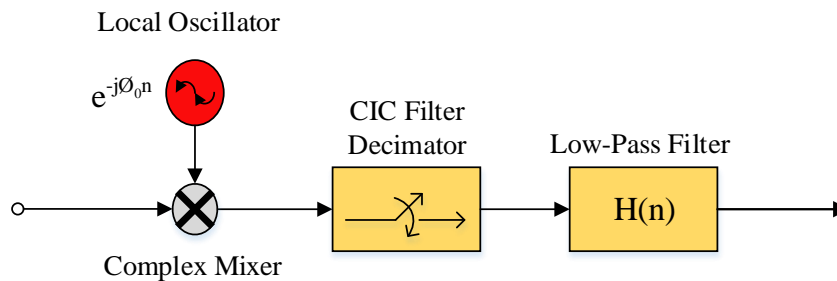


Figure 2-4 Digital Down Converter

This process is graphically shown in the Figure 2-5 where the local oscillator generates a complex sinusoids of frequency $-f_c$ this signal is mixed with the input signal at $+f_c$, as a result input signal is down converted from f_c to baseband. The amplitude

spectrum of both resulting in-phase and quadrature-phase component of the complex baseband signal must be maintained for further processing, which is why all filters in the in-phase and quadrature-phase path must be identical.

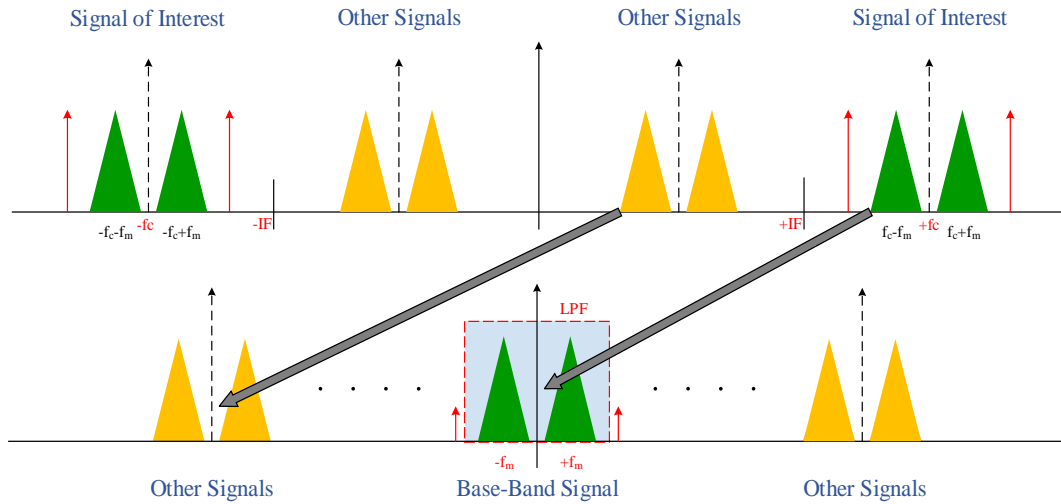


Figure 2-5 Quadrature Mixing in Frequency Domain.

Many techniques have been unveiled to efficiently implement the local oscillator in digital; including, Direct Digital Synthesizers (DDS) and Numerically Controlled Oscillator (NCO). In this thesis, COordinate Rotational Digital Computer (CORDIC) algorithm was used to implement as a numerically controlled oscillator and quadrature mixer combined together because of its simplicity and efficiency. The CORDIC was also used in early calculators and first computers for computing various complex functions like trigonometric, logarithms, complex number multiplications, divisions and square roots. Although the same functions can be implemented using Multiplier and Accumulator units (MAC's), CORDIC can implement these functions just by using shifters and adders while saving a lot of hardware resources which is the primary criteria while designing a large system.

The second stage of the DDC is a filter decimators. Narrowband DDCs use a Cascaded Integrator Comb filter (CIC) since it offers many advantages, such as; implementing high decimation rates within the filter, providing a steep cut-off for a relatively few stages and it is implemented using only delays and adders which makes it very well suited for FPGA implementation. However, multistage CIC filters do not have a flat frequency response in the passband and need a compensating filter after the CIC filter. The response of this additional filter compensates for the droop introduced in the passband. Because of the need for the post compensating filter, CIC filters are preferred to be used with high decimation rates.

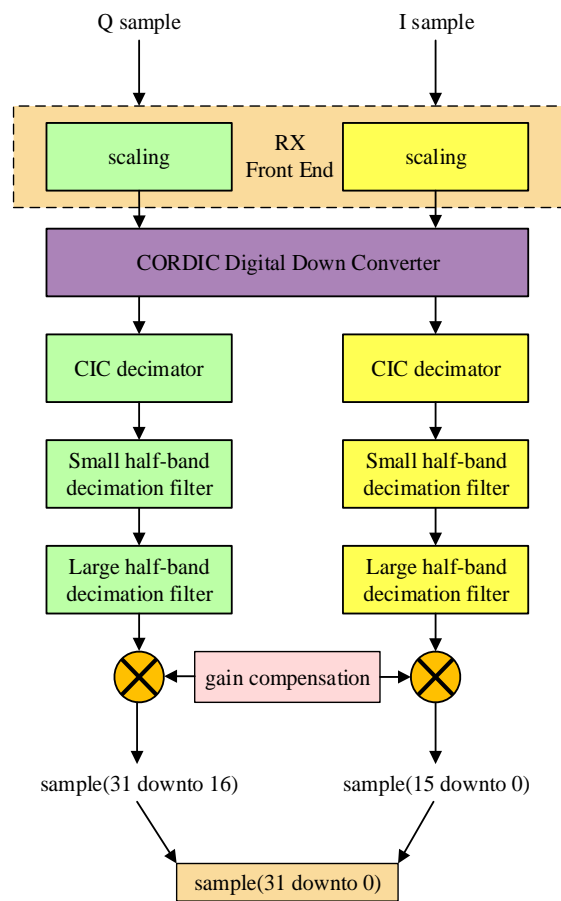


Figure 2-6 Digital Down Converter Chain

The techniques used in this thesis to implement a complex narrow band DDC is shown in the Figure 2-6. In this implementation, the filtering and down sampling was performed in two filter stages. First, a 3-stage CIC filter that performs filtering without multiplications while performing an internal M-to-1 decimation. This CIC filter is followed by a 2 stage half-band filters. The half-band filters can also be used to further decimate the input signal by the factor of 2 or 4 and provide stopband attenuation. This methodology of implementing a complex narrowband DDC is found in the popular Universal Software Defined Radio Peripheral (USRPs) form Ettus Research Inc.

Chapter 3

THEORY OF CORDIC, CIC AND HALF-BAND FILTERS

3.1. CORDIC Processing

The CORDIC processing stage performs the operations of a numerically controlled oscillator (NCO) and complex signal mixer on the incoming data. A numerically controlled oscillator is a digital signal generator which outputs a sinusoidal waveform based on converting a digitally programmed accumulated phase into the sine or cosine of the phase. NCOs offers various advantages for digital signal processing in terms of stability, accuracy, agility and reliability. NCOs offers various advantages for digital signal processing in terms of stability, accuracy, agility, exact repeatability, and reliability. NCOs are used in many digital communication systems, including DDC/DUC for digital radios, digital PLLs, radar systems, function generators, and modulators. There are numerous digital techniques for implementing an NCO with varying degree of complexity and efficiency.

3.1.1 CORDIC Overview

Coordinate Rotational Digital Computer algorithm (CORDIC) was first developed by Jack E. Volder [8] in 1959 at aero-electronics department of Convair. His initial application was to replace the analog resolver in the B-58 bomber's navigation system with a digital computer [18]. Recognizing the potential of the algorithm, it was later generalized and enhanced due to its potential for efficient and low cost implementation

for the computations of various complex functions, such as trigonometric, hyperbolic functions, logarithms, complex number multiplications, divisions and square roots [19]. While all these functions can be implemented using repeated computations with multipliers and accumulator units (MAC's), a CORDIC processor can implement these functions efficiently with the use of a sequence of simple shift and add operations, saving a lot of hardware resources. Furthermore, the CORDIC computing technique is defined to use integer processing; a well-defined number of stages and clock cycles, and can achieve a well-defined numerical precision.

The functionality of CORDIC can be described as the digital equivalent of an analog resolver [8]. Similar to the operation of such a resolver, there are two computing modes, a ROTATIONAL mode and a VECTROING mode. The CORDIC algorithm uses planar rotation and vectoring (r, θ) to compute elementary trigonometric functions when assigned with proper initial conditions. In the rotational mode, given the coordinate components of a vector (X, Y) and the angle of rotation θ , the input vector is rotated by given rotation angle by performing a set of predetermined micro-rotations to obtain a new vector (X', Y') as shown in Figure 3-1. In the vectoring mode, the length r and the angle θ of the vector (X, Y) with respect to the x-axis can be computed. For this purpose, the vector is iteratively rotated towards the x-axis so that the y-component approaches zero. At this point, the sum of all angles is equal to the value of θ , while the value remaining as the x-component corresponds to the length r of the vector (X, Y) .

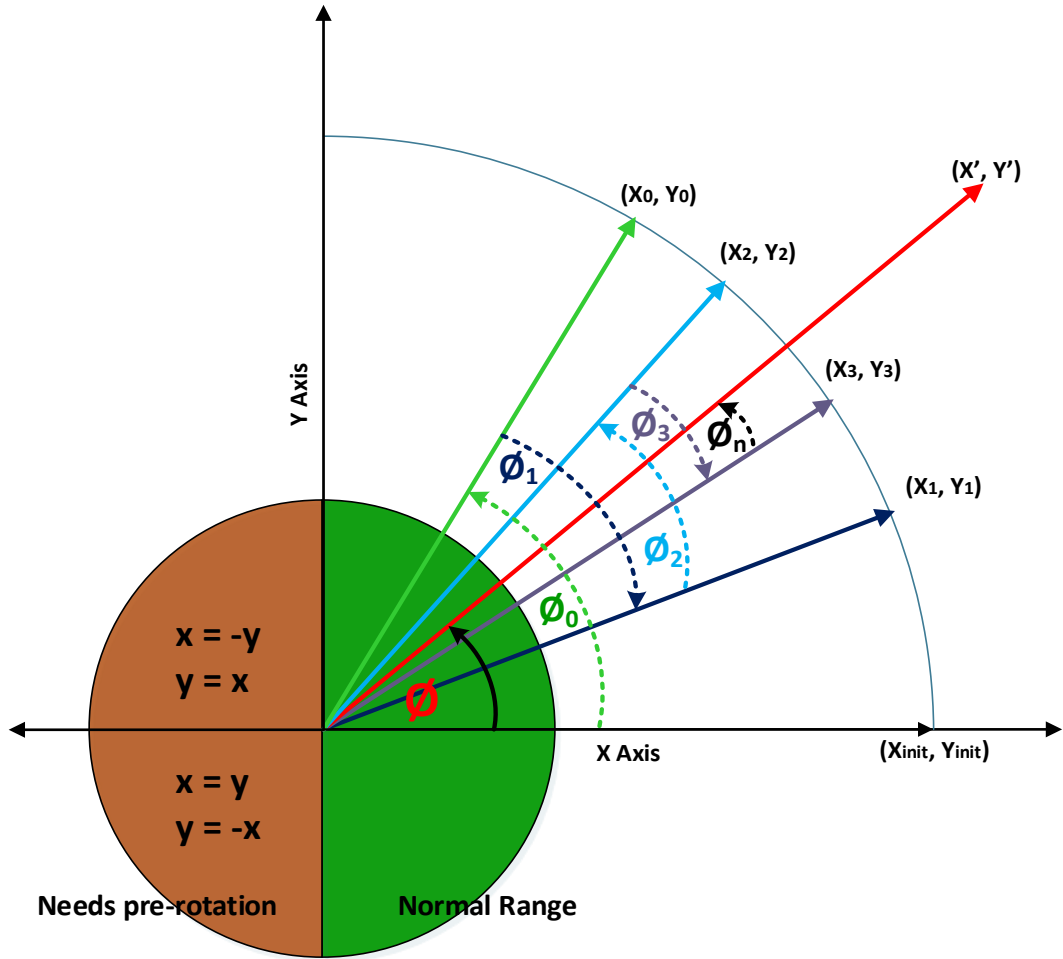


Figure 3-1 CORDIC Micro-Rotations.

3.1.2 CORDIC Algorithm

Consider a 2 dimensional vector at a point v in a complex plane as shown in the Figure 3-2. The coordinate components of v can be represented as

$$v = x + j \cdot y \quad (1)$$

If the vector is rotated by an angle ϕ , then the coordinate components corresponding to the new vector v' in a complex plane is given by [20]

$$v' = v \cdot e^{j\phi} \quad (2)$$

we know that, the exponential term in the above equation can be expressed as

$$e^{j\phi} = \cos(\phi) + j \cdot \sin(\phi) \quad (3)$$

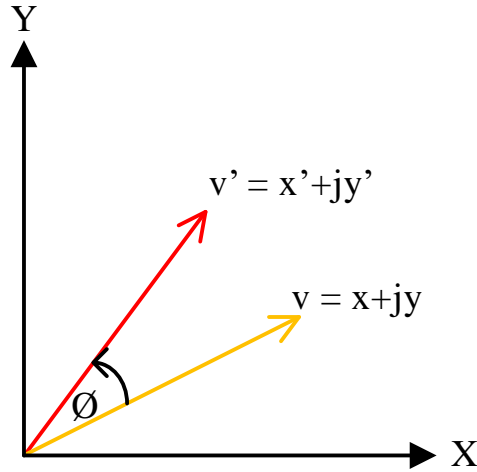


Figure 3-2 Two-Dimensional Vector Rotation

Therefore, by substituting the exponential term in the equation (2) we get,

$$v' = v \cdot (\cos(\phi) + j \cdot \sin(\phi)) \quad (4)$$

By substituting for v and v' , we can simplify the above equation as

$$x' + j \cdot y' = (x + j \cdot y) \cdot (\cos(\phi) + j \cdot \sin(\phi)) \quad (5)$$

$$x' + j \cdot y' = x \cdot \cos(\phi) + j \cdot x \cdot \sin(\phi) + j \cdot y \cdot \cos(\phi) + j^2 \cdot y \cdot \sin(\phi) \quad (6)$$

We know that, $j = \sqrt{-1}$. Then, square of j would be equal to -1 . Therefore, we can rewrite the above equation as

$$x' + j \cdot y' = x \cdot \cos(\phi) + j \cdot x \cdot \sin(\phi) + j \cdot y \cdot \cos(\phi) - y \cdot \sin(\phi) \quad (7)$$

By separating the terms that contains j and rewriting the above equation. We get

$$x' + j \cdot y' = (x \cdot \cos(\phi) - y \cdot \sin(\phi)) + j \cdot (x \cdot \sin(\phi) + y \cdot \cos(\phi)) \quad (8)$$

By equating both sides of the equation, the coordinate components of the new vector at the point v' can be given as

$$x' = x \cdot \cos(\phi) - y \cdot \sin(\phi) \quad (9)$$

$$y' = y \cdot \cos(\phi) + x \cdot \sin(\phi) \quad (10)$$

in order to simplify the CORDIC algorithm for hardware implementation, the equation (9) and (10) can be written in matrix form as

$$\begin{bmatrix} x' \\ y' \end{bmatrix} = \begin{bmatrix} \cos(\phi) & -\sin(\phi) \\ \sin(\phi) & \cos(\phi) \end{bmatrix} \cdot \begin{bmatrix} x \\ y \end{bmatrix} \quad (11)$$

$$\begin{bmatrix} x' \\ y' \end{bmatrix} = R \cdot \begin{bmatrix} x \\ y \end{bmatrix} \quad (12)$$

where R is called rotational matrix and it is defined as

$$R = \begin{bmatrix} \cos(\phi) & -\sin(\phi) \\ \sin(\phi) & \cos(\phi) \end{bmatrix} \quad (13)$$

dividing the equation (13) by $\cos(\phi)$ we get

$$R = \cos(\phi) \cdot \begin{bmatrix} 1 & -\tan(\phi) \\ \tan(\phi) & 1 \end{bmatrix} \quad (14)$$

Furthermore, using the one of the trigonometric identities for $\cos(\phi) = \frac{1}{\sqrt{1+\tan^2(\phi)}}$, we

can modify equation (14) to only have tangent terms as

$$R = \frac{1}{\sqrt{1+\tan^2(\phi)}} \cdot \begin{bmatrix} 1 & -\tan(\phi) \\ \tan(\phi) & 1 \end{bmatrix} \quad (15)$$

Therefore, computation of the coordinate components of a new vector $v' = \begin{bmatrix} x' \\ y' \end{bmatrix}$ can be

represented as

$$v' = \frac{1}{\sqrt{1 + \tan^2(\phi)}} \cdot \begin{bmatrix} 1 & -\tan(\phi) \\ \tan(\phi) & 1 \end{bmatrix} \cdot v \quad (16)$$

where angle ϕ is the rotation angle.

In order to further develop the CORDIC algorithm, we can restrict the values of $\tan(\phi)$ in the above equation such that the total rotation through a desired angle θ is performed as a series of angular rotation steps as shown in Figure 3-3.

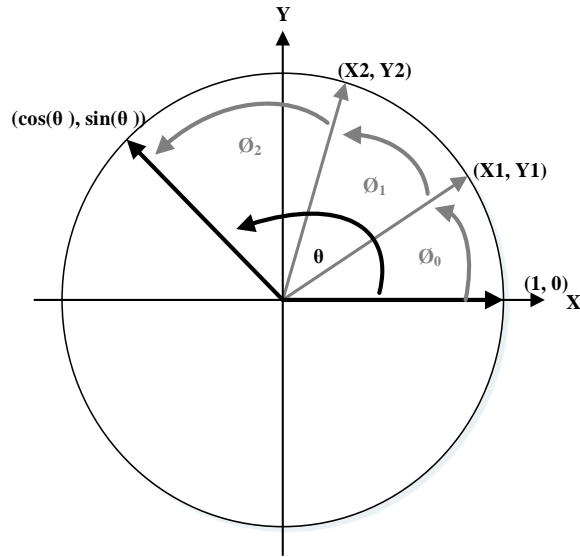


Figure 3-3 Rotation through Iterative Micro-Rotations

The process of rotating through angular rotation steps can be expressed as

$$v_i = \frac{1}{\sqrt{1 + \tan^2(\phi_i)}} \cdot \begin{bmatrix} 1 & -\tan(\phi_i) \\ \tan(\phi_i) & 1 \end{bmatrix} \cdot v_{i-1} \quad (17)$$

the above equation represents the sequence of CORDIC micro-rotations. Under ideal conditions, the sum of all these micro-rotations must be exactly equal to the total rotation angle. That is,

$$\sum_{i=0}^{\infty} \delta_i \cdot \phi_i = \theta \quad (18)$$

where $\delta_i = \pm 1$. For practical applications an infinite summation is not desired.

Therefore, based on the desire numerical precision a limited summation can be formed approximating the angle

$$\sum_{i=0}^{N-1} \delta_i \cdot \phi_i = \delta_0 \cdot \phi_0 + \delta_1 \cdot \phi_1 + \dots + \delta_{N-1} \cdot \phi_{N-1} \approx \theta \quad (19)$$

This is an important design consideration as the instantaneous phase is a numerically scaled integer representing 360 degrees or 2π radians.

Furthermore, the complexity of the numerical calculations that need to be performed during each iterations can be reduced by restricting the $\tan(\phi_i)$ in the equation (17) to take only the values of $\pm 2^{-i}$. Then, the angular steps that $\tan(\phi_i)$ takes can be expressed as,

$$\phi_i = \tan^{-1}\left(\frac{1}{2^i}\right) \quad (20)$$

Resulting in

$$v_i = \frac{1}{\sqrt{1 + 2^{-2i}}} \cdot \begin{bmatrix} 1 & -2^{-i} \\ 2^{-i} & 1 \end{bmatrix} \cdot v_{i-1} \quad (21)$$

From the above equation, we can say that the multiplication with a tangent can be replaced with a simple division operation by a power of 2. This division by power of 2, can be very efficiently implemented through a simple shift right operation on a shift register as shown in the Figure 3-4.

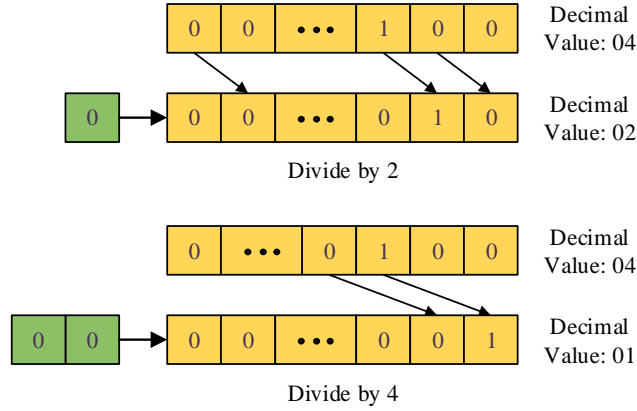


Figure 3-4 Division using Shift Register.

Due to the restriction imposed on $\tan(\phi_i)$, we can substitute $\tan(\phi_i) = \delta_i \cdot 2^i$ in equation (17) as shown below

$$v_i = K_i \cdot \begin{bmatrix} 1 & -\delta_i * 2^{-i} \\ \delta_i * 2^{-i} & 1 \end{bmatrix} \cdot v_{i-1} \quad (22)$$

where $K_i = \frac{1}{\sqrt{1+(\delta * 2^{-i})^2}}$ is the scale-factor.

Until now the CORDIC algorithm is reduced to a few simple shifts and additions, except the multiplication with the scale-factor. During the implementation, the multiplication required by the term K_i in equation (22) can be performed later. In fact, all the multiplication factors can be combined into a single gain normalization step following the completion of all micro-rotations. When this is done, the product of all the individual gains approaches a constant value,

$$\lim_{n \rightarrow \infty} K(n) = \prod_{i=0}^n K_i \approx 0.60725294104140 \quad (23)$$

At this point, a new term called “Z” is introduced. This term represents the intermediate micro-rotations in the CORDIC implementation and it can be represented as

$$Z_{i+1} = \theta - \sum_{i=0}^{N-1} \phi_i \quad (24)$$

where θ is the given rotational angle. On every rotation through an angle ϕ_i , the term Z and δ_{i+1} is computed, where δ_{i+1} is given as

$$\delta_{i+1} = \begin{cases} -1, & Z_{i+1} < 0 \\ +1, & Z_{i+1} \geq 0 \end{cases} \quad (25)$$

3.1.3 CORDIC Pre-Rotation

The CORDIC processor uses a series of micro-rotations that are defined as inverse tangent function as shown in equation (20). As a result, the CORDIC can only compute the coordinate components of vectors whose instantaneous phase values belongs to the region of convergence of inverse tangent function as shown in the Figure 3-5. Any phase angles which are not in this range cannot be processed without some prior manipulation and adjustment.

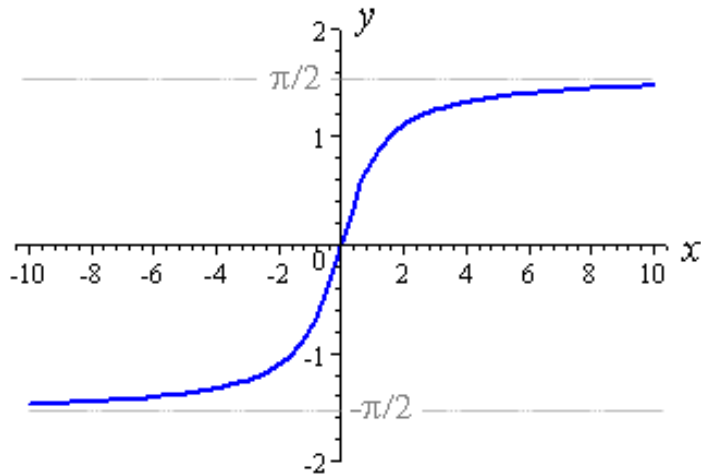


Figure 3-5 Region of Convergence for Inverse Tangent Function

With the phase representation and the symmetry of sine and cosine functions, it is not difficult to define a set of simple pre-rotations based on the phase to allow the CORDIC processor to compute correct values. With the acceptable range of $-\frac{\pi}{2} < \theta < \frac{\pi}{2}$, we need to pre-rotate for two additional regions, as shown in Figure 3-6, $\frac{\pi}{2} < \theta < \pi$ and $-\pi < \theta < -\frac{\pi}{2}$.

For rotations within the first region, $\frac{\pi}{2} < \theta < \pi$, if we apply the substitution based on the trigonometric identities

$$\cos\left(\theta + \frac{\pi}{2}\right) = -\sin(\theta) \text{ and } \sin\left(\theta + \frac{\pi}{2}\right) = +\cos(\theta) \quad (26)$$

$$x \rightarrow y, -y \rightarrow x, \theta \rightarrow \theta - \frac{\pi}{2} \quad (27)$$

The correct result will be computed.

For the second region, $-\pi < \theta < -\frac{\pi}{2}$, the pre-rotation is based on

$$\cos\left(\theta - \frac{\pi}{2}\right) = +\sin(\theta) \text{ and } \sin\left(\theta - \frac{\pi}{2}\right) = -\cos(\theta) \quad (28)$$

$$-x \rightarrow y, y \rightarrow x, \theta \rightarrow \theta + \frac{\pi}{2} \quad (29)$$

and the correct result will be computed.

The relationship between x and y used for pre-rotation can be summarized as shown in Table 3-1. Using this relationship, we can simplify the pre-rotation process as a simple negate and swap operation shown in the Figure 3-6.

Table 3-1 Technique used in CORDIC Pre-Rotation

	$\theta = f\left(+\frac{\pi}{2} \sim +\pi\right)$
x	$\cos\left(\theta + \frac{\pi}{2}\right) = \cos(\theta) \cdot \cos\left(\frac{\pi}{2}\right) - \sin(\theta) \cdot \sin\left(\frac{\pi}{2}\right)$ $\cos\left(\theta + \frac{\pi}{2}\right) = 0 \cdot \cos(\theta) - 1 \cdot \sin(\theta)$ $-\sin(\theta) = -y$
y	$\sin\left(\theta + \frac{\pi}{2}\right) = \sin(\theta) \cdot \cos\left(\frac{\pi}{2}\right) + \cos(\theta) \cdot \sin\left(\frac{\pi}{2}\right)$ $\sin(90 + \theta) = 0 \cdot \cos(\theta) + 1 \cdot \cos(\theta)$ $\cos(\theta) = x$
	$\theta = f\left(-\pi \sim -\frac{\pi}{2}\right)$
x	$\cos\left(\theta - \frac{\pi}{2}\right) = \cos(\theta) \cdot \cos\left(\frac{\pi}{2}\right) + \sin(\theta) \cdot \sin\left(\frac{\pi}{2}\right)$ $\cos(270 + \theta) = 0 \cdot \cos(\theta) + (1) \cdot \sin(\theta)$ $\sin(\theta) = y$
y	$\sin\left(\theta - \frac{\pi}{2}\right) = \sin(\theta) \cdot \cos\left(\frac{\pi}{2}\right) - \cos(\theta) \cdot \sin\left(\frac{\pi}{2}\right)$ $\sin(90 + \theta) = 0 \cdot \sin(\theta) - 1 \cdot \cos(\theta)$ $-\cos(\theta) = -x$

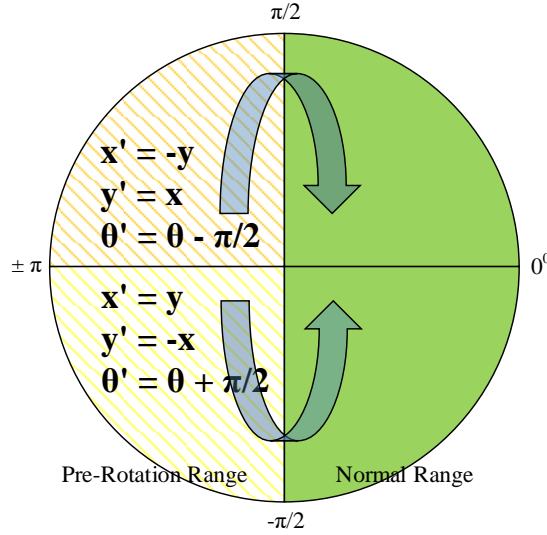


Figure 3-6 Methodology for Pre-Rotation

3.1.3 CORDIC as NCO

We know that the coordinate components of the input vectors for CORDIC can be defined as $v_i = \begin{bmatrix} x_i \\ y_i \end{bmatrix}$. If the coordinate components of this vector is fixed to $v_i = \begin{bmatrix} 1 \\ 0 \end{bmatrix}$, then the output of the CORDIC processor is actually the sine and cosine of an angle through which the CORDIC performed its rotation. Where the angle of rotation θ is defined as a fractional value defined by

$$\theta = \frac{(\text{angle in radians})}{2 * \pi} \quad (30)$$

If this is defined as either an unsigned or signed fractional binary number the instantaneous phase would be represented as

$$\sum_{i=0}^{M-1} b_i \cdot \varphi_i = b_0 \cdot \pi + b_1 \cdot \frac{\pi}{2^1} + b_2 \cdot \frac{\pi}{2^2} + \dots + b_{M-1} \cdot \frac{\pi}{2^{M-1}} \approx \theta \quad (31)$$

or as a two's complement representation,

$$-b_0 \cdot \pi + \sum_{i=1}^{M-1} b_i \cdot \varphi_i = -b_0 \cdot \pi + b_1 \cdot \frac{\pi}{2^1} + \dots + b_{M-1} \cdot \frac{\pi}{2^{M-1}} \approx \theta \quad (32)$$

This significantly simplifies the pre-rotation process, as the quadrants may be directly defined based on the two most significant bits.

With the binary representation, the CORDIC processor can be easily configured to become a NCO and compute the sine and cosine waveforms. This is usually done through the use of a computing a phase accumulator.

The phase accumulator determines and outputs the instantaneous phase of the complex sinusoid. For each clock cycle or time event, the instantaneous phase is added to a predefined phase step to produce a new accumulated value. The phase step and time period between samples defines the frequency at which sine and cosine waveforms would oscillate if the instantaneous phases were presented to CORDIC processor. When the accumulator goes through a complete cycle or full range of summations for the integer width defined, the CORDIC processor would have generated one complete cycle of sine and cosine waveforms. After one cycle, the next phase step will cause a numerical overflow in the accumulator. This is allowed and, in fact, desired as phase is a modulo 2π value and is expected to repeat. With the scaling performed to define the phase, the modulo phase operation perfectly aligns with the binary modulo operation of an integer adder or accumulator.

As mentioned, the frequency of the sine and cosine waves generated by the phase accumulator and CORDIC is directly proportional to the phase accumulator step size. If the frequency is defined as the time derivative (or first order difference) of the instantaneous phase, we have

$$\theta(n) = \theta_{step} \cdot n \quad (33)$$

$$f = \frac{\theta(n) - \theta(n-1)}{\Delta t} = \frac{\theta_{step}}{\Delta t} \quad (34)$$

So, the smaller the step size, the lower the frequency, and the larger the step size, the higher the frequency. In addition, the number of bits, defined as M , will define specific frequencies and frequency steps that can be exactly represented as shown below

$$Phase_{step}(rad) = \frac{NCO_{freq} \cdot 2^M}{2\pi} \quad (35)$$

where NCO_{freq} is the required oscillator frequency in radians, and 2π is the normalized sampling rate.

By incorporating the phase accumulator, the CORDIC processor can be used as a quadrature mixer and NCO. If the frequency of the NCO is chosen to be the carrier frequency of a signal of interest and the input vector represents the in-phase and quadrature-phase components of the signal sampled at RF, the output of the CORDIC processor represents the in-phase and quadrature-phase components of the down-converted baseband signal.

Finally, by using the equation (20), (22) and (24), we can easily implement the CORDIC processor either in hardware and software. The MATLAB and VHDL implementation details are explained in the next chapter of this thesis.

3.2 Filter Decimation for Down Converters

3.2.1 Cascaded Integrator Comb Filter

Many software defined radios are available in the market and each of them have their own set of digital filters used for realizing decimation and interpolation, digital filters are formed by a standard set of resources: memory or delays, adders, multipliers and resamplers. For hardware implementation, filter design can be characterized by the one that minimizes the number of multipliers and accumulators used in the architecture. In 1981, Eugene Hogenauer [21] suggested a new class of economical digital filter called Cascaded Integrator Comb filter also referred to as a CIC filter, the CIC filter belongs to a class of filter that does not require multipliers. Because of the simplicity of the implementation, CIC filter are used in many multirate signal processing applications such as, digital up-sampling/down-sampling. The filter has a lowpass frequency domain characteristics described by *sinc* function with nulls at the output Nyquist rate and multiples, which for narrowband signals can ensure that after down sampling nothing aliases to DC.

CIC filter design and response is derived from a multiplier free sliding window averaging filter also known as a boxcar filter shown in Figure 3-7, whose task is to smooth out the signals and unwanted noise [22]. This boxcar filter computes an output as follows, when a new data sample arrives, the previous contents in the shift register are shifted one place to the right, discards the oldest sample that had arrived M -samples ago. Next, the filter forms the sum of the contents of the register and outputs sum. The

performance of such a direct implementation of system is not very efficient as the summation is repeated for every new sample and the frequency response of this filter does not have significant attenuation outside of the passband. For large M , the number of additions is significant. Meanwhile, the maximum attenuation level of the first side lobe is just -13dB. In addition, it requires $M - 1$ additions to compute every output, which may be a big cost if M is very large. We can try to improve the filter characteristics and reduce signal processing complexity by investigating the mathematics involved behind a sliding window average filter.

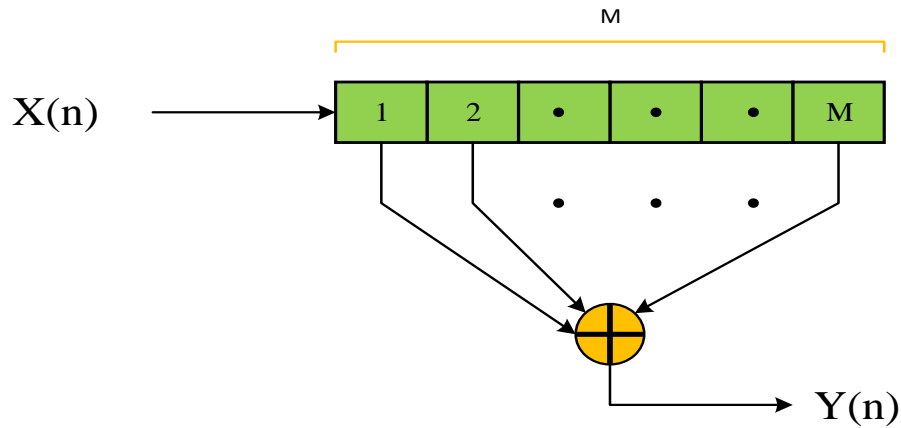


Figure 3-7 FIR Implementation of Boxcar Filter

The impulse response of the sliding window average filter is given by

$$H(n) = \sum_{k=0}^{M-1} \delta(n - k) \quad (36)$$

Hence, the output of the boxcar filter can be written as

$$y(n) = \sum_{k=0}^{M-1} x(n - k) \quad (37)$$

The frequency response of a boxcar filter can be derived by taking the Fourier transform of the equation (36) as

$$H(e^{j\omega}) = \sum_{n=0}^{M-1} 1e^{-j\omega n} \quad (38)$$

we can further simplify the above equation as

$$\begin{aligned} H(e^{j\omega}) &= \sum_{n=0}^{\infty} 1 \cdot e^{-j\omega n} - \sum_{n=M}^{\infty} 1 \cdot e^{-j\omega n} \\ H(e^{j\omega}) &= \sum_{n=0}^{\infty} 1 \cdot e^{-j\omega n} - \sum_{n=0}^{\infty} 1 \cdot e^{-j\omega(n+M)} \\ H(e^{j\omega}) &= \sum_{n=0}^{\infty} 1 \cdot e^{-j\omega n} - \sum_{n=0}^{\infty} 1 \cdot e^{-j\omega(n)} \cdot e^{-j\omega(M)} \end{aligned}$$

taking $e^{-j\omega n}$ common in the above expression we get,

$$H(e^{j\omega}) = (1 - e^{-j\omega(M)}) \cdot \sum_{n=0}^{\infty} 1 \cdot e^{-j\omega(n)} \quad (39)$$

By careful observations of the above expression, we get to know that it is an infinite series expression, which is also a geometric series. So by applying the notable geometric series identity

$$1 + x + x^2 + x^3 + \dots = \sum_0^{\infty} x^n = \frac{1}{1-x} \quad \forall |x| < 1$$

We get

$$H(e^{j\omega}) = (1 - e^{-j\omega(M)}) \cdot \left(\frac{1}{1 - e^{-j\omega}} \right) \quad (40)$$

Taking $e^{-\frac{j\omega M}{2}}$ common in the numerator and $e^{-\frac{j\omega}{2}}$ common in the denominator from the equation (40) we get the following equation

$$H(e^{j\omega}) = e^{-\frac{j\omega M}{2}} \cdot \left(e^{\frac{j\omega M}{2}} - e^{-\frac{j\omega M}{2}} \right) \cdot \left(\frac{1}{e^{-\frac{j\omega}{2}} \cdot \left(e^{\frac{j\omega}{2}} - e^{-\frac{j\omega}{2}} \right)} \right) \quad (41)$$

we know that $\sin(\theta) = \frac{e^{j\theta} - e^{-j\theta}}{2j}$ by substituting in the equation (41). We get,

$$H(e^{j\omega}) = e^{-\frac{j\omega M}{2}} \cdot \left(2 \cdot j \cdot \sin\left(\frac{\omega M}{2}\right) \right) \cdot \left(\frac{1}{e^{-\frac{j\omega}{2}} \cdot \left(2 \cdot j \cdot \sin\left(\frac{\omega}{2}\right) \right)} \right) \quad (42)$$

the above equation can be re-written as

$$H(e^{j\omega}) = e^{-\frac{j\omega(1-M)}{2}} \cdot \left(\frac{\sin\left(\frac{\omega M}{2}\right)}{\sin\left(\frac{\omega}{2}\right)} \right) \quad (43)$$

we know that $\frac{\sin(\theta)}{\theta} = \text{sinc}(\theta)$ we can simplify above expression further as shown below.

$$H(e^{j\omega}) = e^{-\frac{j\omega(1-M)}{2}} \cdot M \cdot \left(\frac{\text{sinc}\left(\frac{\omega M}{2}\right)}{\text{sinc}\left(\frac{\omega}{2}\right)} \right) \quad (44)$$

Using MATLAB, we can plot the frequency response of an M length boxcar filter according to equation (44) as shown in the Figure 3-8. We notice that, in order to achieve higher attenuation outside the passband, the length of the filter should be significantly high. As a result, it requires huge amount of adders for realizing this filter in hardware.

We also notice that nulls are at the integer multiples of $\omega = \frac{2\pi}{M}$ which is an important property of this filter.

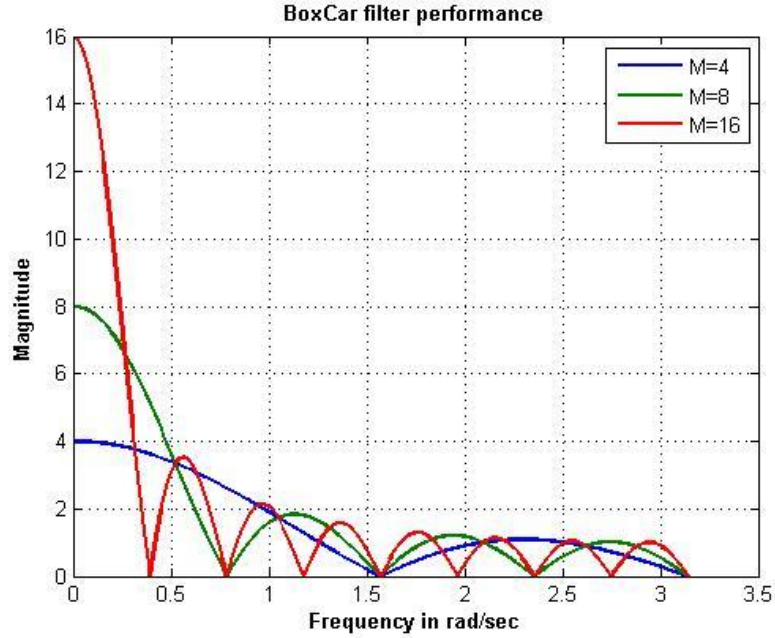


Figure 3-8 Boxcar Filter Frequency Response

We can reduce the number of addition required to implement this filter by considering a recursive form of the boxcar filter. That is, by altering the previous sum by adding the new sample and subtracting the oldest sample, this recursive form can be expressed as

$$y(n) = \sum_{k=0}^{M-1} x(n-k) = x(n) - x(n-M) + \sum_{k=0}^{M-1} x(n-1-k) \quad (45)$$

We know that $y(n-1)$ can be written as

$$y(n-1) = \sum_{k=0}^{M-1} x(n-1-k) \quad (46)$$

Substituting the above expression in the equation (18), we get

$$y(n) = x(n) - x(n-M) + y(n-1) \quad (47)$$

The recursive implementation can be realized as shown in the Figure 3-9. The resulted filter structure is called as CIC filter and could be broken into two parts; one as a comb section of length M and the other as an integrator section. In this type of implementation, the computation of each output sample would require only two adders as compared to $M - 1$ adders in the simple boxcar filter structure.

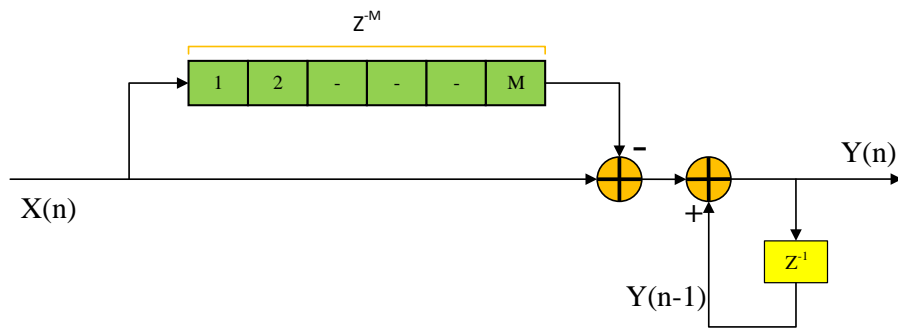


Figure 3-9 Single Stage CIC Filter

While the signal processing complexity is now reduced to just two simple adders, the frequency response of the filter has not changed from that seen in Figure 3-10.

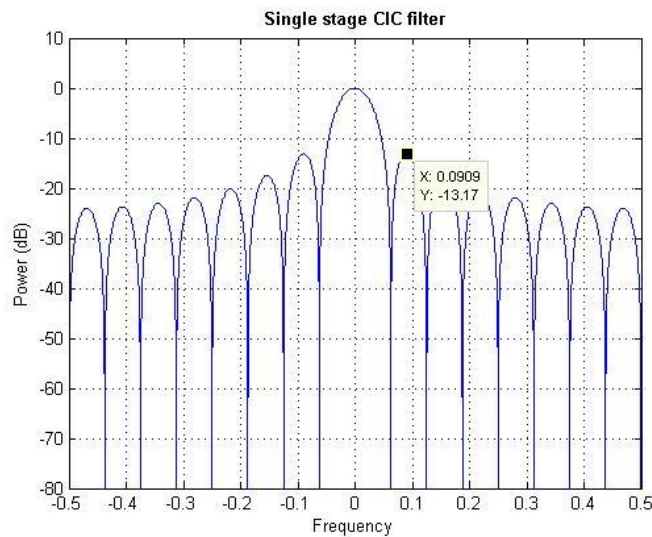


Figure 3-10 Frequency Response of Integrator Comb (CIC) Filter

We can improve the spectral domain performance of this filter by forming a cascade of multiple recursive boxcar filters. It is common to use 3-to-5 cascade stages with many applications. The transfer function and the corresponding frequency response is shown in equation (48) and (49).

$$H_k(Z) = \left[\frac{1 - Z^M}{1 - Z^{-1}} \right]^K \quad (48)$$

$$|H(e^{j\omega})| = \left[M \cdot \frac{\text{sinc}\left(\frac{\omega M}{2}\right)}{\text{sinc}\left(\frac{\omega}{2}\right)} \right]^K \quad (49)$$

where, M is the length of the comb section in the CIC structure and K is number of cascaded stages. The effect of this implementation is to increase attenuation of the first side-lobe level by multiples of -13dB at output of successive cascaded stages as shown in the Figure 3-11. Another possibly more important feature of this cascaded form is that the stopband nulls are getting broader, providing wider notches in the spectrum at frequencies of $\omega = \frac{2\pi}{M}$ or $f = \frac{f_s}{M}$. If the CIC low pass filter is decimated by a factor of M , the wider notches at multiples of the sampling rate in the spectrum fall exactly on the frequency images that would be aliased, as shown in Figure 3-12.

The main disadvantage of this type of implementation is that the low pass filter passband is not flat and the -3dB point on the main-lobe is getting narrower as K increases. This effect is called “droop” in passband. To compensate for this droop, CIC filter decimators are usually followed by a cleanup filter which provides spectral flattening and reshaping.

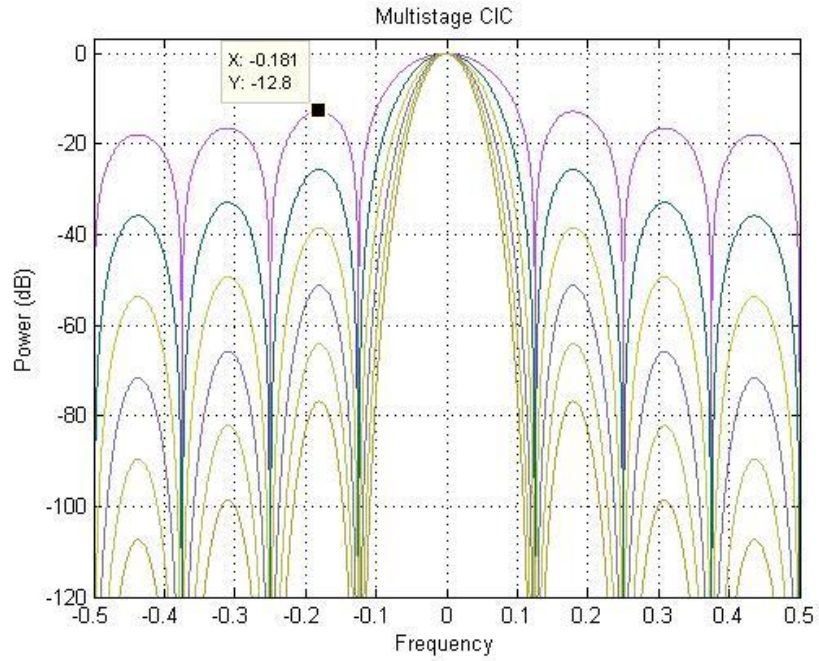


Figure 3-11 Spectrum of a Multistage CIC

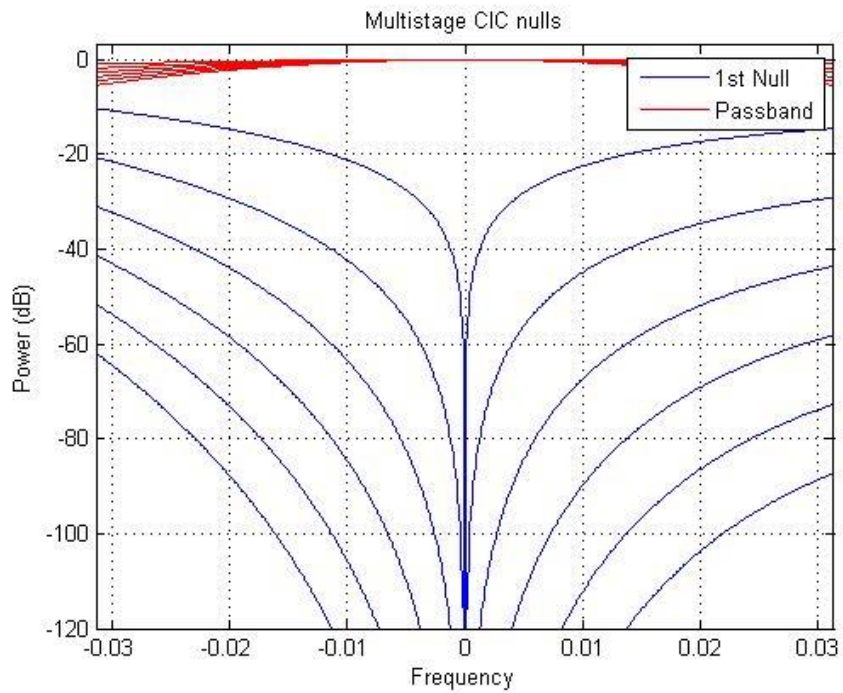


Figure 3-12 Broadening Nulls at Successive Stages of CIC

Furthermore, when the CIC filter is applied for an up-sampling task, the comb section is placed at the input followed by resampling switch and then integrator section. On the other hand for down sampling applications the integrator section is placed at the input followed by resampling switch and then the comb section. This reordering is established to permit the application of multirate signal processing identity of the reordering the resampling switch and the comb filter as shown in Figure 3-13. When the CIC filter absorbs the resampling switch, the comb filter together with the resampling switch becomes a differentiator on the lower data rate side [21] and the filter structure is known as Hogenauer filter. A CIC filter with any number of stages can be converted to a Hogenauer filter by first ordering all the integrators on one side of the filter and the comb filters on the other side, then applying the sample rate identity to interchange the resampling switch and the comb filters. The goal of this thesis is to implement a 3 stage CIC filter as shown in the Figure 3-14.

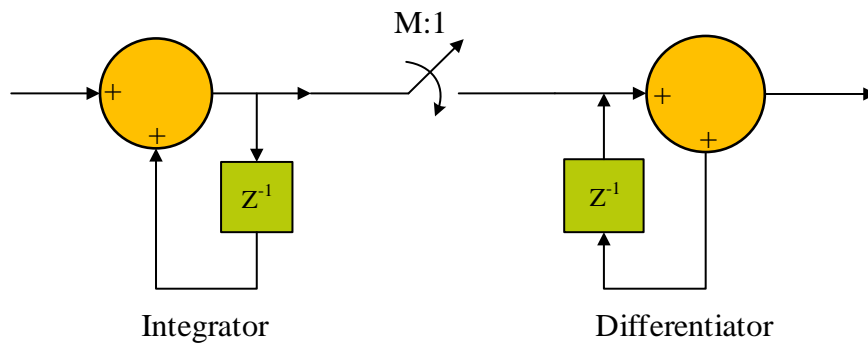


Figure 3-13 Hogenauer Filter Structure of a Single Stage CIC Filter

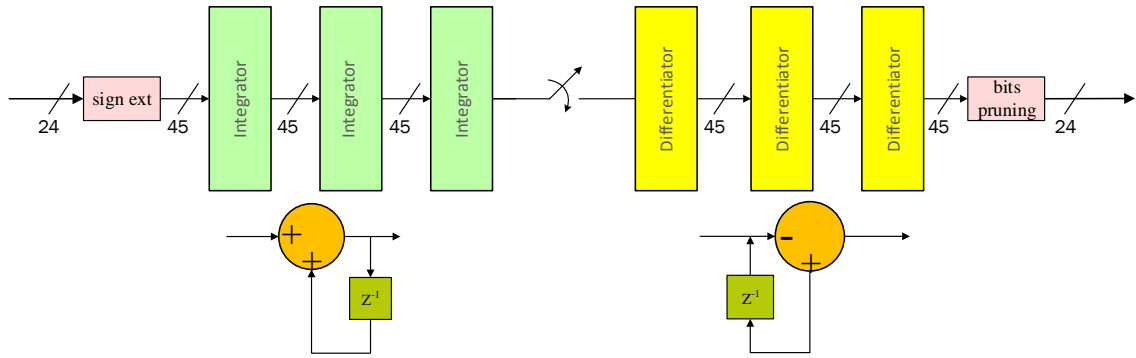


Figure 3-14 Hogenauer Structure of a 3-stage CIC Filter

The integrators in a CIC filter is very unstable and can easily go to infinity will results in a register overflow in all integrator stages in the filter. However, it will not be a problem if these two condition are met [21].

1. The filter is implemented with a number system which allows “wrap-around” between the most positive and most negative numbers.
2. The range of the number system is equal to or greater than the maximum output expected at the output stage of the entire decimation filter structure.

Based on these conditions high attention to the bit growth in each successive stages of the accumulators of the CIC filter. From [22] and [21] the required bit width to design an accumulator which can accommodate the maximum and/or worst case register bit growth is defined as the maximum output magnitude from the worst possible input signal relative to the maximum input magnitude. Using this definition, the maximum register growth from the first stage up to and including the last stage is given by equation (50).

$$G_{max} = R \cdot M^K \quad (50)$$

Where R is the decimation rate, M is the length of comb filter and K is the number of cascaded stages. If the input data has a bit width of B_{in} , then the register growth is given by the equation (51). This growth is used in the CIC filter design process to insure that no data are lost or corrupted due to register overflow.

$$B_{max} = B_{in} + CEIL[\log_2(G_{max})] \quad (51)$$

In most practical cases where decimation rate is very large, B_{max} is very large hence it has to be truncated or rounded at the output stage. The bit growth in the CIC filter reflects the filter gain between the input and output of the filter. During down sampling, we can scale the output of the CIC filter to remove the filter processing gain by pruning the least significant bits to the level corresponding to the filter processing gain. The implementation details are further explained in the next chapter.

3.2.2 Half-Band Filters

The second stage of filtering in the DDC chain consists of two half-band decimating filters. A half-band filter is a non-recursive Finite Impulse Response (FIR) filter designed to have a passband bandwidth between $\pm \frac{1}{4}f_s$ of the sampling rate as shown in the Figure 3-15. The impulse response of an ideal non-casual continuous half-band filter with two sided bandwidth $\frac{f_s}{2}$ is shown in (52) [22].

$$h_{LP}(t) = \frac{f_s}{2} \cdot sinc\left(\frac{2\pi f_s}{2} t\right) \quad (52)$$

Based on the above equation, we can define the half-band filter as, a filter whose impulse response which has a *sinc* characteristics that is symmetric about the origin and has zero crossing at the integer multiples of twice the sampling period. The frequency response of this filter has the same passband and stopband ripples. By zooming into the response, it can be verified that the peak-to-peak ripples in passband and stopband are the same.

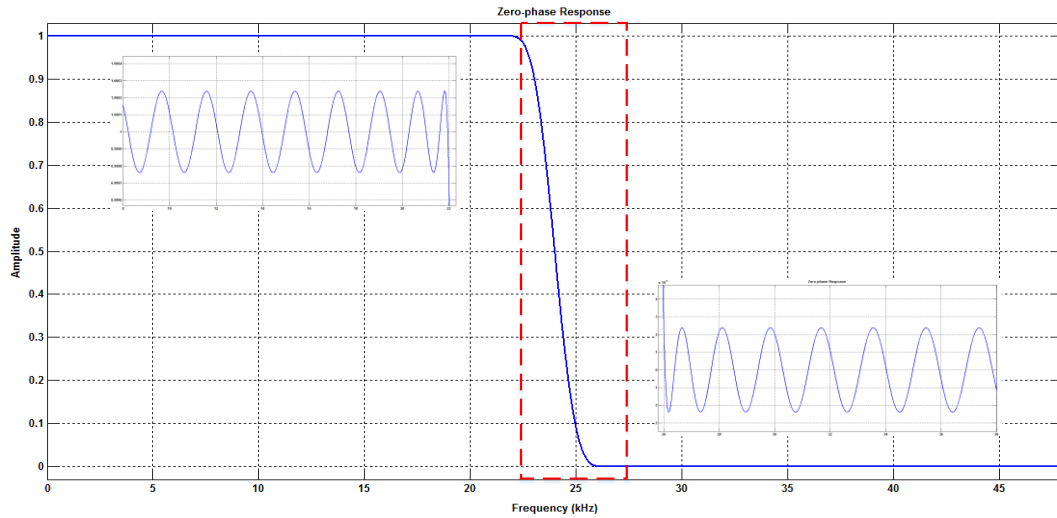


Figure 3-15 Zero-Phase Frequency Response

The discrete impulse response can be obtained from the above equation (46) by sampling it with the sample rate of f_s as shown in (53) and the simplified equation is shown in (54).

$$h_{LP}(n) = \frac{f_s}{2} \cdot \text{sinc}\left(\frac{2\pi f_s/2}{2} \frac{n}{f_s}\right) \quad (53)$$

$$h_{LP}(n) = \frac{1}{2} \cdot \text{sinc}\left(\frac{n\pi}{2}\right) \quad (54)$$

The special property of (54) is that its discrete impulse response has multiple zero valued coefficients [23]. In fact, all the even numbered samples of $h(n)$, except $h(0)$, are

$\frac{\pi}{2}$, and adding both the responses together as shown in (58) we get a filter which has a flat frequency response from DC to f_s , which is also known as an all pass filter.

$$H(Z) + H(-Z) = 2c \quad (58)$$

By default, the resulting sum should be equal to 1, therefore assuming that c in (58) is normalized to 0.5. This shows that, $H\left(e^{j\left(\frac{\pi}{2}-\theta\right)}\right)$ and $H\left(e^{j\left(\frac{\pi}{2}+\theta\right)}\right)$ add up to unity for all θ . In other words, we have a symmetry with respect to the half-band frequency $\frac{\pi}{2}$, justifying the name “half-band filter”.

A digital filter is basically a real-time processor with an arithmetic unit for additions and multiplications, and a memory to store the filter coefficients. A direct is shown in the Figure 3-17. As the number of filter coefficients increases, the implementation of this filter becomes more complicated and requires a larger number of multipliers and adders and the filter would consume a larger area. By proper design of the filter coefficients, many implementation methodology can be followed which can help us in saving the hardware resources required to implement this filter.

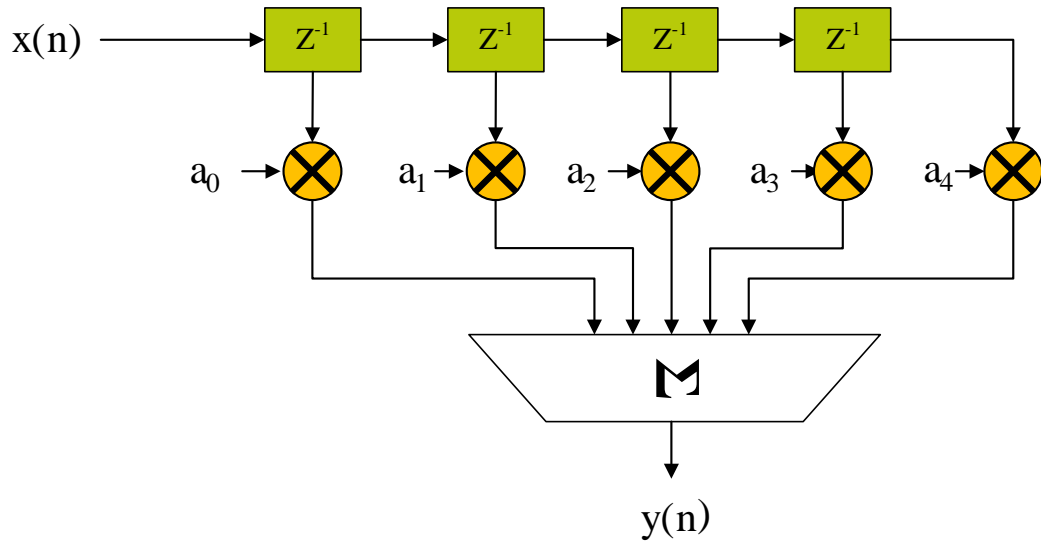


Figure 3-17 FIR Filter Structure

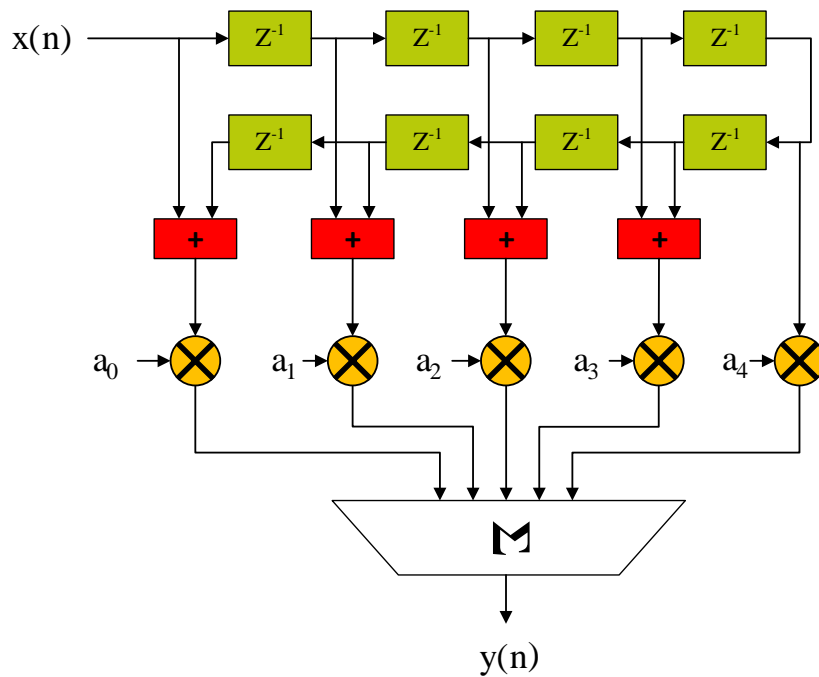


Figure 3-18 Symmetric FIR Filter Structure

The efficiency of half-band filters derives from the fact that nearly 50 percent of the filter coefficients are zero and the remaining coefficients are symmetric with respect

to the single nonzero even coefficient. Hence, the input samples can be pre-added before multiplying with the coefficients as shown in the Figure 3-18. That is, 2 multiplications can be replaced by 1 addition and 1 multiplication operations. Table 3-2 summarizes the computational gain of the half-band filters over the conventional FIR filters. With this result, the half-band filter demonstrates a potentially saving of $\frac{1}{4}$ the multiplications and $\frac{1}{2}$ the additions.

Table 3-2 Half-Band Computation Efficiency

Filter Category (FIR)	Special Conditions	Taps	Number of Multiplications	Number of Adders
Conventional		4M	4M	4M-1
Half-Band		4M+3	2M+3	2M+2
Half-Band	No multiplies at h(0)	4M+3	2M+2	2M+2
Half-Band	No multiplies at h(0) and symmetric	4M+3	M+1	M+1

In this thesis, two half-band filters were implemented which exhibits a strict linear passband characteristics, both the half-band filters also have a fixed decimation by a factor of 2. Amongst the two filters, the first half-band filter has only 7 coefficients. In which, only 3 coefficients are nonzero including the middle coefficient and it has a fairly poor performance in terms of out of band attenuation but in combination with the second filter provides improved transition bands and stopband. The impulse and frequency response of 7-Tap half-band filter is shown in the Figure 3-19. The second half-band filter has 31 coefficients constructed as a 2 path polyphase filter structure. Out of these 31 coefficients, 14 coefficients are zeros and filter is constructed with only using 16 coefficients since the center tap is considered to be equal to 1. This half-band filter has a

significantly better performance compared to first half-band filter with respect to the stopband attenuation levels as shown in Figure 3-20. The implementation details of these half-band filters are further explained in the next chapter.

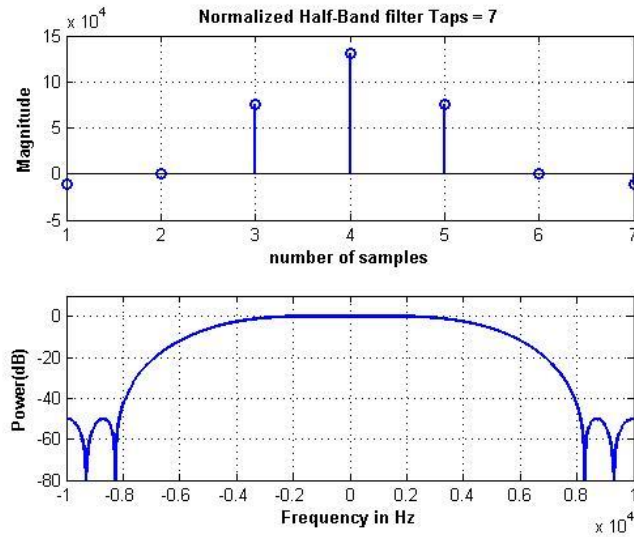


Figure 3-19 First Stage Half-Band Filter

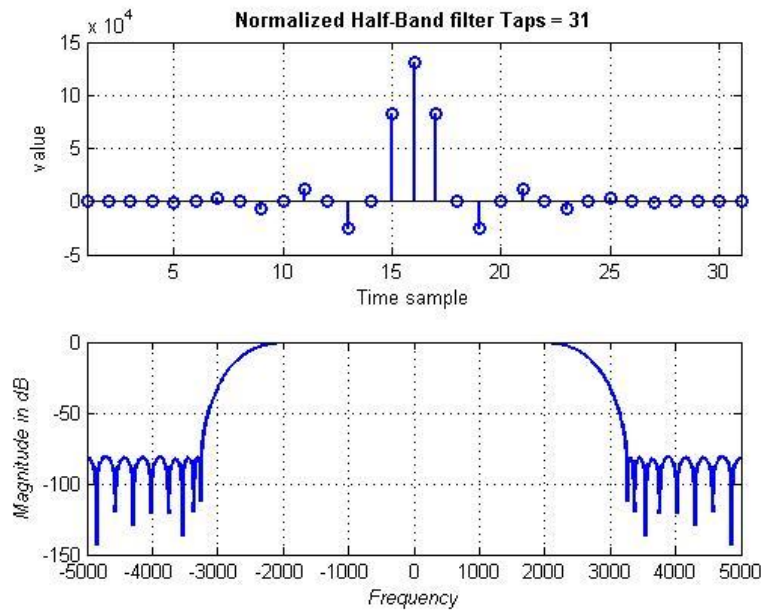


Figure 3-20 Second Stage Half-Band Filter

Chapter 4

METHODOLOGY AND IMPLEMENTATION

This section will provide a detailed description of MATLAB and VHDL implementation of the DDC chain discussed in the previous chapter. The communication signal processing board designed uses a fractional 2's complement integer number system to represent the data samples. The processor is capable of receiving a 32-bit complex word as interleaved 16-bits of a quadrature phase sample and 16 bits of in phase sample. This configuration is intended to support the signal output of two quadrature sampling ADCs. If 16-bit ADCs are used, the data is fed directly into the in-phase and quadrature inputs. If an ADC with less than 16-bits is used, the data must be left shifted so that the ADC Most Significant Bits (MSBs) is the input MSBs and the remaining Least Significant Bits (LSBs) are zero filled. As an integer processor it is very important to maintain proper input bit positioning, as the processing stages have been designed to maximize dynamic range and performance for left aligned data inputs.

After the input stages, the communication signal processor attempt to maintain a 24 bit integer data path. This would allow a wider input ADC to be used in the future while maintaining a higher signal dynamic range in the current processing. The 24-bits representation is not maintained at all signal processing stages as 18x18 multipliers are used in half-band filtering and gain adjustment processing stages. Where this occurs, the signal will be reduced in dynamic range (typically rounded) prior to multiplication and

24-bit results will be maintained. The architectural model of the complex narrow band DDC chain implemented in this thesis is shown in the Figure 4-1.

4.1 CORDIC Processing Unit

The CORDIC processing unit implemented in this thesis can be conceptualized as a combination of NCO and quadrature mixer. The designed CORDIC processor is operating at a full sampling rate, and it allows the full bandwidth of a sampled signal to be down converted to baseband.

Generally, the number of stages in CORDIC is dependent on the number of bits of precision required in the system. For a CORDIC processor working at 24 bits of precision, the maximum number of stages for an efficient implementation is 24, i.e., one stage per bit. Any additional stages would result in same output vectors with no or insignificant change. For a specific input bit precision, the expected operation and resultant vectors from each CORDIC micro-rotations are examined to determine at which stage, or after how many micro-rotations the CORDIC processor has approached the desired angle. As a result, the implementation of the CORDIC processor can be simplified in order to save the area required on the silicon die.

For the architecture selected in this thesis, a 20 stage 24-bit CORDIC processor was designed on a Spartan 6 (xc6slx16-3-csg324) FPGA, and the design was verified with a fixed-point iterative model implemented in MATLAB. The necessary functional components and data flow for implementing the CORDIC processor is shown in the Figure 4-2.

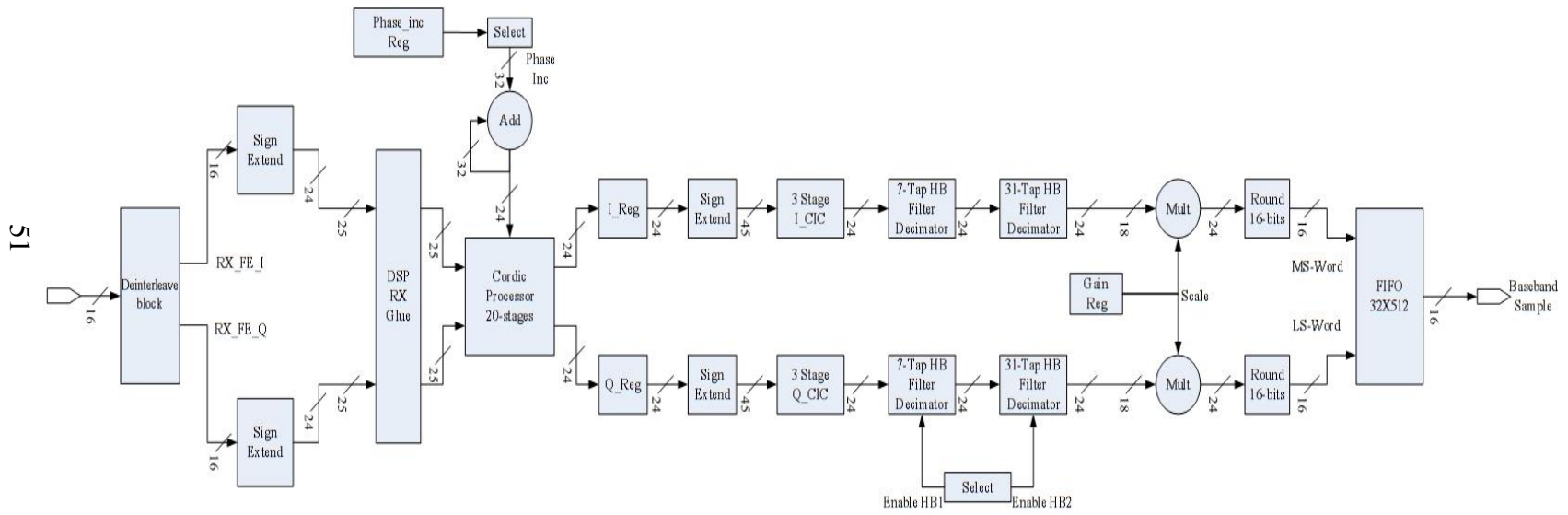


Figure 4-1 Architecture of Communication Signal Processing Board

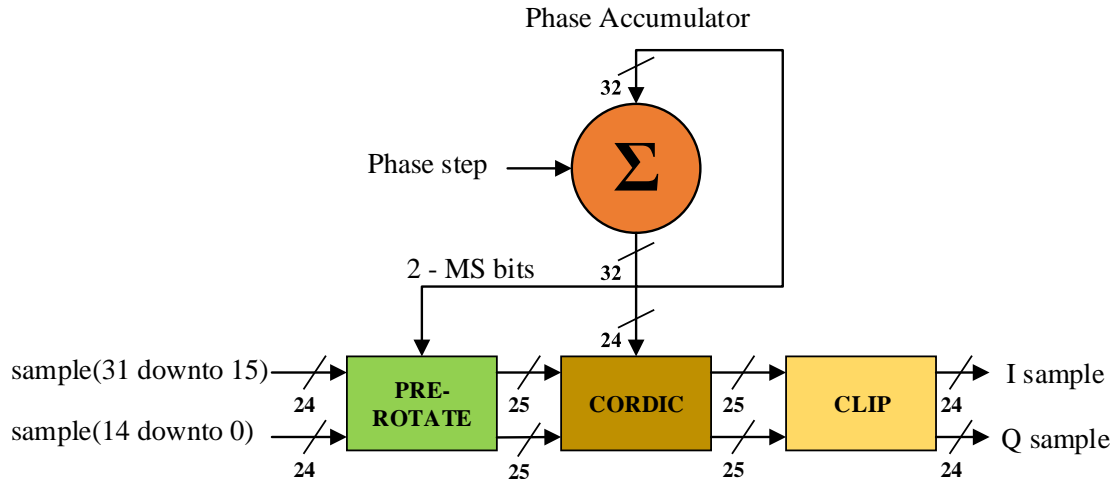


Figure 4-2 CORDIC Processing Unit Core

The CORDIC processor designed uses four fundamental blocks; the phase accumulator, the pre-rotator, the clipper and the actual CORDIC engine.

The CORDIC processor computes an output as follows:

1. The step size of the phase accumulator for a particular frequency that needs to be generated is predetermined and loaded into the phase accumulator. The phase accumulator is updated to the next phase value.
2. The input vectors are first pre-rotated if necessary before the CORDIC engine.
3. The CORDIC engine obtains the data from pre-rotation module and phase accumulator and rotates the coordinate components of the input vector through an angle specified by the phase accumulator.
4. Finally, the outputs from the CORDIC engine are truncated to a required bits precision by the clipping module.

This process is repeated infinitely and the output of CORDIC processing unit will be a frequency translated version of the input signal. The techniques involved in phase

accumulator, pre-rotation and CORDIC engine are explained individually in the following parts of this section.

4.1.1 Phase Accumulator

The CORDIC implemented in this thesis uses a 32-bit phase accumulator, which is implemented as a simple 32-bit adder, which adds the previous phase with a specified step size on every clock cycle. The 32-bit value from phase accumulator is then truncated to a 24 MSBs before being used by the CORDIC engine. The extra 8 LSB in the phase accumulator are used to provide higher frequency resolution for the NCO and a better resolution in the output signal.

A fixed-point 32-bit phase accumulator for the CORDIC processing unit was implemented in MATLAB using a wrap-around method to restrict the integers to a fixed number of bits as shown in the code below.

```
% #####-----[32 bit integer wrap around]-----#####  
if (phase > 2147483647)% if > 2^31 - 1 roll it back to -ve's  
    phase = phase - 4294967295; %(2^31-1 + 2^31)  
else if (phase < -2147483648) % -2^31  
    phase = phase + 4294967295;  
    end  
end
```

In the example shown, the datatype for the “phase” variable was chosen to be int64, and every time the “phase” gets a value greater than $2^{32} - 1$, the value is rolled back to a negative value within the range of a 32-bit integer. This wrap-around logic is shown in the Figure 4-3.

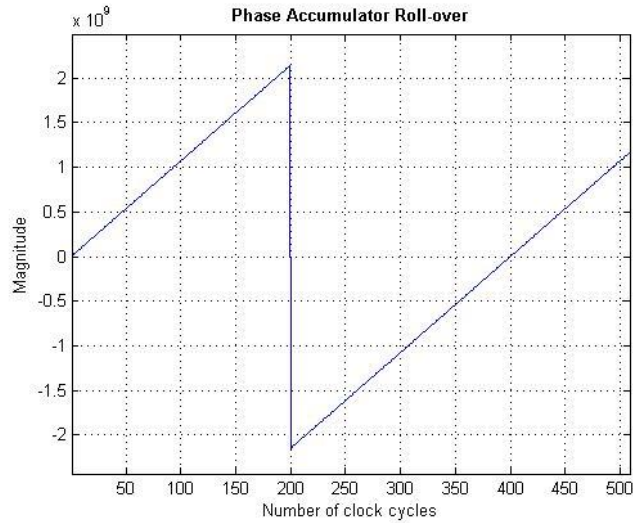


Figure 4-3 CORDIC Phase Accumulator

4.1.2 Pre-Rotation

In the 24-bit MSBs of the phase accumulator, 2^{23} is represented as -180° and 2^{22} is represented as $+90^{\circ}$ and so on. Using this information, we can determine the quadrant of the instantaneous phase values. Therefore, we can implement the pre-rotation block as a multiplexer using quadrant information from 2 MSBs of angular arguments computed in the phase accumulator as shown in the Table 4-1.

Table 4-1 Input Vector Quadrants

Z(23)	Z(22)	Quadrant	
0	0	0 to 90	No pre-rotation
0	1	90 to 180	Needs pre-rotation
1	0	0 to -90	No pre-rotation
1	1	-90 to -180	Needs pre-rotation

The pre-rotation of a 24-bit input angles was done using the MATLAB's predefined bitwise operators in-order to closely match the hardware implementation and ease the verification process as shown in the code below.

```

% Phase pre rotation since cordic is limited to +pi/2 to -pi/2
if (zin>=2^22 && zin<2^23)% interval between 90 to 180 degrees
    xpast = x;
    x = -y;
    y = xpast;
    zin = bitand(zin, 4194303);
else if(zin>=-2^23 && zin<-2^22)% interval between -180 to -90
degrees
    xpast = x;
    x = y;
    y = -xpast;
    zin = bitor(zin,-12582912);
end
end

```

The VHDL code snippet implementing the pre-rotation block as a multiplexer using the two most significant bits of the phase vector as the select lines is shown below.

```

case (Zin(24-1 downto 24-2)) is
when "00" => -- interval between 0 to 90 degrees no pre-rotation
    I0 <= (Iin_ext);
    Q0 <= (Qin_ext);
    Z0 <= (Zin);
when "01" => --interval between 90 to 180 degrees
    I0 <= -(Qin_ext);
    Q0 <= (Iin_ext);
    Z0 <= ("00" & Zin(zwidth-2-1 downto 0)); -- phase
rotation to -90 deg
when "10" => --interval between -180 to -90 degrees
    I0 <= (Qin_ext);
    Q0 <= -(Iin_ext);
    Z0 <= ("11" & Zin(zwidth-2-1 downto 0)); -- Phase
rotation to +90 deg
when "11" => -- interval between -90 to 0 degrees no pre-rotation
    I0 <= (Iin_ext);
    Q0 <= (Qin_ext);
    Z0 <= (Zin);
when others =>
    I0 <= (others => '0');
    Q0 <= (others => '0');
    Z0 <= (others => '0');
end case;

```

4.1.3 CORDIC Engine

As mentioned before in Chapter 3, the CORDIC processor can be easily implemented using the simplified CORDIC equation (59). According to this equation, a single stage CORDIC processor could be implemented just by using two shift registers and three adders as shown in the Figure 4-4.

$$v_i = K_i * \begin{bmatrix} 1 & -\delta_i * 2^{-i} \\ \delta_i * 2^{-i} & 1 \end{bmatrix} * v_{i-1} \quad (59)$$

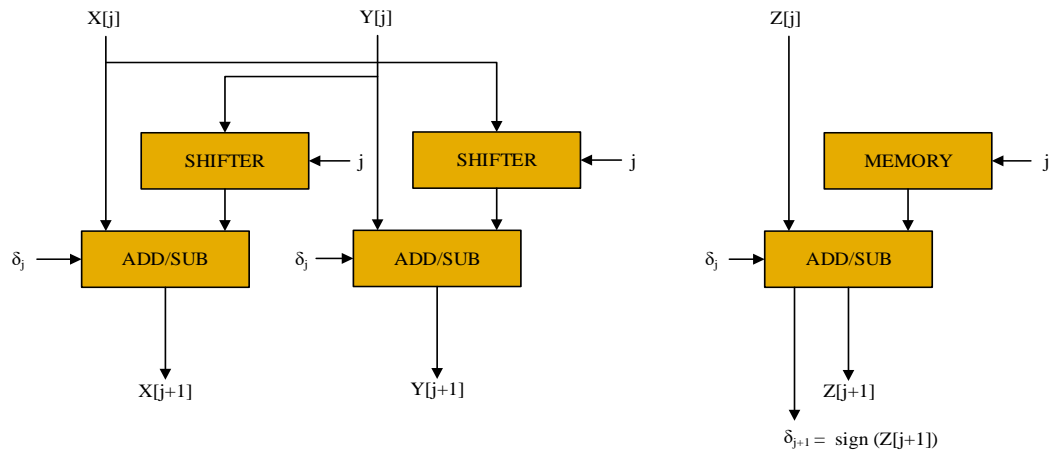


Figure 4-4 Single Stage CORDIC using Shift Registers

Furthermore, to increase the throughput of the CORDIC processor, all micro-rotations defined by the tangents are precomputed and stored on the block RAM or on the Look Up Tables (LUT). These precomputed micro-rotations for a 24-bit CORDIC is shown in the Table 4-2.

Table 4-2 CORDIC Constants or Arc Tangent Radix Constants

Iterations	Angle (radians)	Angles (degrees)	Phase Constants: 24 Bits(radians)
I = 1	$\tan^{-1}(2^{-1})$	45	2097152
I = 2	$\tan^{-1}(2^{-2})$	26.56505118	1238021
I = 3	$\tan^{-1}(2^{-3})$	14.03624347	654136
I = 4	$\tan^{-1}(2^{-4})$	7.125016349	332050
I = 5	$\tan^{-1}(2^{-5})$	3.576334375	166669
I = 6	$\tan^{-1}(2^{-6})$	1.789910608	83416
I = 7	$\tan^{-1}(2^{-7})$	0.89517371	41718
I = 8	$\tan^{-1}(2^{-8})$	0.447614171	20860
I = 9	$\tan^{-1}(2^{-9})$	0.2238105	10430
I = 10	$\tan^{-1}(2^{-10})$	0.111905677	5215
I = 11	$\tan^{-1}(2^{-11})$	0.055952892	2608
I = 12	$\tan^{-1}(2^{-12})$	0.027976453	1304
I = 13	$\tan^{-1}(2^{-13})$	0.013988227	652
I = 14	$\tan^{-1}(2^{-14})$	0.006994114	326
I = 15	$\tan^{-1}(2^{-15})$	0.003497057	163
I = 16	$\tan^{-1}(2^{-16})$	0.001748528	81
I = 17	$\tan^{-1}(2^{-17})$	0.000874264	41
I = 18	$\tan^{-1}(2^{-18})$	0.000437132	20
I = 19	$\tan^{-1}(2^{-19})$	0.000218566	10
I = 20	$\tan^{-1}(2^{-20})$	0.000109283	5

4.1.4 MATLAB Implementation

A 24-bit fixed-point 20 stage CORDIC engine was implemented in MATLAB using an iterative method where j is the iterative index. Each iteration in this implementation can be thought as an individual stage of CORDIC processing as shown in the code snippet below.

```
while j < 20
    if (phase > 0)
        delta = 1;
    else
        delta = -1;
    end
    xpast = x;
    x=xpast - (y* delta *(1/2^j));
    y=y + (xpast* delta *(1/2^j));
    j = j+1;
    phase = phase - (delta *consts(j));
end
```

In each stage, the input vectors (x, y) are right shifted by j times (division by 2^j operation) and added/subtracted together depending on the value of delta (δ_j) resulted from the previous iteration.

In order to configure the CORDIC as a complex sine and cosine signal generator, the initial vectors (x_i, y_i) has to be fixed at $(1,0)$. By doing so, the phase difference between the vectors are explicitly specified as $\frac{\pi}{2}$ as shown in the Figure 4-5. In this example, the CORDIC is used as a NCO for generating a 250 Hz quadrature signals when the sampling rate is 100 KHz. The MATLAB frequency spectrum of the signal generator generating 250Hz is show in the Figure 4-6.

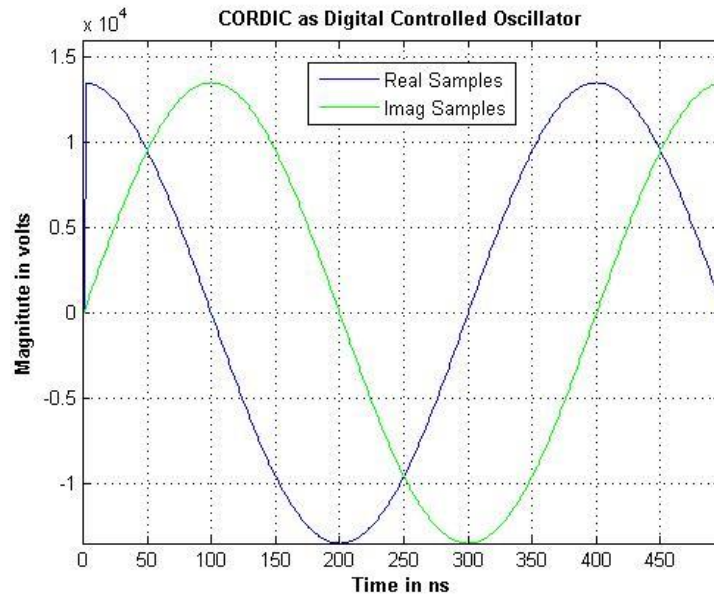


Figure 4-5 CORDIC Implemented as NCO

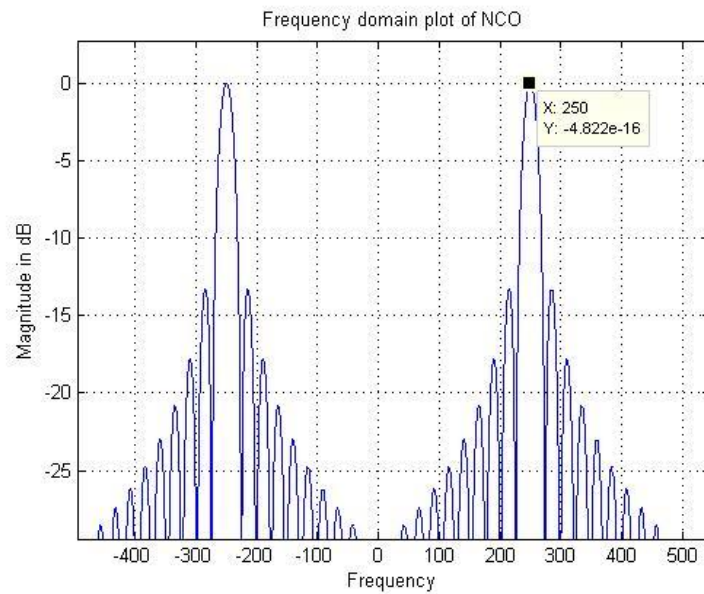


Figure 4-6 Frequency Spectrum of the CORDIC Output (zoomed-in)

4.1.5 VHDL Implementation

The 24-bit input samples are sign extended to 25 bits in order to avoid the overflow involved in the 2's complement arithmetic operations. These 25-bit samples are further sign extended by 3-bits inside the CORDIC engine to compensate with the gain involved in the CORDIC algorithmic. Hence, the CORDIC uses two-27 bit shift registers for (x, y) and a 24-bit register for the phase register(z).

Each stage in the CORDIC processor was implemented as a multiplexer with the sign bit of the angular argument (δ_i) as the select line as shown in the Figure 4-7. In order to attain the highest possible throughput, a pipelined structure was used in this thesis. A 20 stage pipelined CORDIC engine was implemented as a multiple component instantiation of single stage CORDIC as shown in the Figure 4-8.

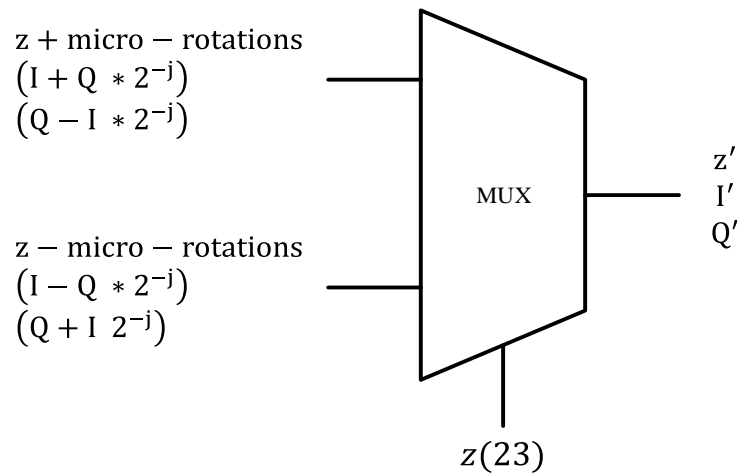


Figure 4-7 VHDL Implementation of a Single Stage CORDIC

In the pipelined CORDIC architecture, each stage is represented as a separate CORDIC block and the pipeline registers are placed after each stage. Each stage in this architecture will be working independently. Thus, when the i^{th} block is performing the

corresponding rotation on the i^{th} data sample, then the $(i - 1)^{th}$ block would be performing the rotation on $(i + 1)^{th}$ data. This way, greater speeds could be achieved by computing many partial results in a parallel processing pipeline.

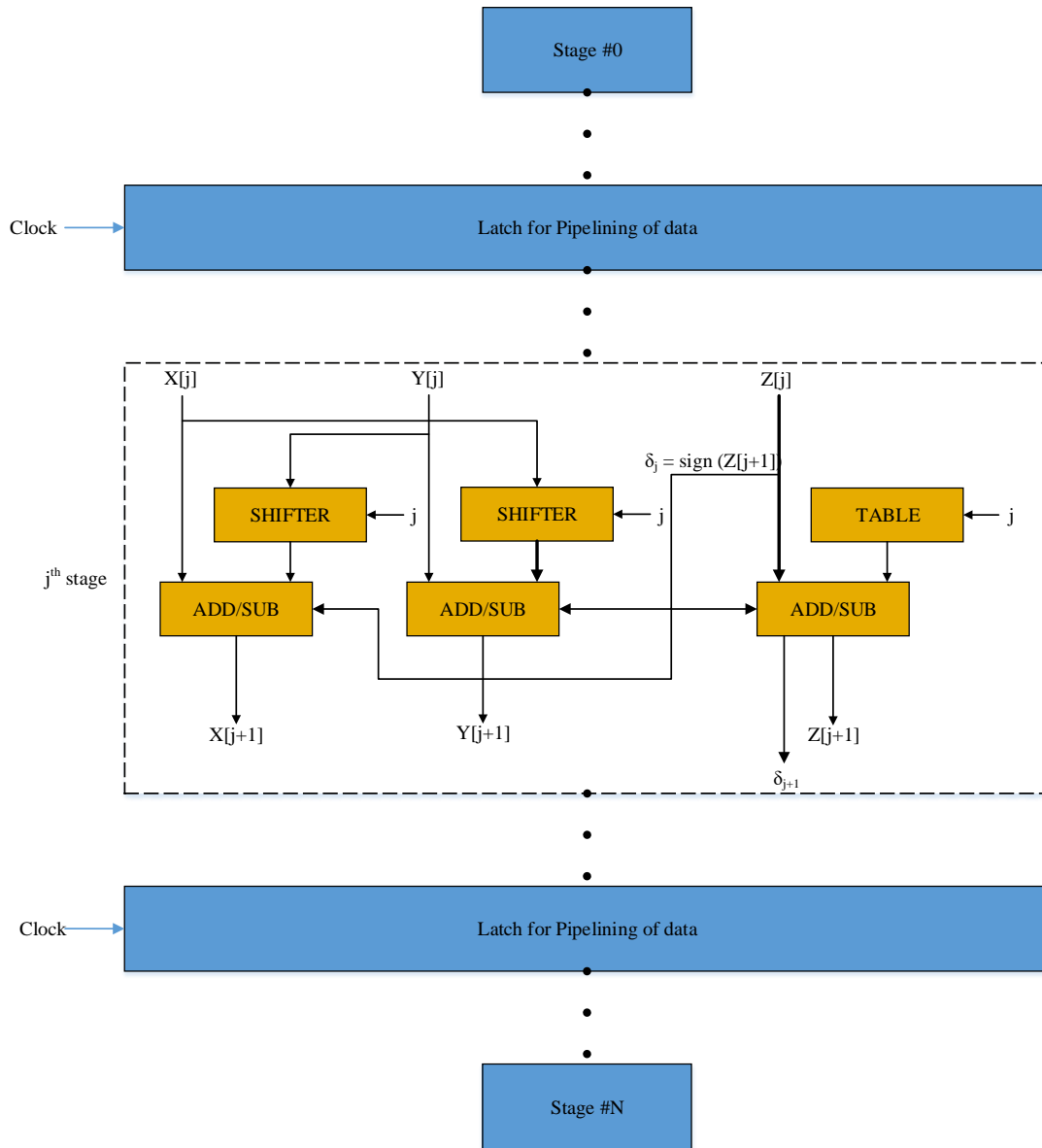


Figure 4-8 CORDIC Pipelined Stages

In the pipelined implementation of CORDIC, the series of micro rotations has to ripple through each stage. Hence, there is an initial 21 clock cycles of latency for the

CORDIC to compute the first output as shown in the Figure 4-9. In this example, once the ddc_en signal goes high (i. e., after the signal processor board is enabled) the signal processor starts capturing the incoming signal (rx_freq_in) and after 21 clock cycles the CORDIC processor result appears on the CORDIC outputs.

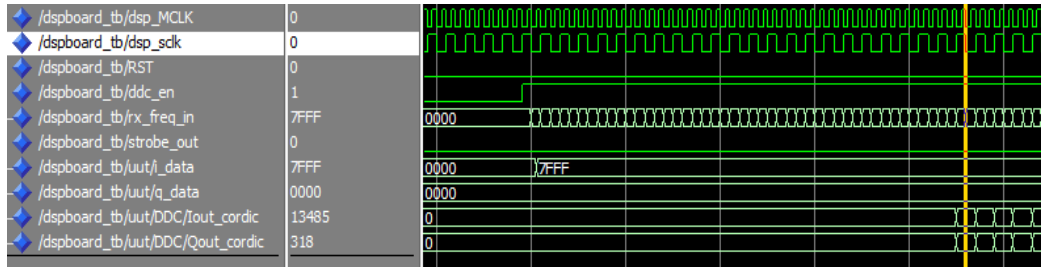


Figure 4-9 CORDIC Initial Latency

The output of the CORDIC is truncated to 24 bit samples and the remaining bits are discarded. In this research, the 27 bit output from the 20th stage of CORDIC is truncated as shown in the Figure 4-10. The bits in yellow represents the valid 24 bit word and the bits in green are discarded. This is done in order to avoid the overflow when the maximum strength of the signal is sent on both I and Q of the same DDC at the same time. The CORDIC operation can be conceptualized for a zero angular phase input as taking the original 16-bit I and Q input samples, shifting them left by 8-bits and then having the CORDIC processor multiplies it by approximately $\frac{1.647}{2^3}$.

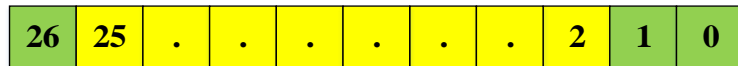


Figure 4-10 CORDIC Output Truncation

The CORDIC implementation was mapped to the target device (Spartan 6 – xc6slx16) as shown in 0Cordic_z24.vhd and CORDIC_STAGE.vhd. The resulted

resource utilization is shown in the Table 4-3. The 19% of LUT utilization is due to storing the CORDIC constants on the LUTs.

Table 4-3 CORDIC Processor Device Utilization Summary

Device Utilization Summary (estimated values)			
Logic Utilization	Used	Available	Utilization
Number of Slice Registers	1670	18224	9%
Number of Slice LUTs	1791	9112	19%
Number of fully used LUT-FF pairs	1624	1837	88%
Number of bonded IOBs	0	232	0%

The ModelSim simulation of this CORDIC processor is shown in the Figure 4-11. Where the output of the CORDIC processor is shown in the analog format for the phase accumulator, in-phase data component and quadrature-phase data component outputs of the CORDIC.

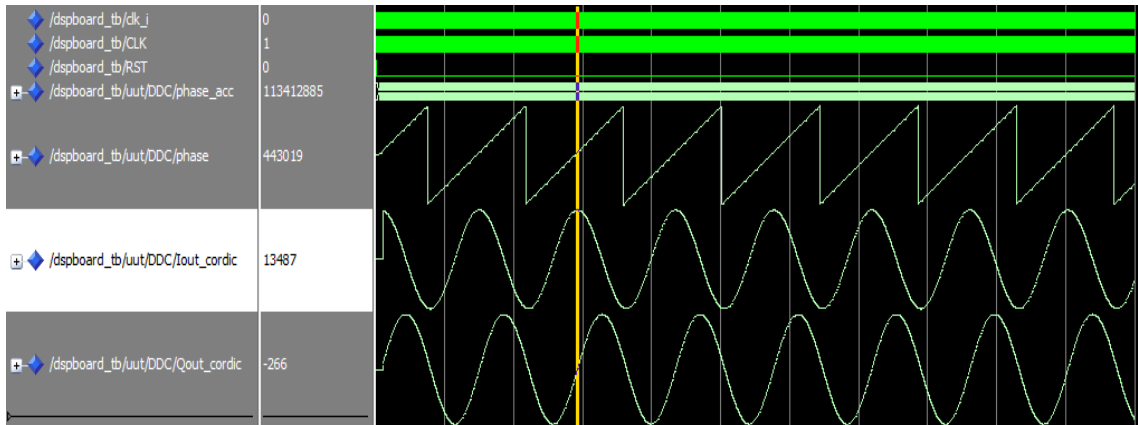


Figure 4-11 Modelsim Simulation of CORDIC

4.2 Cascaded Integrator Comb Filter

When implementing CIC filter decimator at the RTL level, many bit level implementation details need to be considered and are discussed. Both the CORDIC processor and the input data rate to the CIC filter implemented in this thesis must operate at the sampling rate of the incoming signal, while the output rate may be decimated by a factor of between 4 and 127. To design a high throughput CIC filter, the circuit must be implemented in such a way that a high frequency system clock could be used. The highest clock rate at which a combinational logic can be clocked is determined by the maximum delay through combinatorial logic between two adjacent registers.

As we discussed in the previous chapter, the integrator section on the CIC filter is always placed at the higher clock rate when the CIC filters are employed to do decimation or interpolation operations. The clock rate at the integrator section is always higher than the comb section by the factor equivalent to the decimation or interpolation rate. Thus, the integrator section plays a main role in determining the maximum throughput of the whole CIC decimation filter.

To maximize the performance of these CIC filters, a pipelined CIC filter was implemented as shown in the Figure 4-12. In this pipelined filter architecture, the integrator section was implemented as a pipelined structure and the comb section was implemented as a conventional non-pipelined structure [24]. Since, the throughput problem is not as critical in the comb stages of the CIC filter. We can see that in the pipelined CIC filter structure, the integrator stages have no additional pipeline registers. This is an important advantage of the pipelined CIC filter because not only the system

satisfies pipeline structure but also saves power consumption and reduces area on the chip implementation.

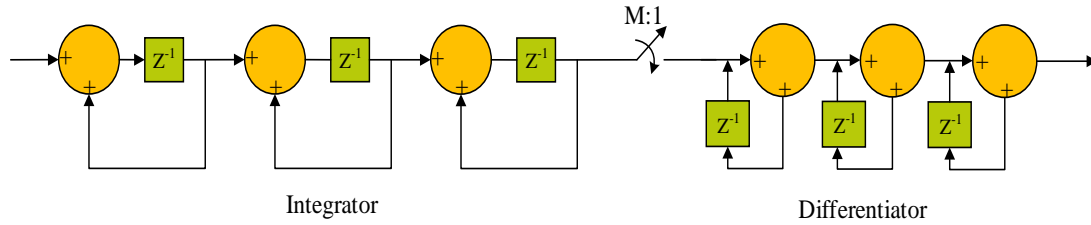


Figure 4-12 3-Stage Pipelined CIC Filter

The register width of all the integrator and comb stages need to be determined to overcome the overflow problem in the integrator section. The maximum register growth is a finite number that can be determined from the sampling rate R and the number of stages used to implement CIC filter. Once these two parameters are determined, we can calculate the worst case bit growth for each individual comb-integrator stages from the equation (60).

The worst case decimate rate that the designed CIC filter can decimate is 127, using this information the worst case bit growth can be calculated as

$$B_{\max} = B_{\text{in}} + \text{CEIL}[\log_2(G_{\max})] \Rightarrow 24 + 3 * \log_2(127) = 44.966 \quad (60)$$

where B_{in} is the bit width of input samples, G_{\max} is the maximum gain of the CIC filter given as $G_{\max} = RM^K$. In this thesis, the bit width of all the registers in the CIC filter was considered as a constant width of 45 bits.

4.2.1 MATLAB Implementation

The accurate MATLAB model of the CIC filter decimator enables functional verification of the designed CIC filter structure. The finite precision MATLAB script

which precisely describes the circuit is designed and incorporated into the model as shown in code below, where the `add_2` function call performs integer addition based on the “bit-width” value provided.

```

for ii = 1:1:nsamples
    x_sign_ext(ii) = sign_ext(int64(x_in(ii)),24,(bitwidth-24));
    integrator(1) = add_2(int64(x_sign_ext(ii)), integrator(1),
bitwidth);
    stage1(ii+1) = integrator(1);
    integrator(2) = add_2(stage1(ii), integrator(2), bitwidth);
    stage2(ii+1) = integrator(2);
    integrator(3) = add_2(stage2(ii), integrator(3), bitwidth);
    stage3(ii+1) = integrator(3);
end

integrator_delay = zeros(1,3); --accounting for the integrator delay
is done here
stage3 = [integrator_delay stage3];

% Down sample the signal this is done in cic_strober.v
sampler = stage3(1:actual_rate:length(stage3));

for jj = 1:1:length(sampler)
    pipeline1(jj) = add_2(sampler(jj), -diff(1), bitwidth);
    diff(1) = sampler(jj);
    pipeline2(jj) = add_2(pipeline1(jj), -diff(2), bitwidth);
    diff(2) = pipeline1(jj);
    pipeline3(jj) = add_2(pipeline2(jj), -diff(3), bitwidth);
    diff(3) = pipeline2(jj);
end

```

All the variables in this implementation have the data type of `int64`. The output of the CORDIC processor is truncated to 24 bits and stored into a file which was used as the input to this CIC filter. These samples are read into the base workspace of the MATLAB and processed in accordance with the CIC algorithm.

Scaling is applied at the output of the CIC to remove the filter processing gain by discarding the lower order bits of the CIC process. We can prune lower order bits early in the filtering chain to the bit position in any stage that cannot grow beyond the least significant bit of the output word [22]. In this thesis, the bits are pruned at the final stage

of the filter. The number of least significant bits discarded/truncated is equal to the gain of the CIC filter decimator. The bit pruning was implemented on MATLAB as shown in the code snippet below.

```
%% Bit pruning CIC decimation filter
shift = round(N*(log2(actual_rate)));
cic_out = bitshift(int64(pipeline3),-shift);
```

The frequency response of the 3-stage CIC filter decimator implemented in this thesis is shown in the Figure 4-13. It can be noted that the attenuation level of the first side lobe is about 39dB and also nulls in the filter are providing wider notch at the multiple of the sampling rate. The droop in the passband is better demonstrated in the lower plot of Figure 4-14.

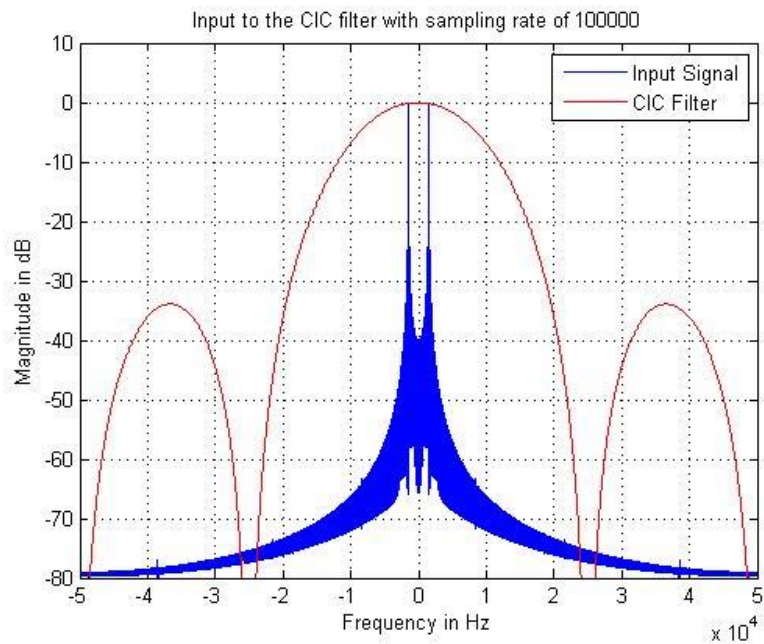


Figure 4-13 Frequency Spectrum of the CIC Filter

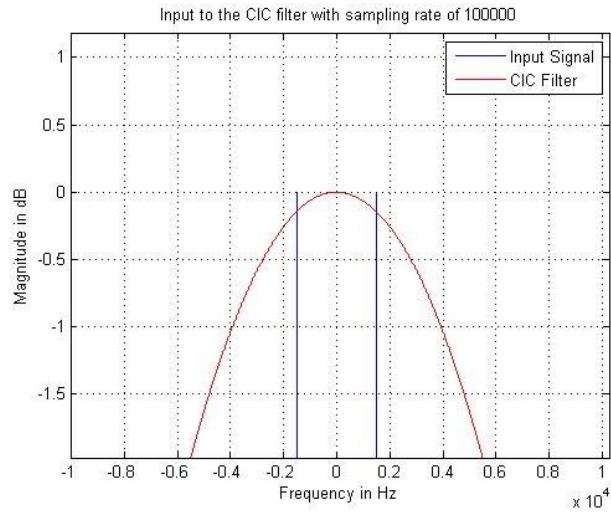


Figure 4-14 Spectral Droop in the Passband

The output of the filter at each intermediate stages is show in the Figure 4-15, the bit growth in the integrator stage is clearly visible as the magnitude of the signal at the integrator section, and the output of the last stage of the differentiator is the output of the CIC filter decimator before the truncation.

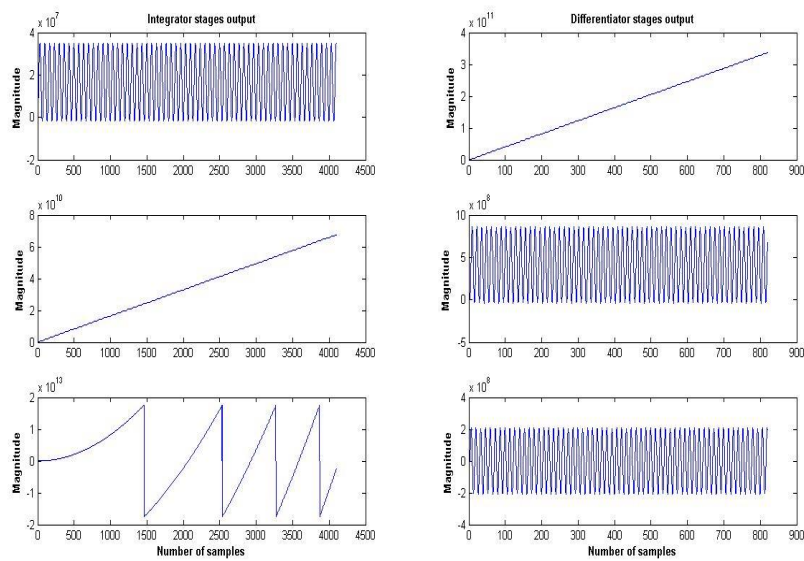


Figure 4-15 Intermediate Outputs of CIC Filter Decimator

The output spectrum of the CIC filter decimator is shown in the Figure 4-16. The comparison between the output of the final stage of the differentiator and truncated samples is also shown in the same figure. It is very clear that the noise introduced by pruning the least significant bits of the filter output is insignificant and almost negligible.

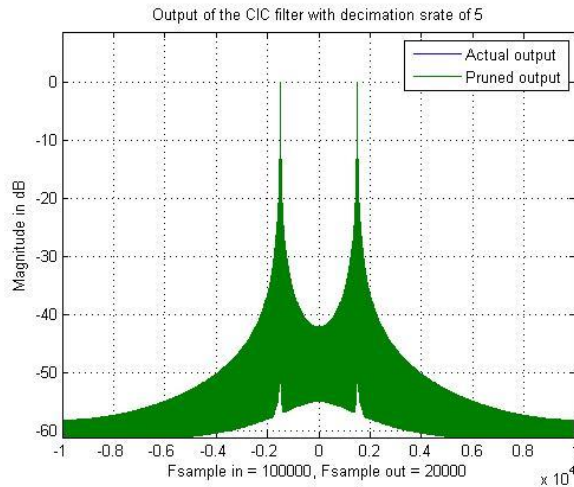


Figure 4-16 3-stage CIC Filter Decimator Output

4.2.2 VHDL Implementation

The pipelined architecture of the CIC filter decimator was implemented in VHDL, the RTL schematic showing the pipeline implementation on the FPGA is shown in the Figure 4-17. The wire connecting the integrator and the register is highlighted to show the pipeline structure at the first stage of the integrator.

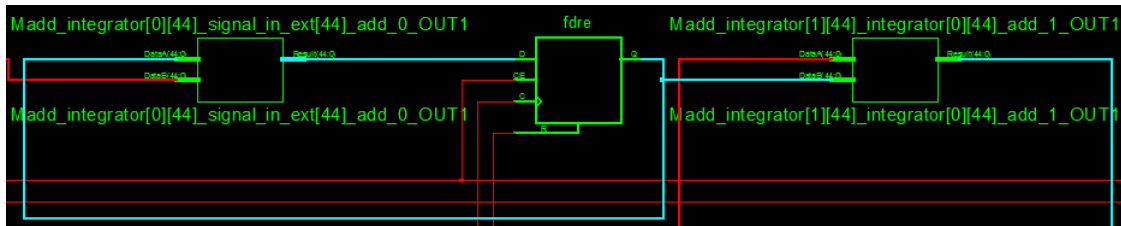


Figure 4-17 RTL Schematic of Pipelined CIC Filter

The resampling switch was implemented as a simple down counter which outputs a pulse of one clock cycle whenever the counter reaches to zero. This strobe enables the differentiator to capture the data from the integrator registers and process the data to compute the output of the CIC filter. The ModelSim simulator is used to verify the functional behavior of the filter as shown in the Figure 4-18.

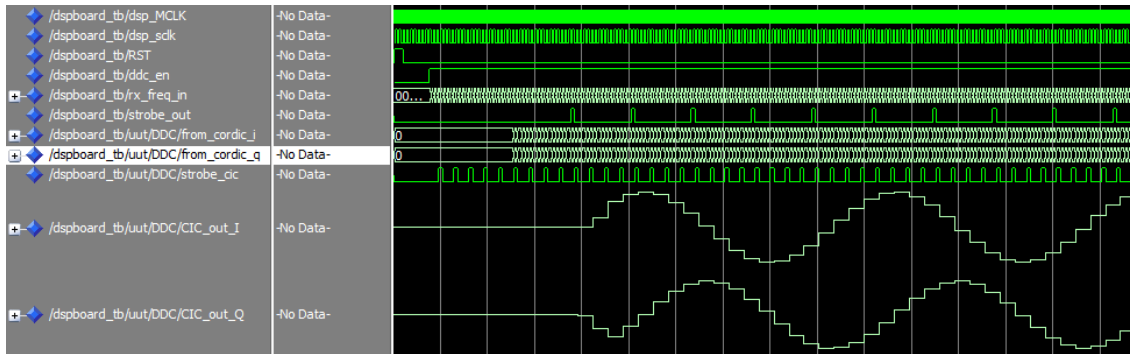


Figure 4-18 CIC Filter Output on ModelSim Simulator

Once the input samples ripples through the integrator and differentiator sections, the 45-bit output from the final stage differentiator is rounded to 24-bit through truncation of the least significant bits. This truncation was hardcoded in the design using an 8-bit 22-to-1 multiplexer as shown in the `cic_decim_prun.vhd` code in the Appendix of this thesis.

A direct mapping of this filter structure was done to a Spartan 6 (xc6slx16-3-csg324) FPGA as shown in `0cic_decim.vhd` results in the following resource utilization shown in the Table 4-4.

Table 4-4 CIC Filter Device Utilization Summary

Device Utilization Summary (estimated values)			
Logic Utilization	Used	Available	Utilization
Number of Slice Registers	482	18224	2%
Number of Slice LUTs	499	9112	5%
Number of fully used LUT-FF pairs	323	658	49%
Number of bonded IOBs	59	232	25%
Number of BUFG/BUFGCTRLs	1	16	6%

4.3 Half-Band Filters

The two half-band filters can be enabled or disabled individually depending on the total system decimation factor. The coefficients for the half-band filters were generated according to [25]. The MATLAB function that implements this algorithm is provided in Appendix A - half-band filter generator MATLAB script. This function accepts a stopband width and the required order of the filter (N), and produces a full set of coefficients of order $4N - 1$. The double precision floating point coefficients generated are then scaled to 17 bit integer values.

The DDC chain implemented in this thesis includes two successive half-band filter decimators. The first stage half-band filter has relatively narrower passband with wider transition band. Hence it requires fewer coefficients. The second stage has relatively larger passband and narrower transition band. Therefore, this filter implementation needs a larger number of coefficients. As a result, if the application needs only requires a single half-band filter to be used, the first half-band filter is always bypassed and only the second one is used.

4.3.1 First Stage Half-Band Filter

The first stage half-band filter has 7 coefficients represented as 18 bit integers, the twos complement representation of these coefficients are shown in the Figure 4-19. As we can see; out of 7 coefficients, 2 of them are zero and the other coefficients are symmetric with respect to the center coefficient.

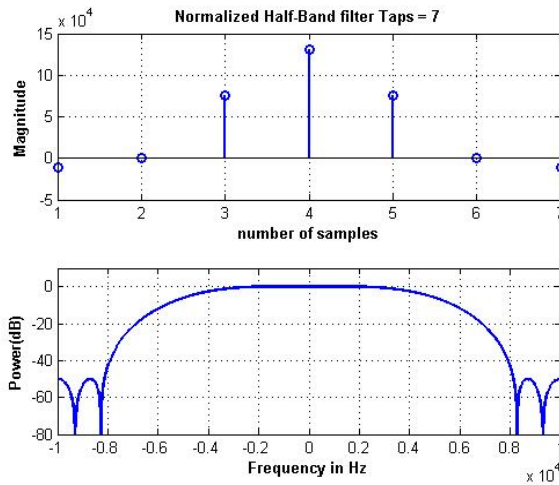


Figure 4-19 7-Tap Half-Band Filter Responses

A direct implementation of this filter would require a multiplier for each nonzero taps. Since, the multipliers are expensive in both hardware and software. This filter was designed much more efficiently with reduced number of required computationally intensive hardware resources by taking into the consideration of the following facts.

1. The half-band filter decimators are implemented at the lower data rate side of the DDC chain and,
2. These filters are configured to decimate the input samples by a factor of 2.

The following part of this section concentrates on the exploiting these two conditions and employing hardware resource sharing. This section also explains how the hardware resources were reused in order to compute the valid output of the filter.

The half-band filter module receives the 24 bit integer samples from the CIC filter decimator and these samples are rounded/truncated to a 17 bit integers. The resulting 17 bit samples are sign extend by 1 bit because the filter structure involves the 2's complement addition of two 17 bit integers. The 18 bit multipliers available on the Spartan 6 FPGA were used to perform the multiplication with the filter coefficients.

4.3.1.1 MATLAB Implementation

The functional block diagram of the first stage half-band filter is shown in the Figure 4-21. This filter was implemented by using 7 shift registers, 2 adders and a multiplier. The exact modeling of this filter was done on MATLAB by taking advantages of arrays as shown in Appendix A - Small (7-Tap) Half Band Filter script.

By visually inspection of the filter structure, many methodologies can be followed to implement this filter on MATLAB. In this work, the filter implementation is divided into three parts.

In the first part the, the outputs of adders and the samples corresponding to the delay element of the center tap were computed as shown in the code snippet below.

```
for n = 1:length(round_in)
    Z = Z*col_sh;
    Z(1) = round_in(n);
    add_1(n) = Z(1)+Z(7);
    add_2(n) = Z(3)+Z(5);
    middle(n) = int32(Z(4)*2);
    m_reg(n) = bitshift(sign_ext(middle(n),18,2),10);
end
```

In the second part, the decimation is employed on the computed samples by only considering every second element in the arrays and the coefficients are multiplied element by element with the summed result as shown in the code below.

```
sum_a = add_1(1:2:length(round_in));
sum_b = add_2(1:2:length(round_in));
middle_reg = [double(m_reg(1:2:length(round_in))) 0];
product_1 = int64(sum_a*(-10690));
product_2 = int64(sum_b*(75808));
product_a = (bitshift(product_1,-(36-accum_W)));
product_b = (bitshift(product_2,-(36-accum_W)));
```

In the final stage, an accumulator was implemented that adds the samples vector from the center tap and product vectors from the multipliers as shown in the code below.

```
% Final accumulator. 30 bit
% NOTE: accum is of double datatype(2^53).
% carefull about the input sizes as accum will overflow
K = 1;
for i = 1:2:nsamples
    accum(i) = middle_reg(K)+product_a(K);
    accum(i+1) = accum(i) + product_b(K);
    K=K+1;
end
```

The fixed-point implementation for adders and multipliers were done using the finite precision wrap-around method. Figure 4-20 shows the input and output spectrum of this half-band filter.

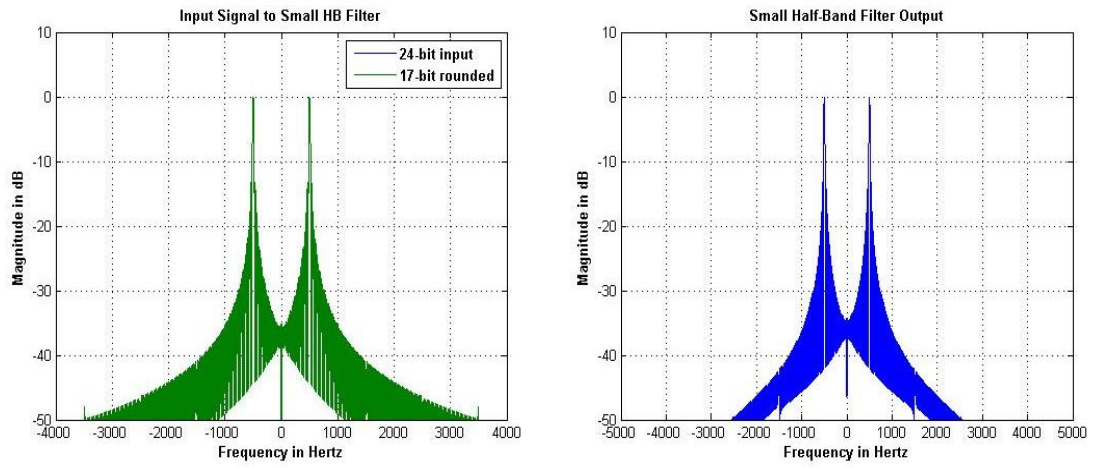


Figure 4-20 Small Half-Band Filter Input and Output Spectrum

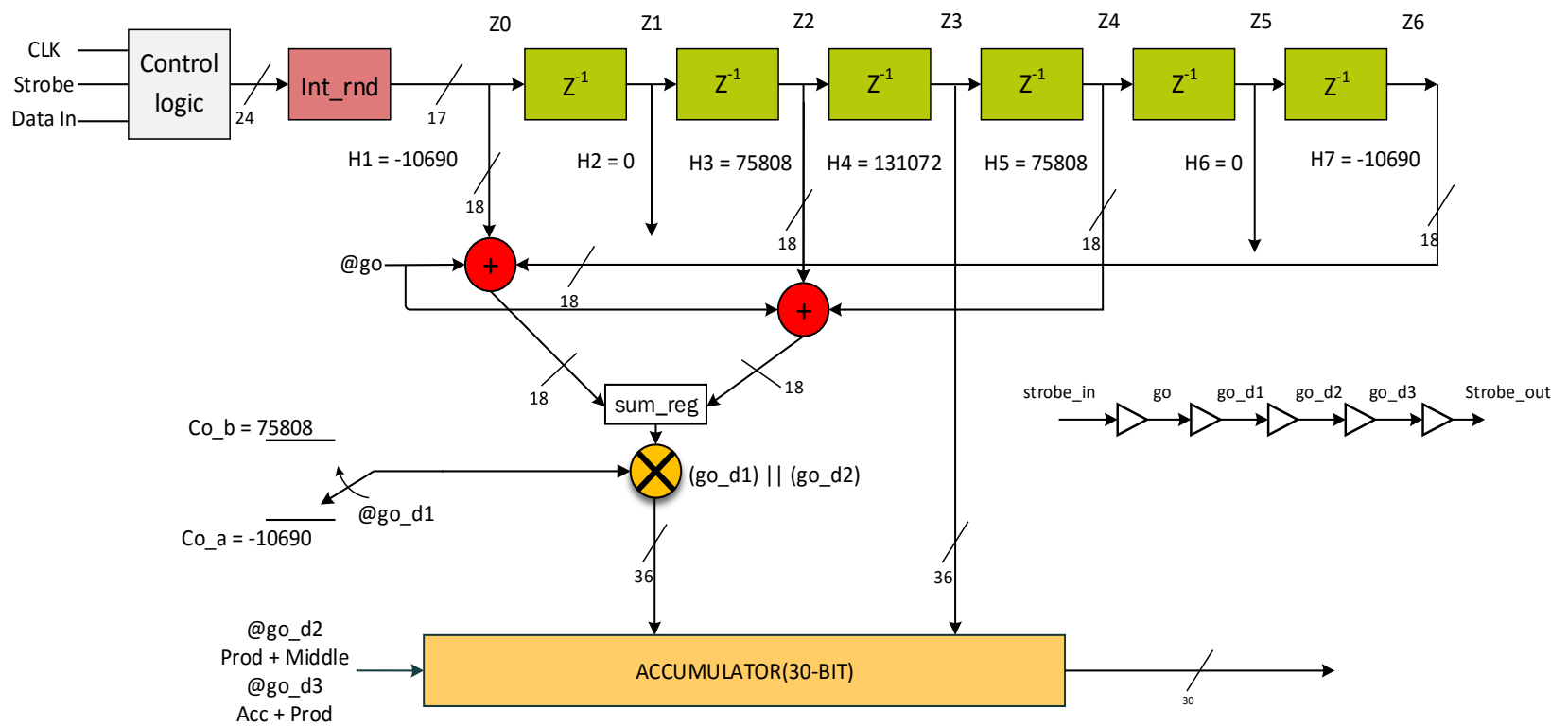


Figure 4-21 Small (7-Tap) Half-Band Filter Circuit Diagram

4.3.1.2 VHDL Implementation

The half-band filter gets the input strobe and the data from the previous stage CIC filter. Since, the filter is intended to decimate the input sample rate by 2, the control logic block in the half-band filter divides this input strobe by 2 in-order to decimate the input as shown in the Figure 4-22. Where, the signal go is $\frac{strobe_{hb}}{2}$ (i.e. capturing every other samples) and the signals $go_{d1}, go_{d2}, go_{d3}, go_{d4}$ are the delayed version of the go signal. These signals are used as the enable signals for adders, multipliers and the accumulator's time window for performing operations.

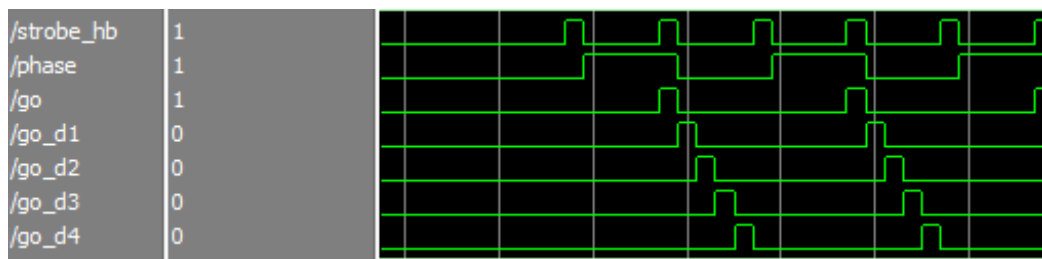


Figure 4-22 Strobe Logic for 7-Tap Half-Band Filter

This filter computes an output as follows:

1. A 17-bit input sample arrives and the data in the shift register shifts one place to the right and discards a sample that had arrived 7-samples ago to accommodate the new sample.
2. On the rising edge of go signal, both the adders are enabled and the samples at shift register corresponding to symmetric coefficients are added together.
3. This addition operation takes one clock cycle to compute an output.

Therefore, on the rising-edge of go_{d1} , the output from $adder_a$ is multiplied

with $coef f_a$ and on the next clock cycle corresponding to go_{d2} , the output from $adder_b$ is multiplied with $coef f_b$. This way, the 18x18 multiplier on the FPGA was reused to compute the product on two consecutive clock cycles.

4. The accumulator is enabled as soon as the multiplier computes its first product after one clock cycle. While the multiplier is still computing the second product, the accumulator starts accumulating the first product and the data from the shift register corresponding to the center tap.
5. Finally, when the multiplier finishes computing the second product (i.e., on the next clock cycle at go_{d3}), the previously computed sum in the accumulator is again added with the second product (product of $adder_b$ and $coefficient_b$).
6. On the next clock cycle i.e., on go_{d4} , the output of the filter is computed and go_{d4} is the strobe out of this 7-Tap filter.

In this filter structure, a 30-bit accumulator was used. This means that the 36-bit output from the multiplier is truncated to 30-bits before being supplied to the accumulator. At the output stage, the 30-bit accumulator output is rounded/truncated to a 24-bit output.

A straight forward mapping of this structure was done onto the Xilinx Spartan 6 (xc6slx16-3csg324) FPGA where all the filter coefficients, taped delay lines were implemented on Configurable Logic Blocks (CLB) slice register as shown in `0small_hb_top.vhd`. The resulting FPGA resource utilization is shown in Table 4-5. It is important to notice that the multiply and accumulated unit of the filter was synthesized as

a DSP48A1s slice which are available on Xilinx devices for computationally intensive DSP applications.

Table 4-5 Small (7-Tap) Half-Band Device Utilization Summary

Device Utilization Summary (estimated values)			
Logic Utilization	Used	Available	Utilization
Number of Slice Registers	430	18224	2%
Number of Slice LUTs	296	9112	3%
Number of fully used LUT-FF pairs	107	619	17%
Number of bonded IOBs	54	232	23%
Number of BUFG/BUFGCTRLs	1	16	6%
Number of DSP48A1s	1	32	3%

4.3.2 Second Stage Half-Band Filter

The second stage half-band filter has higher attenuation level, narrower passband, and steeper transition band when compared to the first stage filter as shown in Figure 4-23. The coefficients for this half-band filter were generated using the same algorithm described in the previous section.

This filter was implemented as a 2 path polyphase filter structure where one component corresponds to all the even coefficients and the other corresponds to all the odd coefficients as shown in the Figure 4-24. The even component has all zero coefficients with just one nonzero center tap which is equal to 1.0. Thus, we just need to add the corresponding delay line value to the output of the filter.

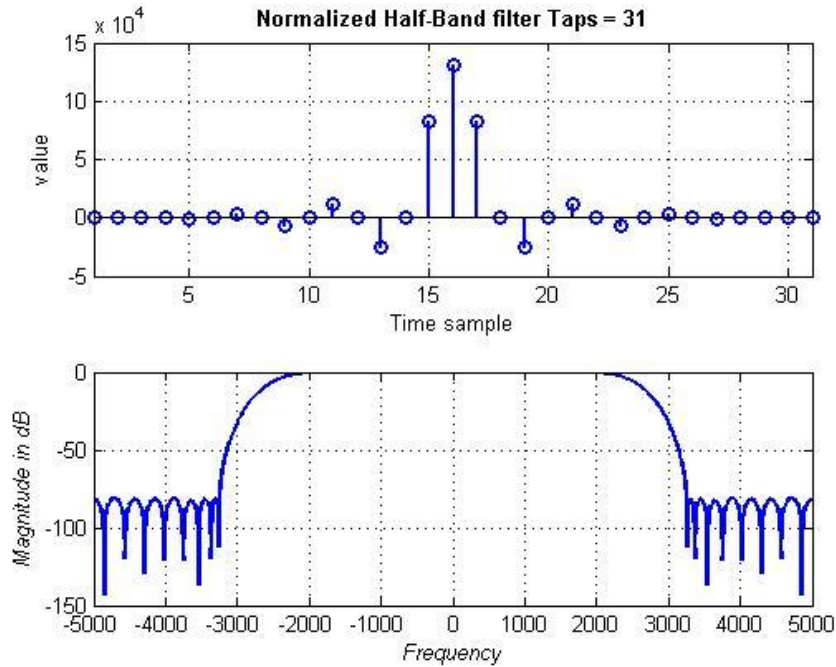


Figure 4-23 31-Tap Half-Band Filter Response

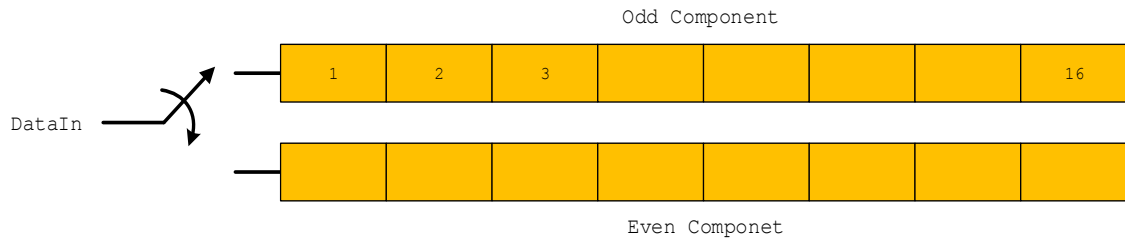


Figure 4-24 2-Path Polyphase Filter Structure Decomposition

Apart from the center coefficient, there are 8 nonzero coefficients on either side, which are in the second component of the polyphase filter. A naive implementation would require a multiplier for each nonzero taps. Because of the symmetry, we can replace 2 multiplies with 1 add and 1 multiply. Thus, to compute each output sample, we need to perform only 8 multiplications since middle coefficient is 1.0.

The filter was implemented using only two multipliers, but it needs minimum of 4 clock cycles to compute a single output. Therefore, this filter implementation can only accept a new data sample every 4 clock cycles. However, we know that this filter is intended to decimate the input samples by 2. Hence, this filter can accept new data sample every two clock cycles. Due to this implementation, the combination of the CIC filter and the first stage half-band filter has to decimate the input sample rate signal at least by a factor of 2. The 31-tap half-band filter structure implemented in this thesis is show in the Figure 4-25.

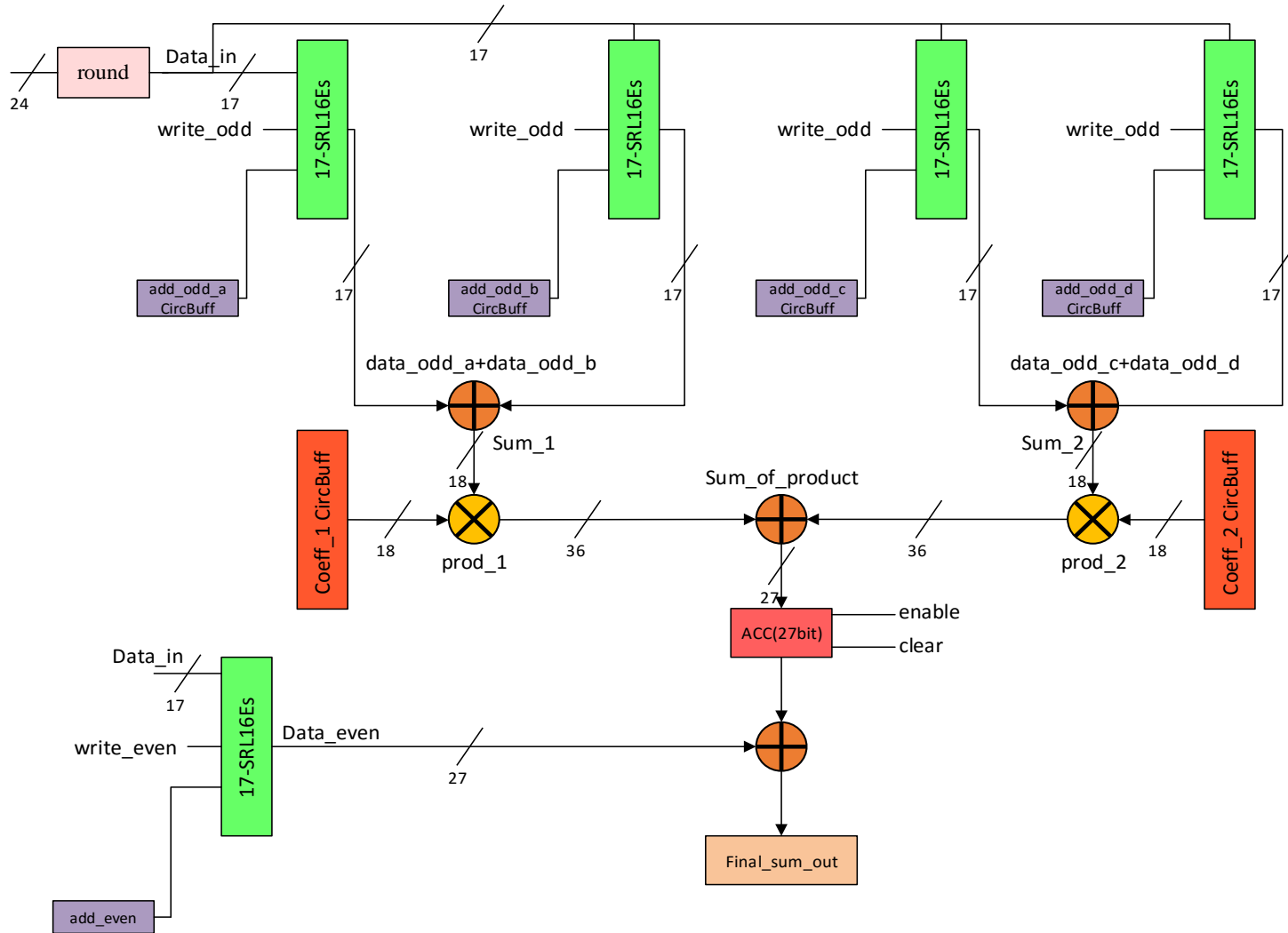


Figure 4-25 Large (31-Tap) Half-Band Filter Circuit Diagram

4.3.2.1 MATLAB Implementation

An exact model of this filter was implemented on MATLAB using a 2 path polyphase structure constructed as a 2x16 matrix as shown in the Figure 4-24, the shift to the left operation was efficiently implemented using the matrix multiplication with the 16x16 upper diagonal matrix. The input samples were rounded/truncated to 17 bit samples and these samples were shifted through the polyphase structure using the commutator. The commutator was implemented as an index generator which generates the corresponding even and odd indices. The MATLAB polyphase structure implementation is shown in the code below.

```
Z = Z*Zshift;  
Tindex = 1+((ii-1)*lambda:ii*lambda-1);  
Z(:,1) = (round in(Tindex))';
```

where, Z is the 2x16 polyphase structure, Zshift is the 16x16 upper diagonal matrix and Tindex is the index generator. Here lambda is equal to 2 since this is a 2 path polyphase structure. Once the indexes are generated, the data corresponding to the indexes are placed in the first column of the Z matrix.

The 8 symmetric coefficients were divided into 2 sets, each consisting of 4 coefficients emulating the coefficients circular buffer as shown in the code below

```
coeff1 = [ -107  445  -1271  2959];  
coeff2 = [-6107 11953 -24706 82359];
```

The sum of the input samples corresponding to the delay line value was computed first and then multiplied with the coefficient vectors. This results in two vectors of 1x4, these two vectors were added to form a sum of product vector and all the elements in the sum

of product vector were summed together to form a partial result in the accumulator. Finally, the sample corresponding to the delay line of the center tap was added to the partial accumulator result to form the final output of the filter. The iterative implementation of this filter is shown in the code below.

```

for ii = 1:1:numblocks
Z = Z*Zshift;
Tindex = ((1+((ii-1)*lambda:ii*lambda-1)))';
Z(:,1) = (round_in(Tindex))';
sum1 = [Z(1,1)+Z(1,16) Z(1,2)+Z(1,15) Z(1,3)+Z(1,14) Z(1,4)+Z(1,13)];
sum2 = [Z(1,5)+Z(1,12) Z(1,6)+Z(1,11) Z(1,7)+Z(1,10) Z(1,8)+Z(1,9)];
prod1 = sum1 .* coeff1; % 36 bit product
prod2 = sum2 .* coeff2;
sum_of_prod = int64(prod1+prod2); % 36 bit
round_sum = bitshift(sum_of_prod,-11); % round to 25 bit number for
accumulator
% actual place for middle is Z(2,8) but due to indexing it is Z(2,9)
middle = bitshift(int32(Z(2,9)),6);%
accum(ii) = sum(round_sum);
final_sum(ii,:) = accum(ii)+ middle; %27 bit accumulator
end

```

The finite precision integer arithmetic operations described in the Figure 4-25 was exactly followed in the MATLAB implementation as shown in the Appendix A - Large (31-Tap) Half Band Filter script.

The bit width of the intermediate results must be carefully accounted in order to avoid the overflow of the two's complement number system. Although the double datatype in MATLAB can represent values up to 2^{53} the integer representation was followed in the filter structure for the sake of convenience.

This half-band filter implementation methodology can be easily verified by using the MATLAB simulations. The input vector and decimated output vector after processing by the filter is shown in the Figure 4-26. We can also observe the filter operation by the

looking at the frequency spectrum at the input and output of the filter as shown in the Figure 4-27.

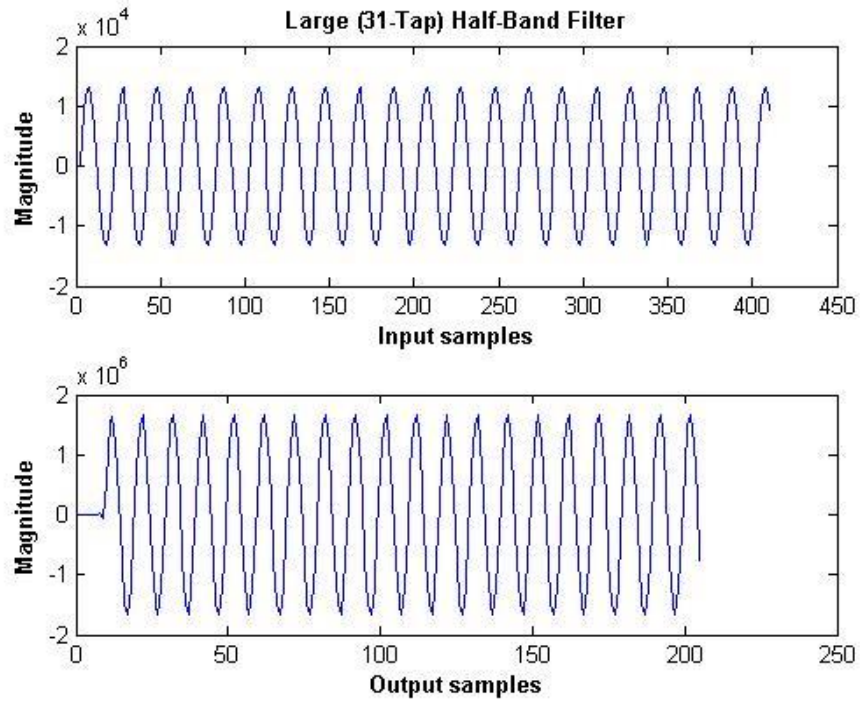


Figure 4-26 Large Half-Band Filter Input and Output Vectors

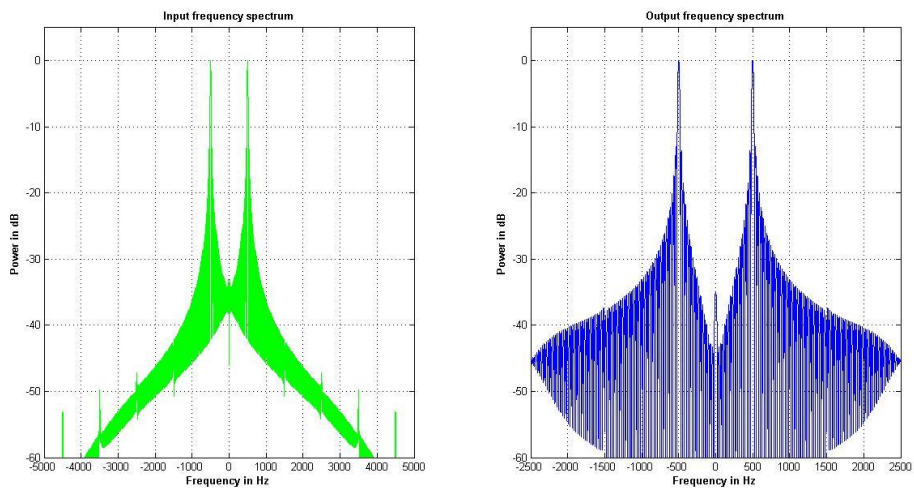


Figure 4-27 Large Half-Band Filter Input and Output Spectrum

4.3.2.2 VHDL Implementation

The final stage half-band filter can get the input samples either from the CIC filter or from the previous stage half-band filter if it is enabled in the signal processing chain. As mentioned before, this filter needs 4 clock cycles to compute one single output sample, which means that this filter can only accept a new value every 4 clock cycles. However, since we're decimating by two we can accept a new input value every 2 cycles. In other words, if the DDC chain is operating at the full clock rate, then the overall decimation rate before the final stage half-band filter must be at least 2 in-order to make sure that this filter has 4 clock cycles. The `strobe_in` is asserted when there's a new input sample available. Depending on the overall decimation rate, `strobe_in` may be asserted less frequently than once every 2 clock cycles. On the output side, we assert `strobe_out` when the output contains a new sample.

In the 2 path polyphase filter structure suggested, only the odd component which has nonzero coefficients needs to be implemented, since the even component only has zeros except the center tap which is equal to 1. This saves resources on the FPGA and achieves the same results as that of a conventional FIR filter with a fewer number of gates. In this thesis, the odd component shown in the Figure 4-24 was implemented as shown in the Figure 4-25. The filter has 4 circular buffers used to generate the address of the delay line corresponding to the nonzero coefficients and 2 circular buffers for holding 8 symmetric coefficients.

The delay line was implemented using four sets of 17 SRL16E shift registers [26]. The arrangement of SRL16Es in each set can be thought as a 17-bit shift registers of length 16 as shown in Figure 4-28 below.

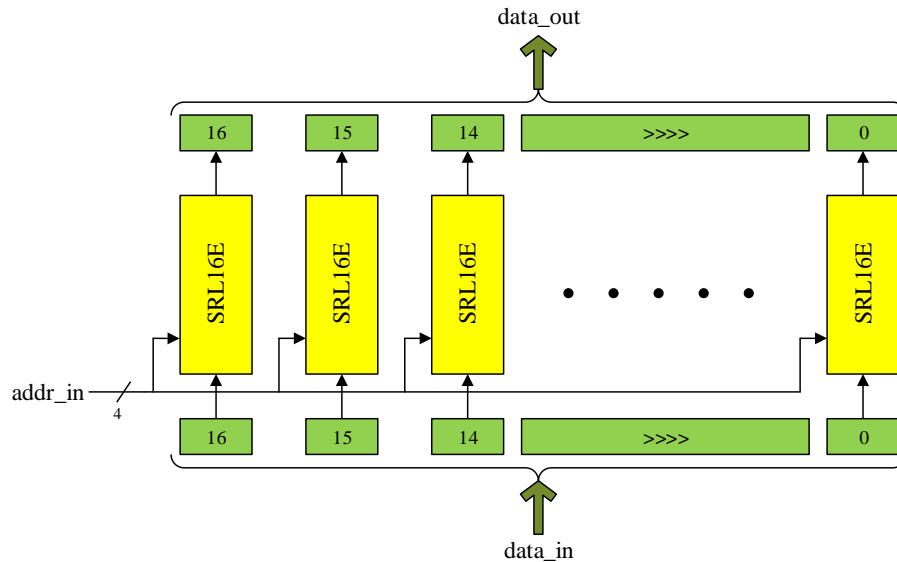


Figure 4-28 17-bit Shift-Register of length 16 using SRL16Es

The Spartan generation FPGAs can configure the Look-Up Tables (LUT) of each slice (SLICEM) as a 16-bit shift register without using the flip-flops available. The Shift-in operations are synchronous with the clock, and shift register length can be dynamically selectable using the length specified externally to this shift register. The use of SRL16E can improve performance and rapidly lead to cost saving of an order of magnitude. Although, SRL16 shift-registers are automatically inferred by the Xilinx Synthesis Tool (XST), the use of primitive instantiation was explicitly specified in this thesis.

The half-band filter module has a counter that counts from 1 to 4 on every alternate input strobe. Depending on the count value, a sequence of output length of shift

register corresponding to the symmetric coefficients are placed on the four select lines (addr_in) of these shift register elements as shown in the Table 4-6.

Table 4-6 Values on the Select Line of SRL16Es

clock	counter	shift_reg-1	shigt_reg-2	shift_reg-3	shift_Reg-4
1	1	0	F	4	B
2	2	1	E	5	A
3	3	2	D	6	9
4	4	3	C	7	8

The 24 bit input samples are truncated to 17 bits at the input stage and loaded to all four shift registers blocks in parallel. The 17-bit output of the shift-registers were again sign extended to 18-bits and added with the delayed samples from other shift-registers. Since this addition takes one clock cycle, the output of the coefficient circular buffer was delayed by one clock cycle to synchronize with the output of the adders, and then multiplied using dedicated 18x18 multipliers. The 36-bit products from two multipliers were further added together using a 36-bit adder to form a sum of product term as described in the filter structure. Until this point, it takes 3 clock cycles for the input samples to ripple through the adders and multipliers and appear at the output of sum of product adder. Hence, on the 3rd clock cycle the accumulator will be cleared and enabled on the 4th clock cycle. For the next 4 consecutive clock cycles, all the adders and multipliers work in parallel to compute the partial filter outputs and the accumulator will be accumulating the sum of products. At the end of the 7th clock cycle the accumulator is disabled and the sample corresponding to the center coefficient delay line value is added on the 8^h clock cycle. Hence at the end of 8th clock cycle the filter outputs its processed

output sample. The timing diagram illustrating the filter operation is shown in the Figure 4-29. The clock_tab signal shows the number of clock cycles elapsed starting from the strobe input.

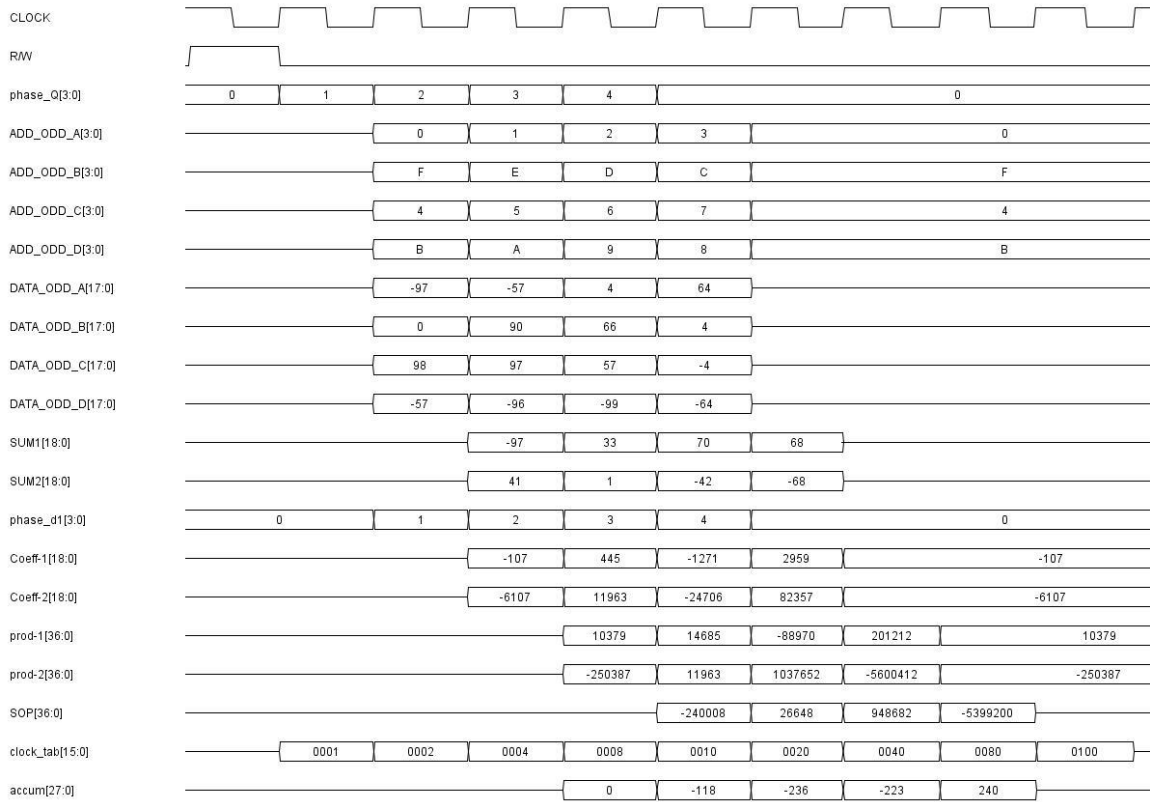


Figure 4-29 Timing analysis of large half-band filter structure

This filter uses a 27-bit accumulator to maintain the extra bits of precision. The final output is truncated to 24-bits. A straight forward mapping of this structure was done onto the Xilinx Spartan 6 (xc6slx16-3csg324) FPGA where all the filter coefficients and the taped delay lines are Configurable Logic Blocks (CLB) slice register based as shown in the 0large_hb_top.vhd. The following resource utilization was observed as shown in the Table 4-7. Notice that the Xilinx Synthesis Tool (XST) has synthesized 2-DSP48A1 slices for implementing the multiply and accumulate unit of this filter.

Table 4-7 Large (31-Tap) Half-Band Device Utilization Summary

Device Utilization Summary (estimated values)			
Logic Utilization	Used	Available	Utilization
Number of Slice Registers	264	18224	1%
Number of Slice LUTs	365	9112	4%
Number of fully used LUT-FF pairs	130	499	26%
Number of bonded IOBs	62	232	26%
Number of BUFG/BUFGCTRLs	1	16	6%
Number of DSP48A1s	2	32	6%

The half-band filters can be enabled or disabled using a control register that can be implemented on FPGA and programmed through an embedded softcore processor in the future. Although, the enable and bypass signals were included in the entity of this half-band filters, these signals are hardcoded and have to be manually changed in the FPGA bitstream.

4.4 DDC Chain Gain Adjustment

There is implicit gain distributed throughout the signal processing chain to give the highest performance from the DDC under worst case signaling. Algorithmic gains anticipated from the signal processing performed is partially incorporated in the CIC and CORDIC processors in order to maximize the dynamic range available in the DDC, but a gain adjustment is applied after the DDC processing elements.

The gain adjustment used in this thesis is given by the equation (61). Where, the numerator is the magnitude of the additional bit growth in CIC filter stage, the term

$GAIN_{CIC}$ is the gain of the CIC filter given as $G_{max} = RM^K$ and $GAIN_{CORDIC}$ is the gain of the 20 stage CORDIC processor which is a constant equal to 1.65.

$$GAIN_{final} = 2^{\left(\frac{CEIL(\log_2(GAIN_{CIC}))}{GAIN_{CORDIC} * GAIN_{CIC}}\right)} \quad (61)$$

This gain was hardcoded and multiplied using the 18x18 multipliers available on the FPGA and the output of the multiplier was truncated to a 16-bit sample. Finally, a 32 bit word was constructed as a concatenation of two 16 bit samples from the in-phase and quadrature-phase components of the DDC chain. Where, 16 most significant bits are in-phase sample and 16 least significant bits are quadrature-phase sample. The DDC chain designed in this thesis can also be used as real mode processor by supplying only zeros to the quadrature-phase component.

4.5 Xilinx Clocking and Clock Distribution

The communication signal processor requires two input clocks; dsp_sclk (SCLK) and dsp_mclk (MCLK). The dsp_sclk is used as the main clock for all the signal processing elements and the dsp_mclk is used for the de-interleave circuit at the input stage of the communication signal processor board.

Both the clock inputs are driven from external source and do not use the on board clocking resources. They are specifically routed to the global clock input pads (GCLK15 and GCLK17) through the VHDCI connector (EXP_IO9_P and EXP_IO10_P). The use of global clock within the FPGA is a recommended way of providing low-skew clock routing to the logic resources within the FPGA.

The Spartan 6 FPGA clock network consists of 4 types of connections [27]:

1. Global clock input pad (GCLK)
2. Global clock multiplexers (BUFG, BUFGMUX)
3. I/O clock buffers (BUFIO2, BUFPLL, BUFIO2_2CLK)
4. Horizontal clock routing buffers (BUFH)

The clock coming through the global input pads, is first routed through an input buffer (IBUF33) and then to the BUFGMUX located in the center of the device. The BUFGMUXEs can be driven by different sources; clock inputs from the 4 different IO banks, clocks from the FPGA logic interconnect and the PLL/DCM. Then the BUFGMUXEs drive a vertical spine which in turn drives the horizontal row clocks (HCLK). The HCLK consists of horizontal clock buffers that provide clock access to all the logic elements and primitives in the FPGA.

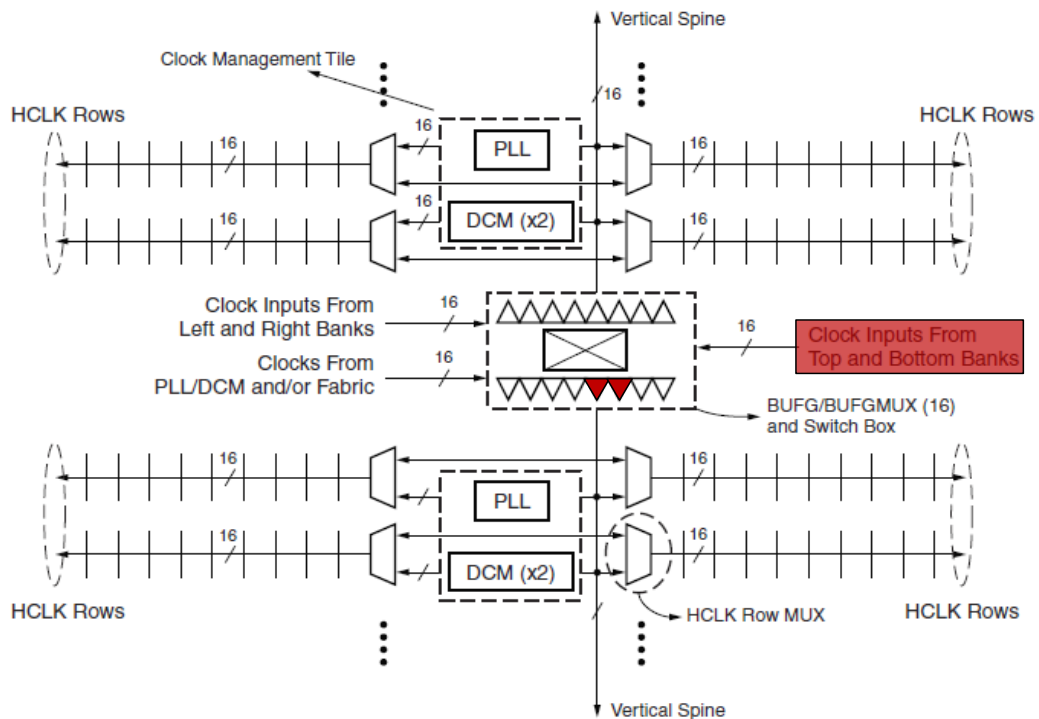


Figure 4-30 Spartan 6 Clock Distribution [27]

Figure 4-30 shows the communication signal processor's global clocking structure using two BUFGMUXes highlighted in red. The inputs to these BUFGMUXes comes from the global clock pads located at the FPGA I/O BANK 0. In this way, the dsp_mclk and dsp_sclk clocks are routed to all the individual elements in the design.

Chapter 5

FPGA BASED DIGITAL PATTERN GENERATOR

The Digilent Nexys 3 development board provided an excellent host for development and demonstration of the DDC signal processing chain for communications, but a means to both source and sink parallel test data to validate correct operation was desired. Assessing the resources and interfaces available on the Nexys 3, it was recognized that a second, identical development board with a different configuration could perform the task and potentially provide a useful resource for future FPGA developments within the WMU ECE Department. Therefore, the objective of this section is to design and develop a flexible FPGA based digital pattern generator and comparator on a Digilent Nexys 3 development board that could be used to source clock synchronized parallel test signals and analyze the synchronously transferred parallel results from any device that is connected.

To successfully accomplish this task, first an architectural design based on the resource available on the Nexys 3 was defined and a parallel interface that could both source clock and data and receive clock and data identified. The Nexys 3, previously described, has the following resources useful for this design: Spartan 6 FPGA, 16MB of Cellular RAM (CRAM) from Micron (Micron part number M45W8MW16), and a high speed 68-pin VHDC connector. The CRAM provides a large memory to hold test data that can be used to both source output patterns and provide reference result to compare to data received. The VHDC connector can be connected to another Nexys 3 using a

commercially available cable. Meanwhile, the Spartan 6 FPGA inherently interfaces to both the CRAM and VHDC interface and has sufficient programmable elements to perform the logical functions required of a pattern generator and result comparator. The following sections describe the test board architecture and the critical interface to a second board for testing.

5.1 Architecture of Digital Pattern Generator

The basic functionality of this board is divided into two parts; first, pattern generator and second, output comparator. The pattern generator section uses a softcore processor operating at 50 MHz to read the predefined data samples stored in the Cellular RAM and provides a periodic 16-bit parallel integer samples using a FIFO at the output stage. The output comparator section receives the processed results through a FIFO at the input stage and the softcore processor reads those results and compares it with precomputed results stored in the Cellular RAM. The 50 MHz clock was generated using a Digital Clock Manager (DCM) on the Spartan 6 FPGA. The functional block diagram of the digital pattern generator and output comparator is shown in the Figure 5-1.

The operating principle of the pattern generator is divided into two aspects; hardware and software that will be described after first considering the data interface.

5.2 Digital Pattern Generator Interface

In order to send and receive the 16-bits of data in parallel, the high speed 68-pin VHDC connector available on Digilent Nexys 3 development board was used as shown in the Figure 5-2.

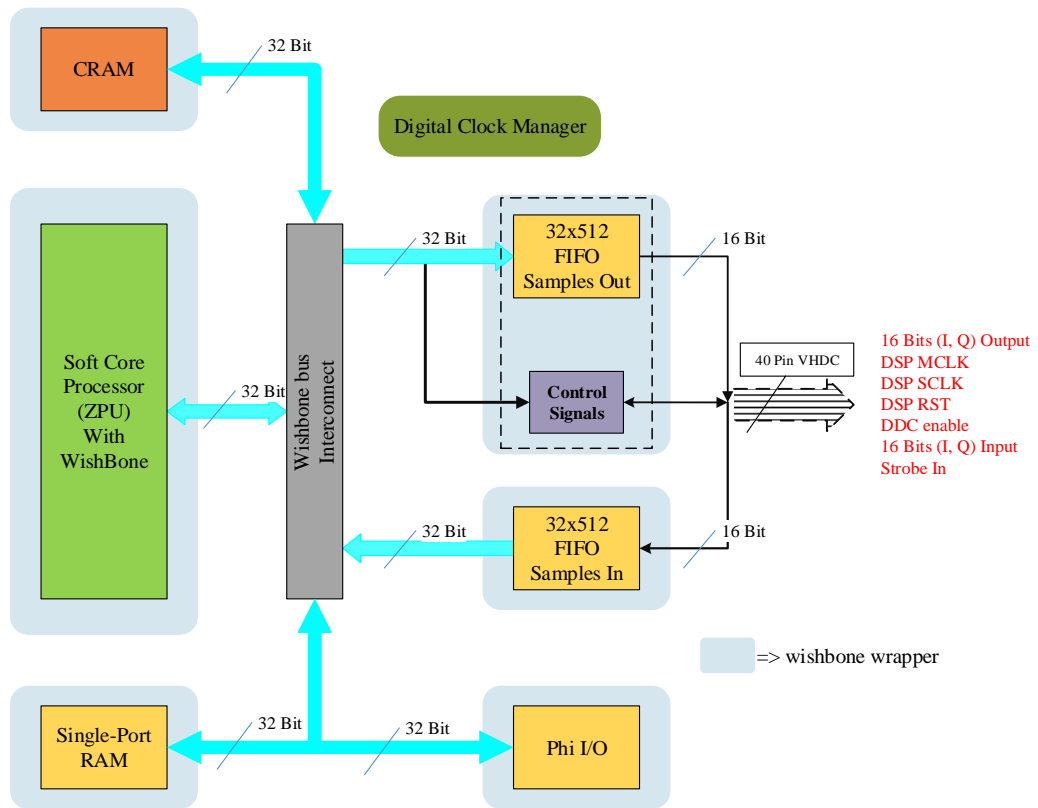


Figure 5-1 Nexys 3 Digital Pattern Generator and Output Comparator

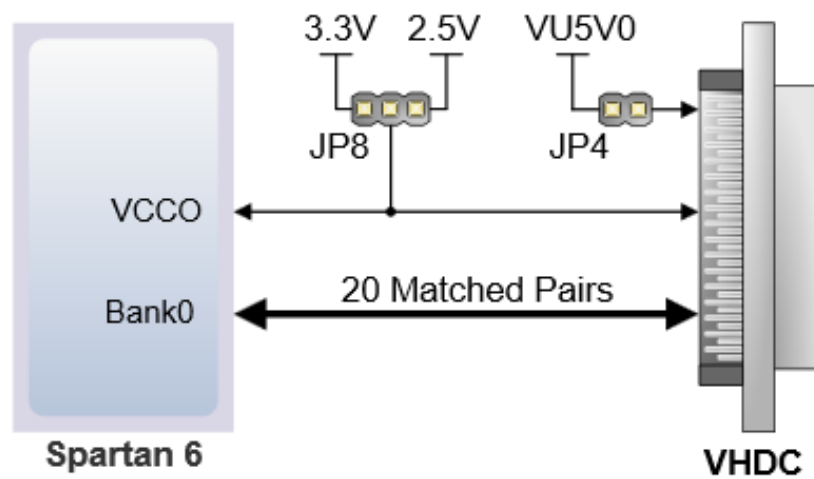


Figure 5-2 Digilent Nexys 3 VHDC Connector [28]

The VHDC connector has 40 data lines which can be routed as 20 impedance- controlled matched pairs or as 40 individual connections, 20 ground lines and 8 power signals. This connector is normally used for Small Computer System Interface (SCSI) 3 applications and each data line supports up to several hundred MHz data rates. The FPGA pins that are connected to the VHDC connector are located at I/O bank 0. The four Vcc pins from the VHDC connector are connected to FPGA I/O bank 0 power supply pins. Although, the VHDC connector are routed as matched pairs to support Low-Voltage Differential Signaling (LVDS), these differential data lines were used as an individual data line to send and receive data simultaneously.

The communication signal processing board is capable of receiving two synchronous system clocks; master clock (MCLK) and dsp clock (SCLK). The master clock should be operating at a rate twice the rate of the dsp clock. The board receives 16-bit data samples in synchronous to the master clock and sends 16-bit processed data samples in synchronous to SCLK. The design also supports a logical high reset and a logical high enable signals which could be used to reset or enable the signal processing chain. The communication signal processing board sends out an enable signal as a reference to the availability of new processed sample. Figure 5-3 shows these interfacing signals.

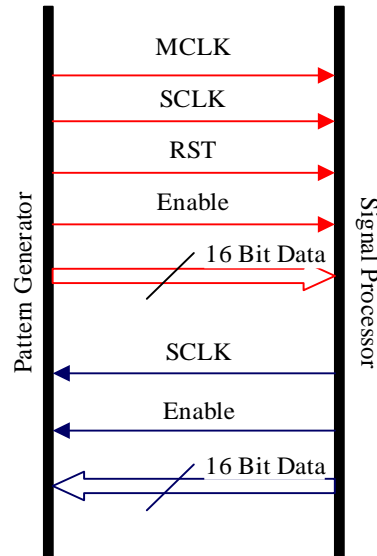


Figure 5-3 Interfacing with Communication Signal Processor

The operating principle of the pattern generator is divided into aspects; hardware and software.

5.2.1 Hardware Aspects

The critical hardware components shown functionally in Figure 5-3 include, a softcore CPU, a Wishbone based peripheral interface bus, a single-port RAM for code and variables, the external CRAM data memory, parallel I/O interface for board resources, and both send and receive FIFOs to source clocked parallel outputs and receive clock enabled parallel inputs. The following sections describe each of these elements.

5.2.1.1 Wishbone - Zylind Processing Unit

The pattern generator board design is based on an embedded softcore processor in order to aid in command, control and transfer of data inside the FPGA. Many FPGA vendors provide their own softcore processor solutions that could be implemented as an

Intellectual Property (IP) in the design. But, the use of an open-source processor was preferred in this thesis so that it can be used without any issues that may arise from copyright laws. One architecture that satisfies all the target features and also compact in size is the Zynlin Processing Unit (ZPU) contributed by Salvador E. Tropea [29]. The ZPU is a 32-bit stack based Reduced Instruction Set Computing (RISC) processor and has a very minimal number of instructions. As a stack-based processor, all the operands for the instruction set are located on a memory stack except for load and store instructions [30]. The most important strength of this architecture is that, it has a simple, easy to read HDL design and is very easy to implement from scratch in-order to suit the specialized application and optimization [29]. This thesis uses the original source files was directly downloaded from [29]. The downloaded package consists of a Zealot version of ZPU processor along with the BRAM, a small peripheral input/output (Phi I/O) core which implements a 64 bit timer, a Universal Asynchronous Receive and Transmit (UART) module and a seven segment display unit.

The architecture suggested in Figure 5-1 has a wishbone interconnect network, a BSD license based project from opencores.org, along with the ZPU core (also called a wishbone-ZPU). This wishbone network was setup as a slave/master architecture such that any number of slaves can be added on this network with very minimal design modifications and define an address space that could be accessed using the ZPU. In this network the ZPU was configured as wishbone master and a small peripheral input/output unit, a single port Random Access Memory (RAM), a Cellular RAM (CRAM) and two FIFOs were configured as the wishbone slaves.

The ZPU does not have any memory map defined in it. However, the software for the ZPU can be written using the memory map that could be defined in wishbone interconnect network as shown in the Table 5-1. The ZPU has 32 bit address space out of which, the 25 down to 2 bits are mapped to the memory map of the wishbone interconnect. The combinational logic designed in the wishbone interconnect uses the most significant 25-to-15 bits to select the individual slaves. The least significant 2nd, 3rd and 4th bits to select specific register locations within the memory space of the selected slaves (other than CRAM and single port RAM) as shown in the Figure 5-4. Therefore, addresses 000000-7FFFFFF are used to address slaves and specific memories in the slaves. Whereas, for the CRAM and signal port RAM, the entire memory space is mapped to that of the ZPU. So, any memory location in the CRAM or the single port RAM can be accessed contiguously by the ZPU starting from 0x00000000 for single port RAM and 0x01000000 for CRAM.

Table 5-1 Wishbone Slaves Memory Map

Slave	Register type	Address
SinglePortRAM	ZPU Memory	0x00000000
CRAM	Data	0x01000000
Phi I/O	GPIO Data	0x080A0004
Phi I/O	GPIO Dir	0x080A0008
Phi I/O	UART_TX	0x080A000C
Phi I/O	UART_RX	0x080A0010
Phi I/O	Counter_1	0x080A0014
Phi I/O	Counter_2	0x080A0018
Phi I/O	Segment_7	0x080A001C
Output FIFO	Status	0x080B0004
Output FIFO	Data	0x080B0008
Input FIFO	Status	0x080C0004
Input FIFO	Data	0x080C0008

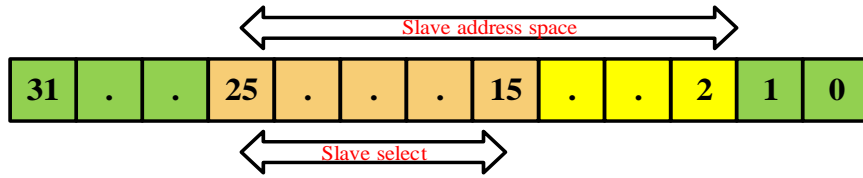


Figure 5-4 Wishbone-ZPU Address Space

When the ZPU software tries to communicate with the slaves, the ZPU places corresponding slave address and data on its address bus and data bus. The communication between ZPU and slaves is shown in Figure 5-5. This communication can be described as follows.

1. All of the communication with the slaves goes through wishbone interconnect, the wishbone interconnect decodes the addresses from the address bus and enables the slave select signal of the corresponding slave.
2. Wishbone interconnect further transfers the wishbone signals like strobe, cycle, write, address and data-out generated from the ZPU to the selected slave.
3. The slave decodes these wishbone signals and performs the required operation such as writing and reading on a specified memory location.
4. The slaves are responsible to generate an acknowledge signal and send it back to wishbone interconnect along with the data if requested by the ZPU.
5. Upon receiving this acknowledgement signal, the ZPU disables all the wishbone signals and continues executing the next instruction.

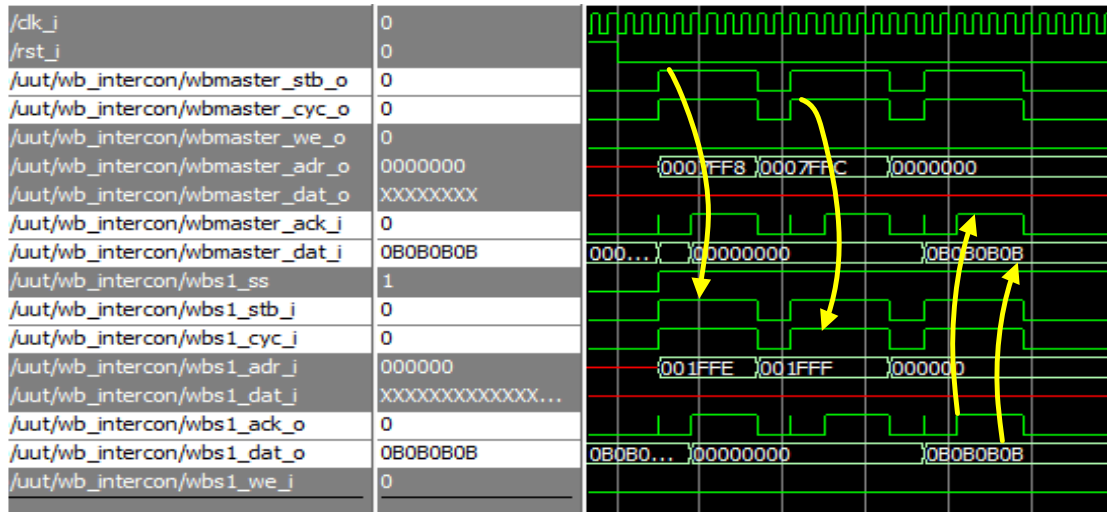


Figure 5-5 ZPU-Slave Communication

5.2.1.2 Cellular RAM

CRAM used in this design has 16-bit wide memory with 8M address spaces and can support both 8 bit and 16 bit data access. Since the ZPU supports 32-bit data transfers, the state machine for the memory interface was designed in such a way that every 32 bit write to or read from the CRAM operates on two consecutive memory locations. Therefore, we can address 4 Meg address spaces through software. This CRAM interface was designed as a part of the class project in ECE5570 in Fall-2013 at Western Michigan University. The detailed state machine design that performs 32-bit reads and writes is described in [31] and the VHDL implementation of the memory interface can be found in Appendix C - wb_slv_cram.vhd and cram_interface.vhd.

5.2.1.3 FIFOs

For data interfacing to a target Nexys 3 board, the design has an input FIFO and output FIFO. The output FIFO is used to source the test signals and the input FIFO is

used to collect the processed signals. The FIFOs were implemented on a block RAM using the Xilinx Native Intellectual Property (IP) and include independent read and write clocks. The FIFO dimensions were chosen to be somewhat large, allowing a block of output data to be written as a block or burst and a block or burst of input data to be read. This allows the software programming in the ZPU to more efficiently support data transfers and have longer time intervals for other processing. The FIFOs are configured to generate the following status flags; full flag, almost-full flag, write acknowledge flag, half-full flag and empty flag.

These flags are asserted on the following events.

1. The full flag is asserted when the data is written to the N^{th} location on the FIFO.
2. The almost full flag is asserted when the data is written to the $(N - 1)^{th}$ location on the FIFO.
3. The write acknowledge flag is asserted when the FIFO write is successful (one clock cycle after the write to the FIFO is initiated).
4. The half full flag is asserted when the data available in the FIFO is less than half of the FIFO capacity.
5. The empty flag is asserted when there is no data available on the FIFO.

The FIFO also has a reset pin where all the locations in the FIFO are initialized to zeros on reset.

5.2.1.3 Output FIFO

The Output FIFO block consists of a wishbone wrapper which send the acknowledge signal upon receiving the wishbone cycle and strobe signals and a FIFO with the following dimensions.

1. Write width of 32 bits wide and write depth of 512.
2. Read width of 16 bits wide and read depth of 1024.

The FIFO status flags were incorporated into an 8-bit status register as shown in the Figure 5-6. The 3 MSBs and the LSB bit are unused. The half full flag is negated in the register, so when the amount of data on the FIFO is less than half full, the register would contain the value “00001000”. The output FIFO interface was designed to send the acknowledge signal as soon as the wishbone strobe and cycle signals arrived. The data is captured into a 32 bit register (data register) which is then written into the FIFO. The status register implemented in this FIFO interface is read only, while the data register is write only.



Figure 5-6 Output FIFO Status Register

The FIFO controller was designed as a state machine which is responsible to decode the read and write operations from the ZPU. The flowchart of this state machine can be described is shown in the Figure 5-7. The VHDL implementation is shown in the Appendix C - fifo_if.vhd source file.

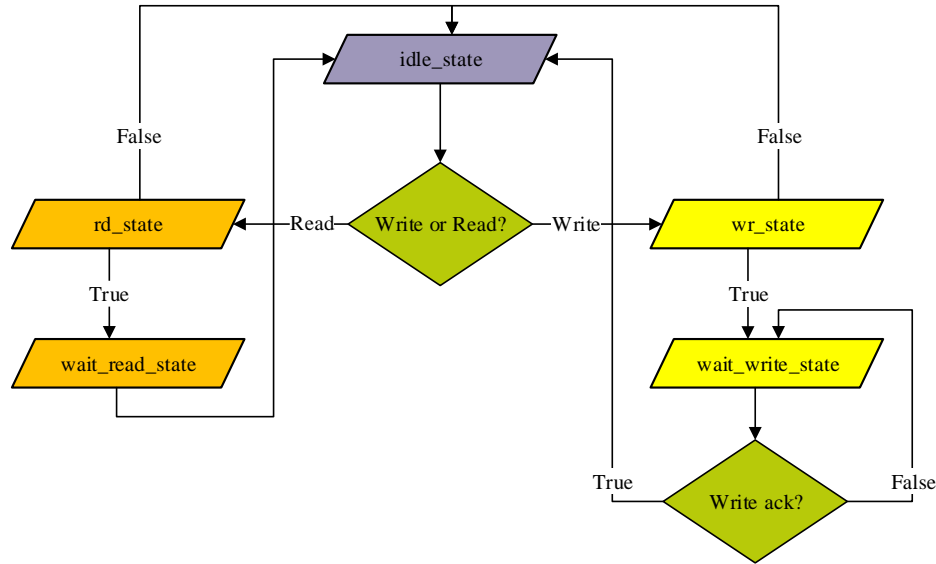


Figure 5-7 Output FIFO State-Machine Flowchart

As shown in the above flow chart, the state machine is designed with 5 states. The operation of the state machine can be described as follows:

1. In the idle state, the state machine continuously checks for a read or write request from the ZPU and transfers control to the appropriate state.
2. In the read state, the state machine checks if the ZPU is requesting to read the status register and copies the contents of status register onto the output data bus. If the ZPU is requesting to read something else then the control is transferred back to idle state.
3. The wait read state is a dummy state, it was just designed to provide one clock cycle time before switching back to the idle state.
4. Likewise, in write state, the state machine checks if the ZPU is writing to FIFO data register. Then the FIFO write enable signal is asserted and data is written onto the FIFO data bus through the FIFO data register.

- In the wait write state, the FIFO write enable signal is disabled and returned to idle state depending on the write acknowledge flag.

The FIFO write process using the above state machine is shown in the Figure 5-8

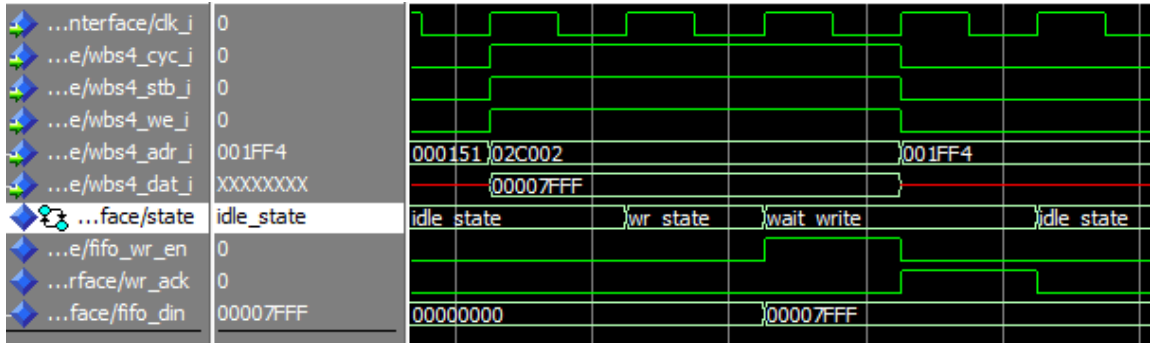


Figure 5-8 Output FIFO Write Process

The reading of the output FIFO and transfer of data to the target board does not occur until the output FIFO is almost filled. The interface was designed in such a way that, the almost full flag generated after writing $(N - 1)^{th}$ word to the FIFO is used to toggle the enable signal for the target processor board.

The read clock (rd_clk) for the FIFO was generated using a 16-bit counter whose count value is set to 0x007D as shown in the code snippet below. If a different read clock is required, the counter needs to be reconfigured to reflect the changes.

```
rd_clk_thingy:
process(clk_i, rst_i, rd_count)
begin
if rising_edge(clk_i) then
if rst_i = '1' then
rd_count <= (others => '0');
rd_clk <= '0';
else
if rd_count = x"007D" then --3F
rd_clk <= not(rd_clk);
rd_count <= (others => '0');
else
rd_count <= rd_count + '1';
end if;
end if;
```

```

end if;
end if;
end process rd_clk_thingy;

```

The above stated logic was used to generate the read clock because, the Digital Clock Manager (DCM) available on Spartan 6 FPGA operating with 100 MHz primary clock was unable to generate this low frequency clock signal. The data from the FIFO is read in synchronous to the read clock. This read clock is also used as the master clock (MCLK) for the communication signal processor.

The serial clock (SCLK) for the communication signal processing board was implemented as a T-flip flop that toggles a signal on every falling edge of the master clock (MCLK). The master clock, serial clock, enable and reset signals, and the data read from the FIFO was sent over the VHDC cable as input signals to the communication signal processing board as shown in Figure 5-9 and Figure 5-10.

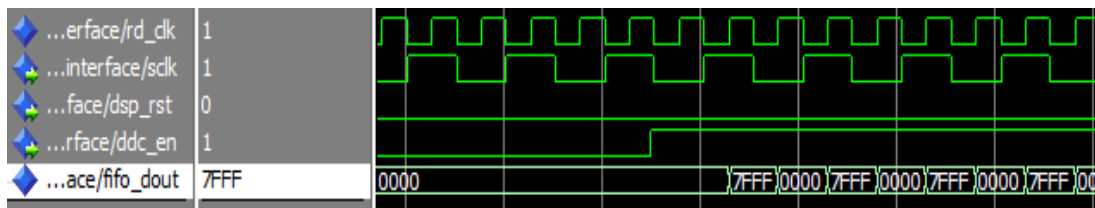


Figure 5-9 Output of the Pattern Generator Board (ModelSim Simulator)



Figure 5-10 Output of the Pattern Generator Board (MSO-X 3034A)

5.2.1.3 Input FIFO

The input FIFO has the exact opposite dimensions as the output FIFO.

1. Write width of 16 bits wide and read depth of 1024.
2. Read width of 32 bits wide and write depth of 512.

Similar to the output FIFO, the input FIFO has a status register as shown below



Figure 5-11 Input FIFO Status Register

Here, the FIFO status register consists of half full, empty and full flags. The 4 MSBs and a LSB are unused bits in the register. The FIFO controller was designed as a state machine which decodes the read requests from the ZPU. In the input FIFO block, both the FIFO data register and the status register are read only. The flowchart of this state machine is shown below

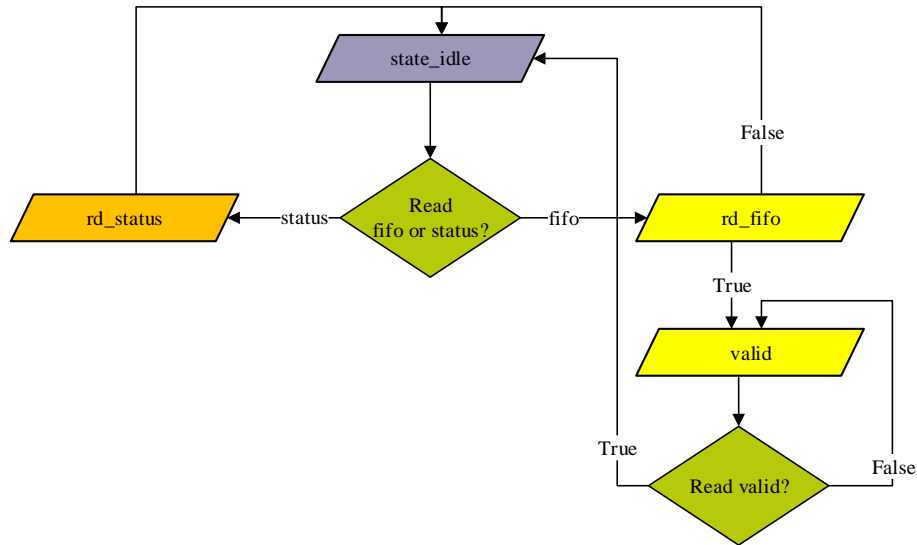


Figure 5-12 Input FIFO State-Machine Flowchart

The operation of the state machine can be described as follows:

1. In the idle state, the state machine continuously checks for a FIFO data read or status register read request from the ZPU.
 - a. If the state machine determines that it is a FIFO data read request, then the FIFO read enable is asserted and the control is transferred to rd_fifo state.
 - b. If the state machine determines that the ZPU is requesting for status register, then the control is transferred to rd_status state.
2. In the rd_fifo state, the read enable signal is deasserted and the data output from the FIFO is sent to the ZPU. It also checks for valid flag if the data validate the data read from the FIFO and then the control is handed over to the idle state.

3. In the rd_status state, the current value in the status register is supplied to the ZPU and the command is returned back to idle state.

The read operation of the state machine is shown in the ModelSim simulation below

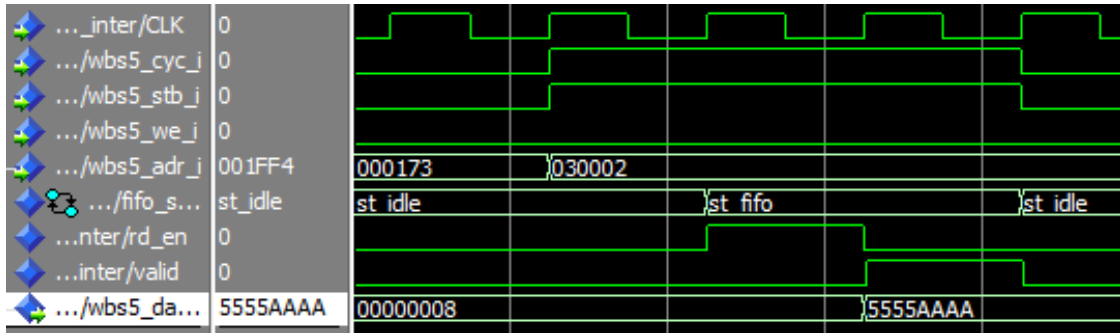


Figure 5-13 Input FIFO Read Process

5.2.1 Software Aspects

The software components involve not only the composition of C code that executes on the ZPU but also data preparation and storage to the CRAM and the appropriate file manipulations to generate appropriate Xilinx configuration code for loading. The following section describes the software and processes required for testing.

5.2.1.1 Generating Test Data

In order to generate the patterns using pattern generator, The 32-bit integer samples were pre-computed in a *.bin file using MATLAB script as shown below

```

cram_top = 65535;
data = (65535);
x = zeros(1,cram_top);
for k = 1:1: cram_top
    x(k) = 2147418112;% data format --> [16bit(I) 16bit(Q)]
end
fileID = fopen('cram_TestData.bin', 'w+', 'l');%%%%%%%%%%
for i= 1:cram_top
    fwrite(fileID,x(i), 'int', 'l'); % int = 32 bits little endian
end
fclose(fileID);

```

Currently, the ZPU supports only little endian data transfers. Hence, the patterns were created in a little endian fashion as shown in the in the Figure 5-14. Since, the pattern generator was used to emulate the data samples from two quadrature sampling ADCs, the data format of a 32 bit integer was designed such that the 16 MSBs represent in phase samples and 16 LSBs represent quadrature phase samples.

Address	0	1	2	3	4	5	6	7	8	9	a	b	c	d	e	f
00000000	00	00	ff	7f	00	00	ff	7f	00	00	ff	7f	00	00	ff	7f
00000010	00	00	ff	7f	00	00	ff	7f	00	00	ff	7f	00	00	ff	7f
00000020	00	00	ff	7f	00	00	ff	7f	00	00	ff	7f	00	00	ff	7f
00000030	00	00	ff	7f	00	00	ff	7f	00	00	ff	7f	00	00	ff	7f

Figure 5-14 32-bit Binary Pattern in Little Endian Fashion

The above mentioned method is one way to generate 32-bit integer patterns. These samples can also be the captured directly from a 16 bit ADC, but it has to be arranged in a specified data format mention above.

5.2.1.2 Copying Data to CRAM

The data generated in the previous section was copied to the on-board CRAM using Digilent adept software. The Digilent Adept software has an option for writing a file to the memory directly from the computer without actually configuring the FPGA. This process is shown in the Figure 5-15. In order to use the Adept memory write option,

the FPGA must be connected to the computer via USB. Once the Adept detects the FPGA board, it displays appropriate tabs as shown in the figure below. Under the memory tab, by selecting the RAM radio button and appropriate file, we can write the generated pattern file to CRAM.

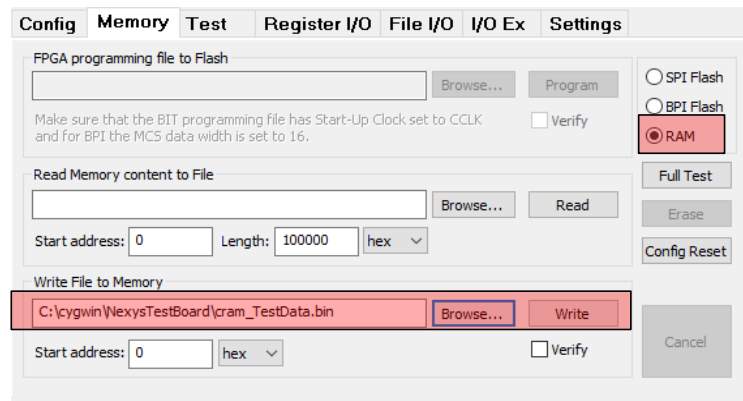


Figure 5-15 Writing Data to CRAM using Adept

5.2.1.3 ZPU Software

The software for the ZPU was written in C language and is compiled using zpu-gcc toolchain under Cygwin environment (Linux). In order to compile the ZPU software we need the following requirements:

1. Cygwin 32-bit environment with bitutils, cmake, gcc, g++, gdb and make packages.
2. ZPUGCC toolchain [32].

The project consists of a header file and a source code. The header file basically defines the pointers pointing to unsigned long int, these pointers were initialized to the

address spaces specified by the wishbone-slave memory map as we discussed in the previous section.

The source code begins by initializing a pointer pointing to the base address of the CRAM. During the initialization cycle, the data is read from the CRAM and written to the output FIFO until the $(N - 1)^{th}$ location. After which, the program enters into an infinite loop. In the infinite loop, the status register of the output FIFO is checked to see if the amount of data available is below half full or if the FIFO is empty. If either of them are true then the ZPU reads the data from the CRAM starting from the last location where it stopped and writes it to output FIFO as bursts. The data in the CRAM is valid until the 65535th location. Hence, when the data is read from the 65535th location, the pointer is initialized back to the bottom of CRAM and this process is continued infinitely. During the time between the two consecutive burst writes to output FIFO, the ZPU checks the status register of input FIFO. If the input FIFO is more than half filled, then the ZPU reads a burst of 32-bit complex words from the FIFO and compares it with the results stored on CRAM. The process of ZPU burst writes and the comparison time between two consecutive burst writes is shown below.

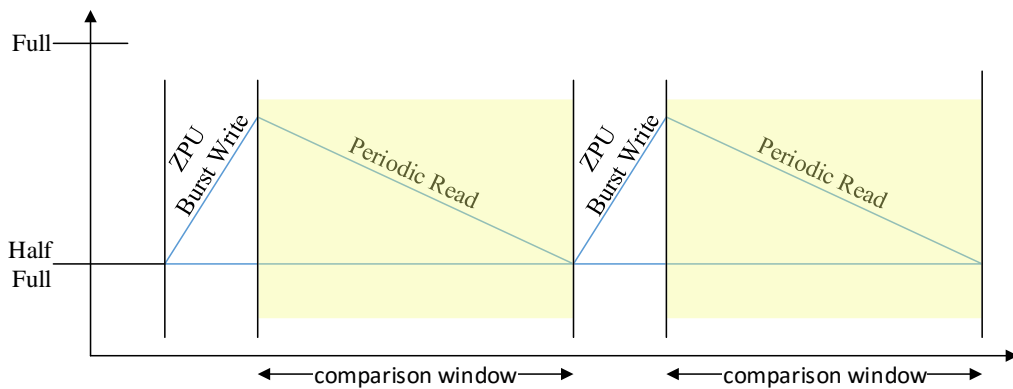


Figure 5-16 ZPU Write and Comparison Scheme

The following process was used to compile the source code and generate the FPGA bit streams:

1. zpu-elf-gcc command was used to compile the C code. This creates an *.elf file in the same director.
2. The *.elf file created would be too big to write it to the BRAM of Spartan 5 FPGA. Hence zpu-elf-strip command was used to strip the *.elf file.
3. The resulting elf file is then converted to a *.bin using the command zpu-elf-objcopy.
4. Finally, the BRAM contents were generated as ASCII character in a *.txt from *.bin file. The *.txt file would contain the program data that needs to be loaded into BRAM.

The detailed explanation for compiling the ZPU software can be found in Appendix D - Compiling process.

Finally, the data2mem tool [33] from Xilinx was used to change the ZPU software source code directly in the FPGA bit stream file instead of re-initializing the ZPUs single port RAM in the design and synthesizing the entire design again. The data2mem tool accepts the *.elf file, *.bit file and *.bmm file and outputs an updated *.bit file which contains the updated ZPU software image and can be used to program the FPGA.

Chapter 6

RESULTS AND PERFORMANCE

The previous chapters have described the theory, operation and implementation of the DDC chain, NCO and CORDIC processor, CIC filter and half band filters. A test board that can provide clocked parallel data vectors as though provided by an ADC has also been described. This section describes the stand alone and combined testing of the circuitry and systems developed.

6.1 Signal Processing Chain Verification

The individual blocks in the signal processing chain was tested using the VHDL test bench. The test vectors emulating the ADC data were created using MATLAB and stored into a file. The file was read by the VHDL test bench in interleaved fashion and fed to DDC chain.

One way of testing this hardware is to feed the binary patterns of 0x7FFF and 0x0000 in interleaved fashion synchronized with the master clock. As was discussed earlier, if the input of the CORDIC is fixed to (1, 0), the CORDIC would act as an NCO generating sine and cosine waveforms of a particular frequency defined by phase accumulator. This concept was exploited to generate 500Hz sine and cosine waveforms. In order to generate the waveforms of this frequency, the phase accumulator was loaded with 0x0147AE14. This value was calculated using the equation

$$Phase_{step}(rad) = \frac{NCO_{freq} * 2^{32}}{f_{sample}} \quad (62)$$

where $NCO_{freq} = 500$ and $f_{sample} = 100 \text{ KHz}$.

When the phase accumulator steps through the given angle, the CORDIC computes the corresponding sine and cosine components at the output. The rate at which this calculation happens is directly proportional to the rate at which the CORDIC processor is clocked. In order to shorten the simulation time required for ModelSim simulator, a 50MHz clock was generated in the VHDL test bench.

The output at each stage of the in-phase component of the DDC chain can be verified by plotting it against MATLAB computed data. In addition, the Chipscope results are also shown and compared to the ModelSim simulation and MATLAB simulation.

1. CORDIC stage:

The output at the CORDIC stage is shown in the Figure 6-1. As we can see, the 24 bit time domain samples computed using MATLAB almost exactly overlaps with the samples captured though the VHDL simulation.

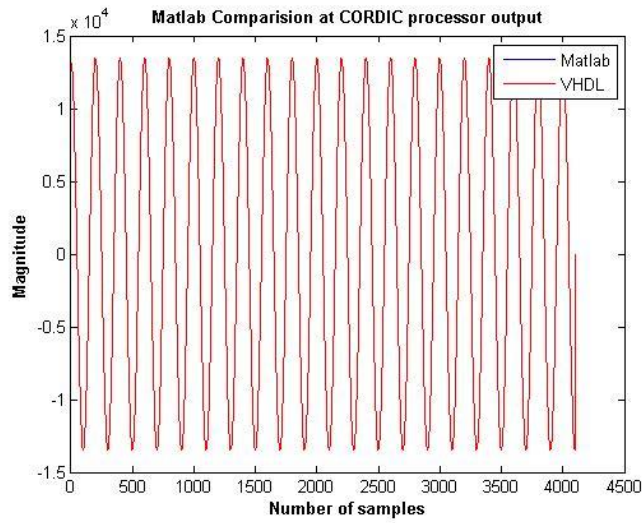


Figure 6-1 CORDIC Time Domain Output

The frequency spectrum was also generated in order to compare the received signal in frequency domain as depicted in the figure below.

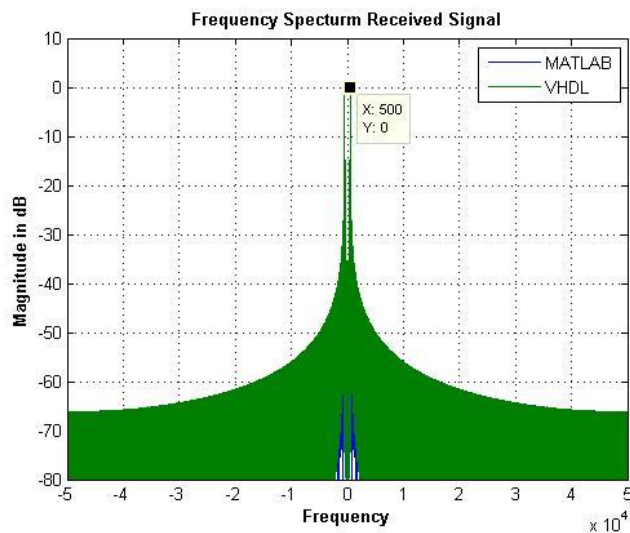


Figure 6-2 CORDIC Output Frequency Spectrum

As we can see, the frequency spectrum of the MATLAB computed samples and the samples exported from ModelSim are nearly identical with each other and the peak is

shown at 500Hz. The error between these two implementation methodologies is shown below.

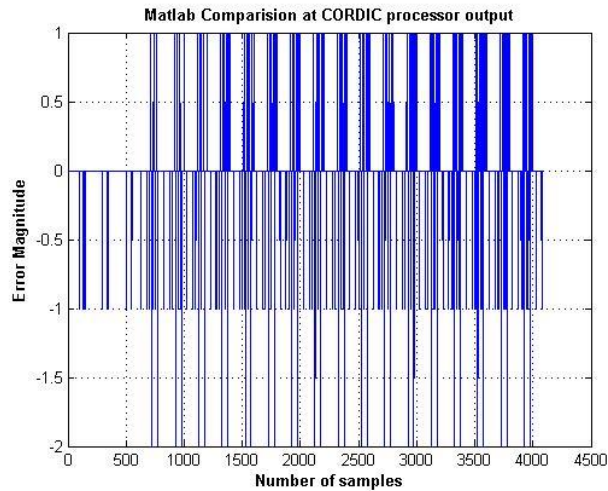


Figure 6-3 Error between MATLAB and VHDL Implementation

From the Figure 6-3 it can be seen that, there is no such significant error between both the implementation, as the error was limited to only 2 bits least significant. The error at the least signification bits can be ignored in this system since truncation on least significant bits are employed at multiple locations. A hardware comparison of the in-phase MATLAB data, Modelsim VHDL simulation, and Chipscope captured Xilinx device data is shown in Figure 6-4. As we can see, the output of the CORDIC processor on FPGA exactly matches with the ModelSim simulation tool.

		X <1x4117 int32>														
		23	24	25	26	27	28	29	30	31	32	33	34	35	36	
n_cordic_i	13430	0	13430	13383	13323	13251	13164	13066	12954	12830	12692	12542	12379	12206	12019	
n_cordic_q	1270	0	1270	1692	2110	2527	2942	3354	3763	4167	4570	4966	5357	5743	6124	
* from_cordic_i	0	0	13483	13430	13383	13323	13251	13164	13066	12954	12830	12692	12542	12379	12206	12019
* from_cordic_q	0	0	847	1270	1692	2110	2527	2942	3354	3763	4167	4570	4966	5357	5743	6124

Figure 6-4 MATLAB-ModelSim-Chipscope Somparisons

2. CIC filter decimator:

The second stages in the signal processing chain is the CIC filter decimator, the 24-bit samples of 500Hz signal sampled at 100 KHz are received at the input from the CORDIC processor. The decimation rate for CIC filter was chosen to be 5. The output of the CIC filter would have a sample rate of 20 KHz. The time domain comparison of the output from MATLAB and VHDL implementation is shown in the figure below.

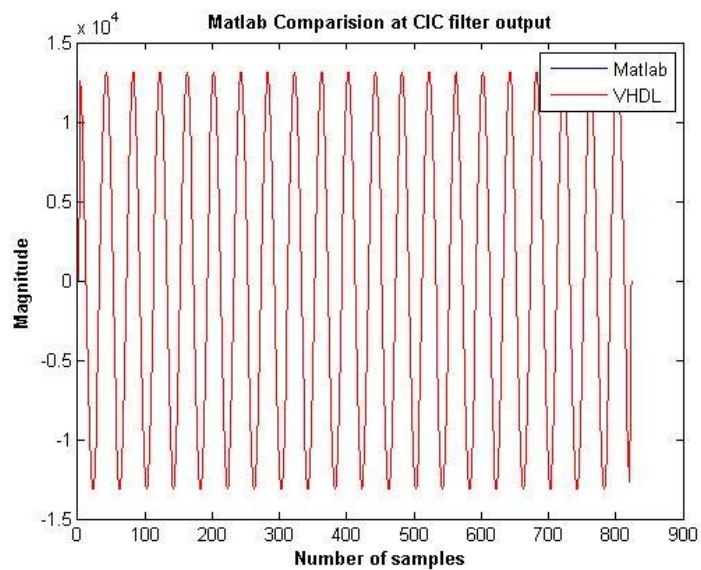


Figure 6-5 CIC Filter – Time Domain Comparison

As we can see, the time domain samples from both MATLAB and ModelSim exactly overlaps each other. The frequency response of the received samples is shown in the Figure 6-6.

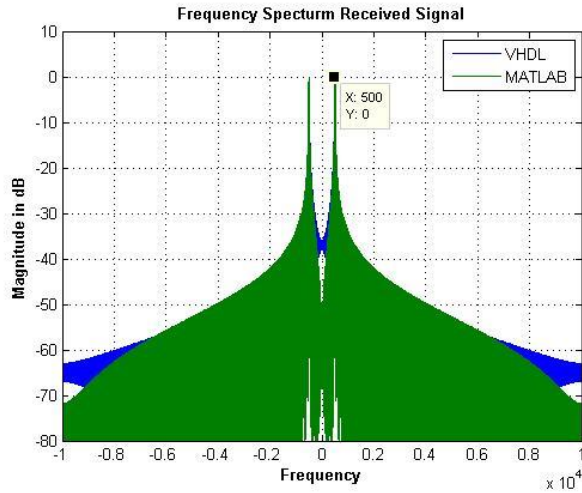


Figure 6-6 Frequency Response of the CIC Filter Output

Although, the time domain samples appear to overlap on each other, again there are small errors between the MATLAB computed samples and the samples exported from ModelSim is shown in the Figure 6-7. Again these errors corresponds to the LSB and can be ignored in this implementation since, the LSBs are going to be truncated in further stages of the signal processing chain.

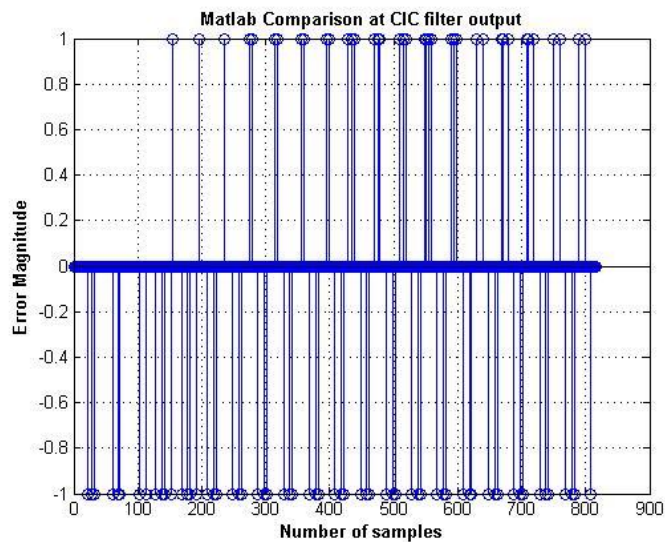


Figure 6-7 Error between MATLAB and VHDL implementation

3. First stage half-band filter:

The next stage of the signal processing chain is the 7-tap half-band filter. The half-band filter implemented in this thesis has a fixed decimation of 2. Therefore, the output sample rate of this filter is always half of the input sample rate. The 24-bit samples of a 500Hz signal are received from the CIC filter decimator, the sampling rate at this stage would be 20 KHz. These samples are further truncated to 17 bits and processed through adders and multipliers involved in the filter structure as previously described. The output of this filter is a 24-bit processed time domain samples, the Figure 6-8 shows the time domain comparisons of the processed samples from MATLAB and VHDL implementation.

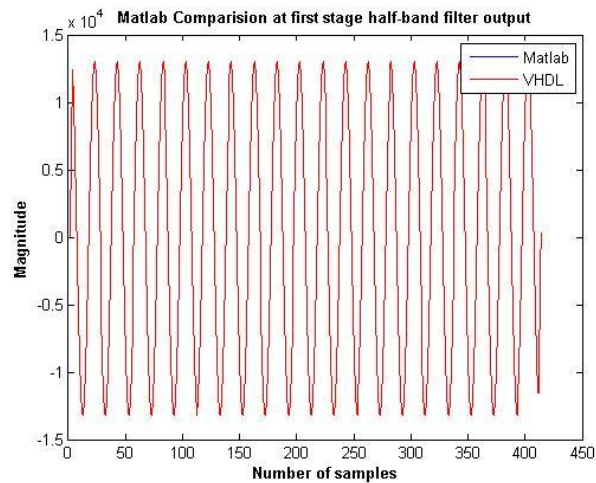


Figure 6-8 First Stage Half-Band Filter – Time Domain Comparison

The frequency spectrum of the half-band filter output is shown in the Figure 6-9. As we can see, the sample rate at the output is exactly half of the input sample rate. The sample by sample comparison of the 24 bit output is shown in the Figure 6-10. It is evident from

the figure that the VHDL implementation exactly matches with the MATLAB computed output.

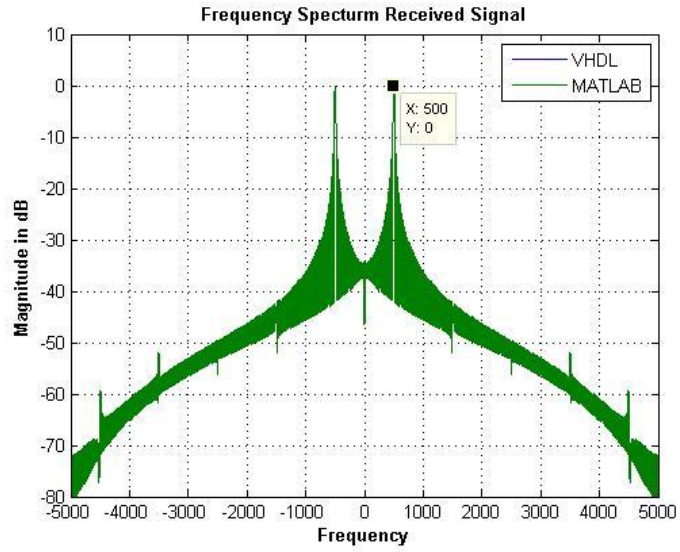


Figure 6-9 Output Spectrum of the First Half-Band Filter

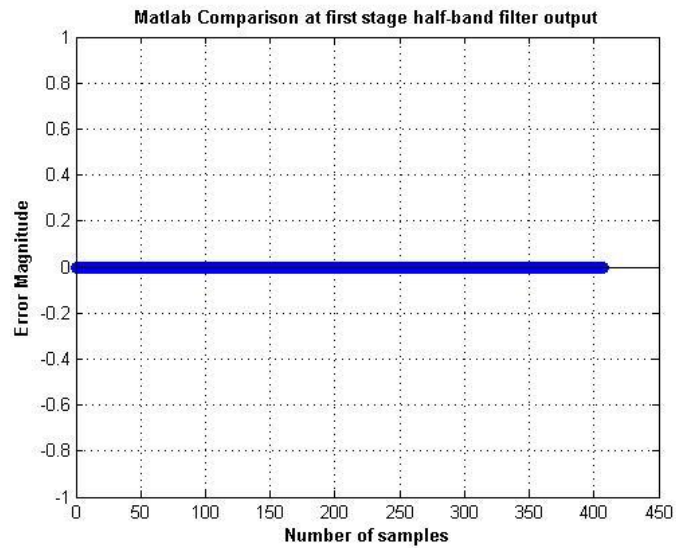


Figure 6-10 Error between MATLAB and VHDL Implementation

4. Final stage half-band filter

The final stage of the signal processing chain is a 31-tap half-band filter. The 24 bit samples from the previous stage are filtered and further decimated by 2, providing the final bandwidth limitation. The time domain output of both MATLAB and VHDL implementation is shown in the Figure 6-11

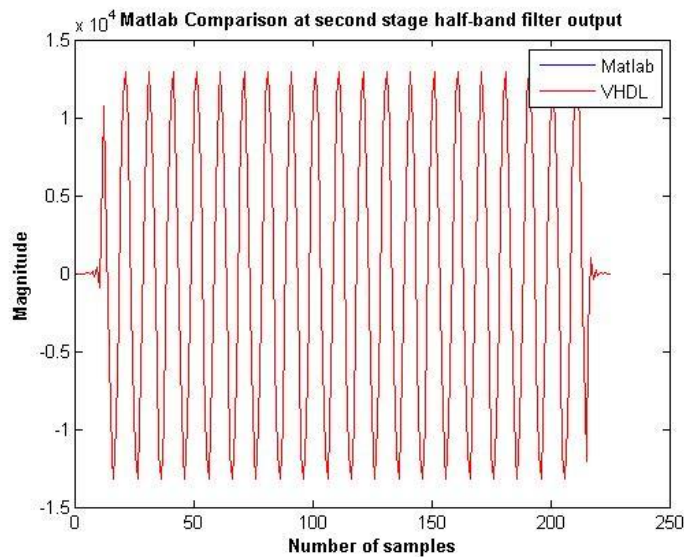


Figure 6-11 Final Stage Half-Band Filter – Time Domain Comparison

The output spectrum of this half-band filter is depicted in the Figure 6-12. The output spectrum contains a small DC component because of 2's complement truncation at the input stage. The sample by sample comparison of the MATLAB and VHDL implementations is shown in the Figure 6-13. The VHDL implementation exactly matched with the MATLAB implementation except for one sample.

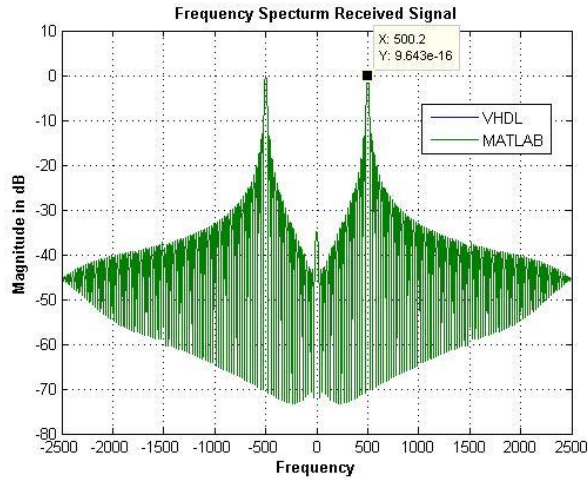


Figure 6-12 Output Spectrum of the Final Stage half-Band Filter

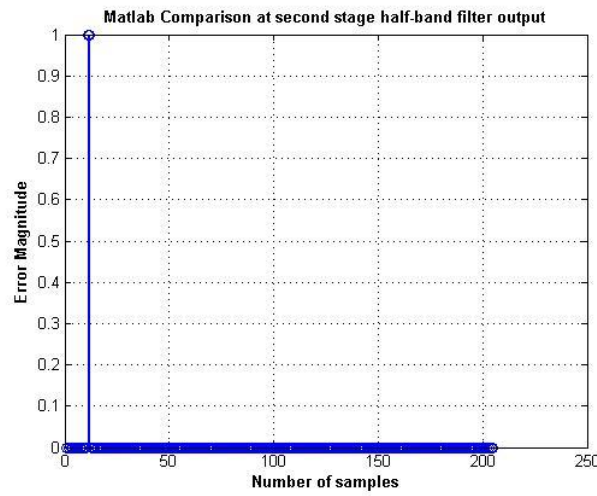


Figure 6-13 Error between MATLAB and VHDL Implementation

The Figure 6-14 shows the Chipscope analyzer data and the corresponding ModelSim and MATLAB data. The data from MATLAB and ModelSim was correlated with Chipscope Pro after the initial transient response of the filter. Once the filter gets to a steady state, the simulated data exactly matches with the data in the hardware.

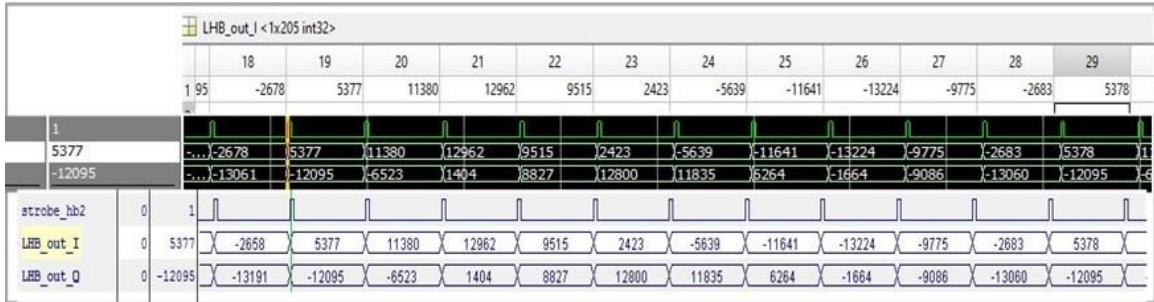


Figure 6-14 MATLAB-ModelSim-Chipscope Comparisons

The final decimated output compared to the input signal can be seen on Chipscope Pro Analyzer (Version 14.7) as shown in the Figure 6-15. The total decimation rate achieved by the entire system was $5 \times 2 \times 2$ or 20 (i.e., CIC=5, first half-band = 2 and final half-band = 2).

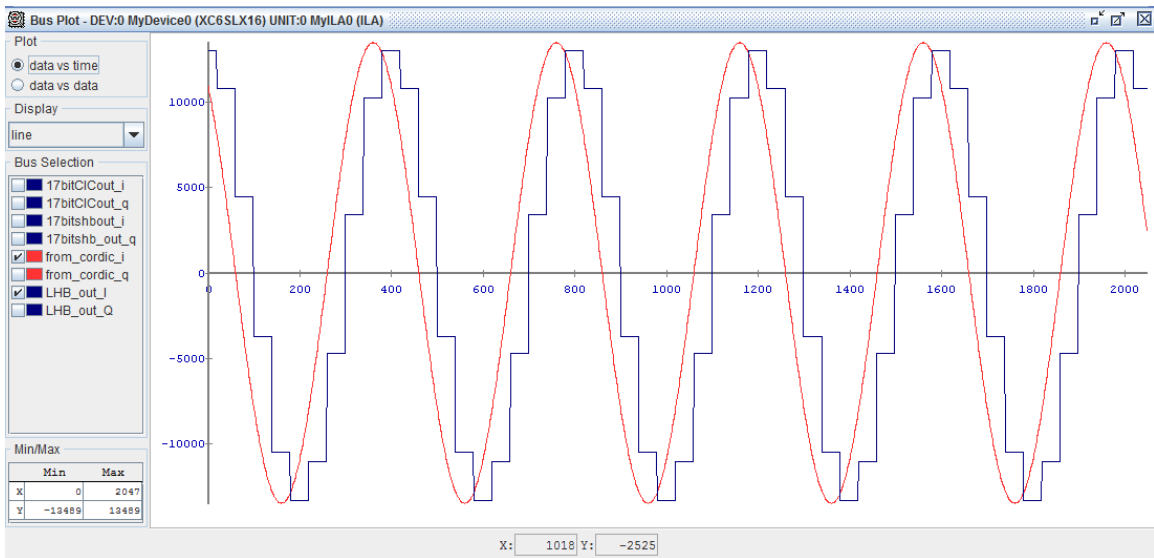


Figure 6-15 DDC Output using Chipscope-Pro Analyzer

6.2 Pattern Generator Board Testing

Once the system has been tested between MATLAB, Modelsim and Chipscope Pro, there was a desire to provide a parallel data input from a separate clock driven device. The following section describes testing performed with the Pattern Generation board implementation.

6.2.1 Maximum Data Rate Achieved using ZPU

The maximum data rate at which the pattern generator board is able to source the test data is directly proportional to the read clock that is generated for the output FIFO.

The read clock rate was determined as follows:

The CRAM takes about “70ns” [34] to read or write 16 bits of data in an asynchronous mode. When operating with 32 bit data transfers at a 50 MHz clock, the designed memory interface requires approximately “200ns” for two-16 bit data access. The ZPU being a stack based processor, the number of clock cycles required to execute a particular set of instructions is larger than compared to a regular register based processor. Based on these facts, the time taken by the ZPU to read the data from CRAM and write it to the FIFO is approximately 5.22us as shown in the Figure 6-16. In this figure, the $\sim half_{full}$ flag (D7) and the FIFO $write_{enable}$ (D15) signal are depicted.

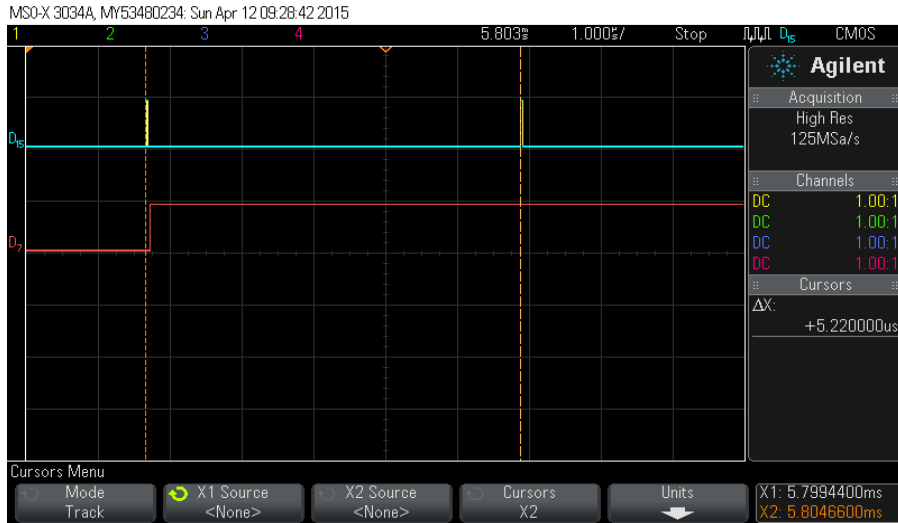


Figure 6-16 Time Delay between 2 Successive FIFO Writes

In order to maintain the periodicity at the output of the pattern generator, the ZPU software was designed in such a way that, a burst of 50 data samples of 32-bits gets written into the FIFO every time the amount of data available in the FIFO is less than half full as shown in the Figure 6-17. The total time taken by the ZPU to write these 50 data sample bursts was found to be approximately “260us”. Therefore, the maximum rate at which the data can be read from the FIFO was approximately 385.6 kilo samples per second (ksps). Since, the pattern generator board was also intended to do the results comparison, the read speed of the FIFO is limited to less than or equal to 200 ksps. The data read from the FIFO is actually the 16-bit interleaved data samples emulating the ADC. Thus, the actual sample rate for the communication signal processor is half of the rate at which the samples are read from the FIFO (i.e., 100 ksps).

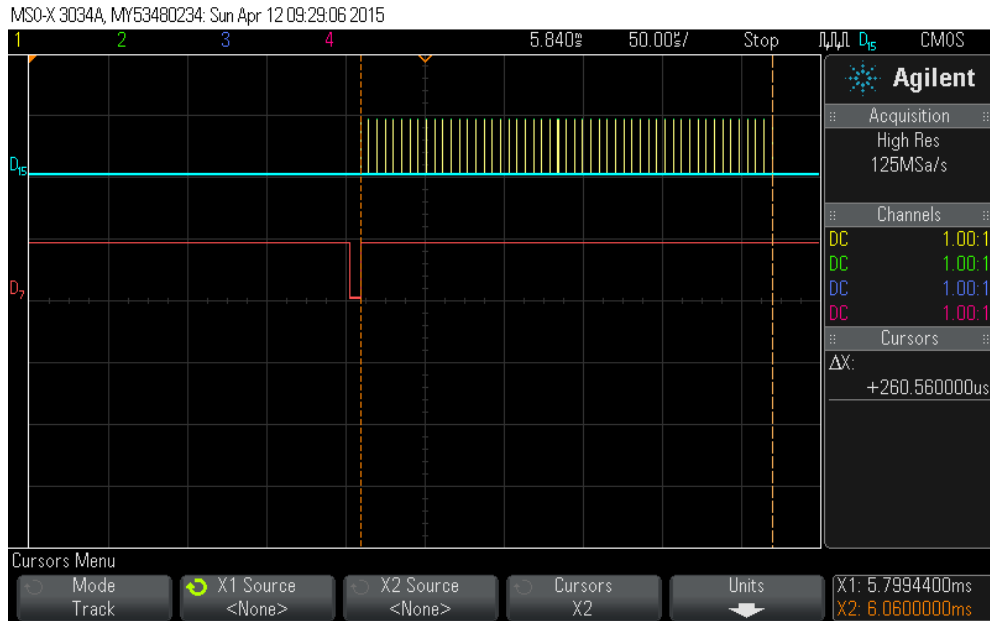


Figure 6-17 FIFO Burst Write

6.2.2 MATLAB limitations to Account for Hardware Transients

A major challenge with testing digital filters that are implemented in hardware involves the transient responses associated with initialization. Although, many techniques are suggested in the literature in order to eliminate these transients, their implementation was not considered in this thesis in order to save hardware resources. Instead, the initial set of output samples were simply discarded in this work.

The transient effect is clearly visible at the output of the final stage half-band filter shown in Figure 6-18. Due to the difficulty in perfect time sample alignment when decimation is performed, an exact MATLAB modeling for this transients was not implemented. As a result, the pattern generator and result analyzer board was just used as pattern generator for this application. Overall, the pattern generator readily sends out the

stored patterns along with the necessary clocks and control signals in order to test the communication signal processor developed.

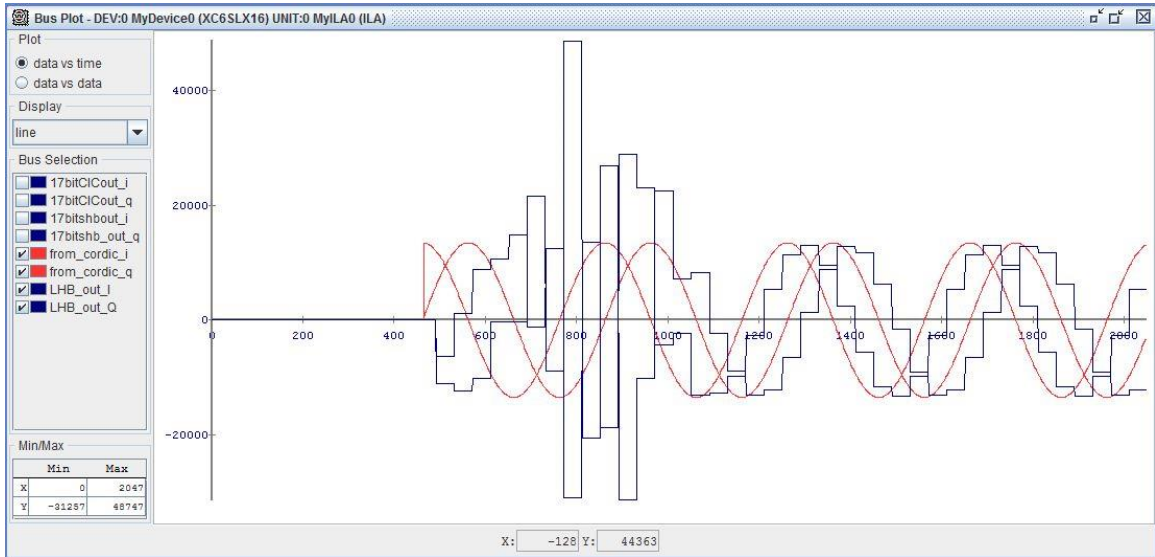


Figure 6-18 Transient Response at the Output of the Final Stage Half-Band Filter

6.3 Signal Processor Device Utilization Summary

The complete device utilization summary for the communication signal processing board is shown in the Table 6-1 below. It can be clearly seen that, only about 55% of the slices have been utilized, the utilized memory both single port and dual port is also only 14% and only a quarter of the available 31-DSP48A1 slices have been utilized. In general, we can approximate about 50% of logic resources still available in the FPGA with significantly more DSP and memory resources available. This allows for more signal processing blocks like equalizers, FEC and other communication specific algorithms to be implemented.

Table 6-1 Signal Processor Device Utilization Summary

Device Utilization Summary			
Slice Logic Utilization	Used	Available	Utilization
Number of Slice Registers	5,118	18,224	28%
Number used as Flip Flops	5,117		
Number used as Latches	1		
Number of Slice LUTs	4,308	9,112	47%
Number used as logic	3,511	9,112	38%
Number used as Memory	323	2,176	14%
Number used as Shift Register	323		
Number used exclusively as route-thrus	474		
Number with same-slice register load	468		
Number with same-slice carry load	6		
Number of occupied Slices	1,620	2,278	71%
Number of MUXCYs used	2,864	4,556	62%
Number of LUT Flip Flop pairs used	5,350		
Number with an unused Flip Flop	994	5,350	18%
Number with an unused LUT	1,042	5,350	19%
Number of fully used LUT-FF pairs	3,314	5,350	61%
Number of unique control sets	97		
Number of slice register sites lost to control set restrictions	418	18,224	2%
Number of bonded IOBs	37	232	15%
Number of LOCed IOBs	37	37	100%
Number of RAMB16BWERs	20	32	62%
Number of RAMB8BWERs	1	64	1%
Number of BUFG/BUFGMUXs	3	16	18%
Number used as BUFGs	3		
Number of BSCANs	1	4	25%
Number of DSP48A1s	8	32	25%
Number of RPM macros	9		
Average Fanout of Non-Clock Nets	3.26		

6.4 Signal Processor Timing Verification

In this section, we will analyze the worst case delay for the data path between the input and the output of the signal processor board. This analysis was performed using the Xilinx's built-in timing analyzing tool. The table is shown in Figure 6-19 and contains the minimum and the maximum delay between the dsp_clk (SCLK) input and the FIFO output of the signal processor board. The theoretical minimum clock speed that the processor can be run is determined by the fifo_dout(15) signal. Based on this worst case delay, the maximum useable clock frequency is approximately 87 MHz, if operated at a higher frequency, invalid parallel output data would be generated.

Clock dsp_sclk to Pad						
Destination	Max (slowest) clk (edge) to PAD	Process Corner	Min (fastest) clk (edge) to PAD	Process Corner	Internal Clock(s)	Clock Phase
fifo_dout<0>	10.076 (R)	SLOW	5.883 (R)	FAST	dsp_sclk_BUF	0.000
fifo_dout<1>	9.973 (R)	SLOW	5.795 (R)	FAST	dsp_sclk_BUF	0.000
fifo_dout<2>	9.858 (R)	SLOW	5.759 (R)	FAST	dsp_sclk_BUF	0.000
fifo_dout<3>	9.945 (R)	SLOW	5.828 (R)	FAST	dsp_sclk_BUF	0.000
fifo_dout<4>	10.158 (R)	SLOW	5.977 (R)	FAST	dsp_sclk_BUF	0.000
fifo_dout<5>	10.166 (R)	SLOW	6.006 (R)	FAST	dsp_sclk_BUF	0.000
fifo_dout<6>	10.164 (R)	SLOW	5.978 (R)	FAST	dsp_sclk_BUF	0.000
fifo_dout<7>	10.390 (R)	SLOW	6.138 (R)	FAST	dsp_sclk_BUF	0.000
fifo_dout<8>	10.252 (R)	SLOW	6.051 (R)	FAST	dsp_sclk_BUF	0.000
fifo_dout<9>	10.737 (R)	SLOW	6.376 (R)	FAST	dsp_sclk_BUF	0.000
fifo_dout<10>	10.615 (R)	SLOW	6.315 (R)	FAST	dsp_sclk_BUF	0.000
fifo_dout<11>	10.675 (R)	SLOW	6.323 (R)	FAST	dsp_sclk_BUF	0.000
fifo_dout<12>	10.790 (R)	SLOW	6.423 (R)	FAST	dsp_sclk_BUF	0.000
fifo_dout<13>	10.908 (R)	SLOW	6.475 (R)	FAST	dsp_sclk_BUF	0.000
fifo_dout<14>	11.139 (R)	SLOW	6.657 (R)	FAST	dsp_sclk_BUF	0.000
fifo_dout<15>	11.402 (R)	SLOW	6.861 (R)	FAST	dsp_sclk_BUF	0.000
strobe_out	8.732 (R)	SLOW	4.996 (R)	FAST	dsp_sclk_BUF	0.000

Figure 6-19 Signal Processor Timing Summary

Chapter 7

CONCLUSION AND FUTURE WORK

7.1 Conclusion

In this thesis, the successful implementation and verification of a narrowband digital down converter chain has been demonstrated on a Spartan 6 development board. In addition to this signal processor board, a digital pattern generator and output comparator system was developed on a second Spartan 6 development board.

The DDC implemented in this thesis consists of a 20 stage pipelined CORDIC processor, implemented in VHDL. The corresponding iterative model was also designed in MATLAB for functional verification. A 3-stage CIC filter decimator was implemented in order to perform the high rate decimation followed by a 2 stage half-band filters, one with 7 taps and other with 31 taps both performing a fixed decimation by a factor of 2. Again, MATLAB was used to design a finite precision integer model of the CIC and half-band filters in order to verify the functionality of the hardware developed.

In addition, a pattern generator and result comparator board was designed using an embedded softcore processor called a Zylon Processing Unit. The pattern generator board consists of the CRAM containing the test vectors that are generated using MATLAB. The ZPU was used to source these test signals and collect the results from the device that is being tested in real time. For a more predictable combinatorial result

without transients, the board would also compare the results with the pre-computed results that are stored in the CRAM.

7.2 Future Work

Based on the experiences gained during the course of this research, the following recommendations are possible areas that may be explored in the future: First specific improvements to the current system are described. This is followed by broader application of the elements developed.

1. The CIC and the half-band filter stages contain sections that truncates the 24-bit data input to the signal processing board. Though truncation serves multiple purposes, it does result in loss of precision as compared to options like rounding. More research is required in analyzing the cost and performance benefits of various rounding algorithm on the overall system, before such a technique can be incorporated in to the system.
2. Another aspect of the implementation that can be significantly improved is the soft core ZPU processor. The small footprint RISC based processor was an ideal candidate for the type of operations being performed in this research. But the large execution times in the ZPU, owing to its stack based architecture proved to be a limiting factor in the maximum throughput that can be achieved on a board to be tested. The latest Zynq based FPGA development boards combine the software programmability of an ARM core processor with the hardware programmability of an FPGA and would be an ideal replacement for the ZPU.
3. The comparator section of the pattern generator could not be validated with MATLAB results due to the presence of transients in the CORDIC and the filter stages.

Simulating CORDIC, CIC and half-band with all possible transients in MATLAB could provide a way to perform end to end testing the DDC chain.

4. Most of the parameters of the CORDIC can be reconfigured to suit the DDC requirements for a broad range of wireless communication technologies. However, the number of pipelined stages in CORDIC is fixed currently to 20-stages. This can be modified by using VHDL 'generate' statements to instantiate an array of CORDIC stages.

The DDC processing elements developed provide key components required by Dr. Bazuin to develop a customized, open-source Xilinx design for real-time processing of narrowband signals. This could replace and/or extend the capability of existing Ettus Research USRP devices available or provide a means to use the existing USRP RF daughter cards with new Xilinx Zynq-based development boards. As defined, the DDC elements can also be readily configured for transmitting, performing the mathematical inverse operations involved in digital up-converting (DUC). A DUC reverses the processing element ordering and converts the CIC filter-deciminator into a CIC interpolator-filter.

7.3 Summary

In the course of this thesis, it was a great experience learning about multi-rate signal processing concepts. This thesis is a great way to learn about the implementation of digital filter on FPGA and employing hardware resource sharing to reduce the number of logic resources required. In addition, to further continue this research we can develop a Gigabit Ethernet interface on a Zynq-based development board to establish the

communication between PC and FPGA. This along with DDC/DUC chain and AD-FMCOMMS1-EBZ [35] we can develop a custom software defined radio peripheral.

REFERENCES

- [1] Falciassecca, G; Valotti, B., "Guglielmo Marconi: The pioneer of wireless communications," *Microwave Conference, 2009. EuMC 2009. European*, vol. no., pp. 544-546, Sept. 29 2009-Oct. 1 2009.
- [2] www.gsma.com, "The Mobile Economy 2015," GSM Association, 2015.
- [3] "Annual wireless Industry Survey," CTIA The wireless Association, [Online]. Available: http://www.ctia.org/docs/default-source/Facts-Stats/ctia_survey_ye_2014_graphics.pdf?sfvrsn=2. [Accessed 7 10 2015].
- [4] G. Manganaro and D. Leenaerts, *RF IC Design for Wireless Communication Systems*, MA, USA: Elsevier's Science & Technology, 2013.
- [5] M. Maupin, "Implementing Sub-GHz wireless connectivity in Embedded Devices," *Wireless Design and Development*, pp. 32-36, June 2014.
- [6] Raychaudhuri, D.; Mandayam, Narayan B., "Frontiers of Wireless and Mobile Communication," *Proceedings of the IEEE*, Vols. 100, no.4., pp. 824-840, April 2012.
- [7] Texas Instruments, "OMAP3430 Processor," [Online]. Available: <http://www.ti.com/general/docs/wtbu/wtbuproductcontent.tsp?contentId=14649&navigationId=12643&templateId=6123#chipDiagram>. [Accessed 11 November 2015].
- [8] Volder, Jack E., "The CORDIC trigonometric computing technique," *Electronic Computers, IRE Transactions on*, Vols. EC-8, no.3, pp. 330-334, Sept. 1959.
- [9] Harris,F.J.;Dick,C.;Rice,M., "Digital receivers and transmitters using polyphase filter banks for wireless communications," *Microwave Theory and Techniques, IEEE Transactions*, Vols. 51, no.4, pp. 1395-1412, Apr 2003.
- [10] W. Tuttlebee, *Software Defined Radio: Origins, Drivers and International Perspectives*, New York: John Wiley, 2002.

- [11] Mitola, J., III, "Software radios: Survey, critical evaluation and future directions," *Aerospace and Electronic Systems Magazine, IEEE* , Vols. 8, no.4, pp. 25-36, April 1993.
- [12] "Wireless Innovation Forum," June 2015. [Online]. Available: http://www.wirelessinnovation.org/Introduction_to_SDR.
- [13] Shannon, C.E., "Communication In The Presence Of Noise," *Proceedings of the IEEE*, no. vol.86, no.2, pp.447-457, Feb. 1998.
- [14] "WARP: Wireless Open Research Platform," [Online]. Available: <http://warp.rice.edu/>. [Accessed June 2015].
- [15] "USRP Software Defined Radios," [Online]. Available: <http://www.ettus.com/>.
- [16] "GENI Cognitive Radio Kit," [Online]. Available: <http://crkit.orbit-lab.org>.
- [17] "SORA: SDR Platform from Microsoft," [Online]. Available: <http://research.microsoft.com/en-us/projects/sora/>. [Accessed June 2015].
- [18] "CORDIC," Wikipedia The Free Encyclopedia, [Online]. Available: <http://en.wikipedia.org/wiki/CORDIC>. [Accessed April 2015].
- [19] J.S. Walther, "A unified algorithm for elementary functions," in *AFIPS Spring Joint Computer Conference*, 1971.
- [20] Monash University, "A VHDL Implementation of a CORDIC Airthmetic Processor Chip," Monash University, Australia, Clayton VIC 3168, 1994.
- [21] Hogenauer, E., "An economical class of digital filters for decimation and interpolation," *Acoustics, Speech and Signal Processing, IEEE Transactions*, Vols. 29, no.2, pp. 155-162, Apr 1981.
- [22] fredric harris, *Multirate Signal Processing for Communication Systems*, San Diego, California: Pearson Education, Inc., 2011.
- [23] Vaidyanathan, P.P., "Multirate digital filters, filter banks, polyphase networks, and applications: a tutorial," *Proceedings of the IEEE*, Vols. 78, no.1, pp. 56-93, Jan 1990.
- [24] Xilinx, "LogiCORE IP CIC Compiler v3.0," Xilinx, Inc, San Jose, CA, June 22, 2011.

- [25] Larry Doolittle, LBNL, "Filtering and Decimation by Eight in an FPGA for SDR and Other Applications," November, 2006.
- [26] K. Chapman, "Saving Costs with the SRL16E," White Paper: Xilinx FPGAs, 2008.
- [27] Xilinx, "Spartan-6 FPGA Clocking Resources," www.xilinx.com, June 19, 2015.
- [28] "Digilent, Inc," [Online]. Available:
https://www.digilentinc.com/Data/Products/NEXYS3/Nexys3_rm.pdf.
[Accessed 21 October 2015].
- [29] "ZPU Repository," [Online]. Available:
http://repo.or.cz/w/zpu.git?a=blob_plain;f=zpu/docs/zpu_arch.html.
[Accessed 21 October 2015].
- [30] A. Lopes, "ZPUino, 32 bit processor, for all your needs," [Online]. Available:
http://www.alvie.com/zpuino/zpu_instructions.html. [Accessed 21 October 2015].
- [31] Dr. Bradley J. Bazuin, "ECE 5570 Web Site: Dr. Bazuin," [Online]. Available:
<http://homepages.wmich.edu/~bazuinb/ECE5570/CellularRam-External%20Memory%20Interface.pdf>. [Accessed 22 October 2015].
- [32] Á. Lopes, "GitHub," 28 April 2015. [Online]. Available:
<https://github.com/zylin/zpugcc>. [Accessed 3 November 2015].
- [33] Xilinx Inc, "Data2MEM User Guide," www.xilinx.com, June 24, 2009.
- [34] Micron Technology, "Micron Technology, Inc.," [Online]. Available:
<http://www.micron.com/parts/psram/cellularram/mt45w8mw16bgx-701-it>.
[Accessed 22 October 2015].
- [35] Analog Devices, "AD-FMCOMMS1-EBZ User Guide," 15 July 2015. [Online]. Available: <https://wiki.analog.com/resources/eval/user-guides/ad-fmcomms1-ebz>. [Accessed 19 November 2015].

Appendix A - MATLAB Scripts

CORDIC Processor

```
% Cordic Implementation

clc
clear all
close all
nsamples = 4096;
fftsize = 65536;
fsample = 100e3;
fsignal = 10e3;
frange = (-0.5:1/fftsize:0.5-1/fftsize)*fsample;
[I, Q] = TestSigGen(fsignal,fsample,nsamples,0);
Isample = fix(I*2^14-1);
Qsample = fix(Q*2^14-1);
x_in = (I+i*Q)*2^14-1;
fileID = fopen('C:\Users\Nagarjun\Documents\MATLAB\Thesis\cordicI.txt', 'w+');%%%%%%%%%%
for i= 1:nsamples
    fprintf(fileID, '%d\n',int32(Isample));
end
fclose(fileID);
fileID = fopen('C:\Users\Nagarjun\Documents\MATLAB\Thesis\cordicQ.txt', 'w+');%%%%%%%%%%
for i= 1:nsamples
    fprintf(fileID, '%d\n',int32(Qsample));
end
fclose(fileID);
figure('NumberTitle', 'off',...
       'Name', 'Received signal');
plot(0:nsamples-1,x_in)
title('\bfReceived signal')
xlabel('\bfTime')
ylabel('\bfMagnitude')
sigspec = fftshift(fft(x_in,fftsize));
figure
```

```

plot(frange,dB(psdg(SigSpec/max(SigSpec))));
title('\bfFrequency Specturm Received Signal')
xlabel('\bfFrequency')
ylabel('\bfMagnitude in dB')
ylim([-80,10]); grid on
input_str = sprintf('Please enter center freq (less than %dHz)',fsample);
NCO_Freq = input(input_str);
PhaseInc = 2*((NCO_Freq * 2^(32-1)) / fsample)
STG = 20; % Number of rotations
K = 0.60725294104140; % Cordic Gain
for i = 0:1:(23)
    c = (round((atan(1.0/(2^i))/(2*pi)) * (2^24)));
    consts(i+1) = c;
end
% pre allocate the vectors and parameters
phasepast = 0;
init_0padding = 1;
Isample = Isample*2^8;
Qsample = Qsample*2^8;
Is = int32([zeros(1,init_0padding) Isample(1:nsamples-init_0padding)]);
Qs = int32([zeros(1,init_0padding) Qsample(1:nsamples-init_0padding)]);
phase = (0);
initial = 1;
x = int32(1)*(2^(16)-1);% 24 bit input to cordic
y = int32(0);
for N = 1:nsamples
#####
%           CORDIC PROCESSOR
#####
    x = sign_ext(Is(N),24,1);% 25 bit Cordic processor
    y = sign_ext(Qs(N),24,1);
% Phase accumulator
    phase = phase + PhaseInc;
% phasepast = phase;
% #####-----[32 bit Integer Wrap Around]-----#####
    if (phase > 2147483647)% if > 2^31 - 1 roll it back to -ve's
        phase = phase - 4294967295; %(2^31-1 + 2^31)
    else if(phase < -2147483648) % -2^31
        phase = phase + 4294967295;

```

```

end
end
zin_24 = floor(phase/256);% right shift by 8 since zwidth is 24
zin = int32(zin_24);
% Phase pre rotation since cordic is limited to +pi/2 to -pi/2
if (zin>=2^22 && zin<2^23)% interval between 90 to 180 degrees
    xpast = x;
    x = -y;
    y = xpast;
    zin = bitand(zin, 4194303);
else if(zin>=-2^23 && zin<-2^22)% interval between -180 to -90 degrees
    xpast = x;
    x = y;
    y = -xpast;
    zin = bitor(zin,-12582912);
end
end
% 20 stage, 27 bit cordic pipeline
x = sign_ext(x,25,2); % sign extend to accomodate bit growth
y = sign_ext(y,25,2);
j = 0;
d=1;
P_vec(N) = phase;
% z = phase;
while j < STG
    if (zin > 0)
        d = 1;
    else
        d = -1;
    end
    xpast = x;
    x = xpast - (d*bitshift(y,-j));
    y = y + (d*bitshift(xpast,-j));
    j = j+1;
    zin = zin - (d*consts(j));
% #####-----[27bit OverFlow Compensation]-----#####
    if (x > 134217727)% if > 2^27 -1 roll it back to -ve's
        x = x - 268435455;
    else if(x < -134217728)

```

```

        x = x + 268435455;
    end
end
if (y > 134217727)% if > 2^27 -1 roll it back to -ve's
    y = y - 268435455;
else if(y < -134217728)
    y = y + 268435455;
end
end
end
% Clip the cordic output to 24 bit
X(N) = bitshift(x,-2);
Y(N) = bitshift(y,-2);
Z(N) = zin;
end
% Save Real and Imaginary values to test.mat file.
X_fft = fftshift(fft(double(X), fftsize));
save('C:\Users\Nagarjun\Desktop\Mathworks\Matfiles\cordic_out.mat', 'X',
'Y','X_fft','NCO_Freq', 'fsample','nsamples');
% Time Domain Plots.
figure('NumberTitle', 'off',...
        'Name', 'CORDIC output');
plot(X,'b')
hold
plot(Y,'g')
grid on
title('CORDIC time domain')
legend('Real Samples', 'Imag Samples')
xlabel('Time')
ylabel('Magnitute')
% Frequency Plots
figure('NumberTitle','off',...
        'Name','Power Spectral Desity plot')
plot(frange, dB(psdg(X_fft/max(X_fft))))
axis([-fsample/2 fsample/2 -80 10])
grid on;
title('Frequency domain plot of NCO')
xlabel('Frequency')
ylabel('Magnitude in dB')

```

```

% Phase shift the CORDIC output to match the FPGA
cordic_delay = 21;
x = [zeros(1,cordic_delay) X];
fileID = fopen('C:\Users\Nagarjun\Documents\MATLAB\Thesis\cordicI2cic_TB.txt',
'w+');%%%%%%%%%%
for i= 1:nsamples
    fprintf(fileID, '%d\n',X(i));
end
fclose(fileID);
fileID = fopen('C:\Users\Nagarjun\Documents\MATLAB\Thesis\cordicQ2cic_TB.txt',
'w+');%%%%%%%%%%
for i= 1:nsamples
    fprintf(fileID, '%d\n',Y(i));
end
fclose(fileID);

```

Cascaded Integrator Comb Filter

```

% CIC Decimation Filter Design Simulation for SDR
clc
clear all
close all
load('C:\Users\Nagarjun\Desktop\Mathworks\Matfiles\cordic_out.mat') % Cordic output
fftsize = 65536;
fsample_in = fsample;
actual_rate = 5;% odd decimation would give better results;
decim_rate = actual_rate-1;
fsin = NCO_Freq;
Fs_out = fsample_in/actual_rate;
bits_in = 24;
N = 3; %number of stages
% nsamples = 512*4;
maxbitgain = ceil(log2(127));
% input signal

% x_in = (cos(2*pi*(0:nsamples-1)*(fsin/Fs_in)));%+rand(1,nsamples); %input signal

```

```

x_in = X;
nsamples = length(x_in);
figure
plot((0:1:nsamples-1),x_in)
title('Input signal')
xlabel('Time')
ylabel('Magnitude')
freq_in = (-0.5:1/fftsize:0.5-1/fftsize)*fsample_in;
x_infft = fftshift(fft(double(x_in), fftsize));
figure
plot(freq_in, dB(psdg(x_infft/max(x_infft))))
stitle = sprintf('Input to the CIC filter with sampling rate of %g', fsample_in);
title(stitle)
xname = sprintf('Fsin = %g', fsin);
xlabel('Frequency in Hz')
ylabel('Magnitude in dB')
hold on
% CIC freq Response
freqrange = (-0.5:1/fftsize:0.5-1/fftsize);
ZeroIdx=find(freqrange==0);
NotZeroIdx=find(freqrange~=0);
H0freq(NotZeroIdx)= sin(pi*decim_rate*freqrange(NotZeroIdx)) ./
sin(pi*freqrange(NotZeroIdx));
H0freq(ZeroIdx)=decim_rate;
H0freq=(H0freq/decim_rate).^N;
plot(freq_in, dB(psdg(H0freq)), 'r')
hold off
ylim([-80 10])
grid
legend('Input Signal', 'CIC Filter')
% integrator implementation
integrator = int64(zeros(1,N));
diff = int64(zeros(1, N));
% bitwidth=bits_in+ceil(N*log2(decim_rate));
bitwidth=bits_in+ceil(N*maxbitgain);
for ii = 1:1:nsamples
    x_sign_ext(ii) = sign_ext(int64(x_in(ii)),24,(bitwidth-24));
    integrator(1) = add_2(int64(x_sign_ext(ii)), integrator(1), bitwidth);
    stage1(ii+1) = integrator(1);

```



```

    integrator(2) = add_2(stage1(ii), integrator(2), bitwidth);
    stage2(ii+1) = integrator(2);
    integrator(3) = add_2(stage2(ii), integrator(3), bitwidth);
    stage3(ii+1) = integrator(3);
end
accu_delay = zeros(1,3);
stage3 = [accu_delay stage3];
% Down sample the signal this is done in cic_strober.v
sampler = stage3(1:actual_rate:length(stage3));
%Comb implementation
for jj = 1:1:length(sampler)
    pipeline1(jj) = add_2(sampler(jj), -diff(1), bitwidth);
    diff(1) = sampler(jj);
    pipeline2(jj) = add_2(pipeline1(jj), -diff(2), bitwidth);
    diff(2) = pipeline1(jj);
    pipeline3(jj) = add_2(pipeline2(jj), -diff(3), bitwidth);
    diff(3) = pipeline2(jj);
end
##### Integrator plots
figure
subplot(3,2,1)
plot(stage1);
title('\bfIntegrator stages output')
ylabel('\bfMagnitude')
subplot(3,2,3)
plot(stage2);
ylabel('\bfMagnitude')
subplot(3,2,5)
plot(stage3)
ylabel('\bfMagnitude')
xlabel('\bfNumber of samples')
% ##### Differentiator plot
subplot(3,2,2)
plot(pipeline1);
title('\bfDifferentiator stages output')
ylabel('\bfMagnitude')
subplot(3,2,4)
plot(pipeline2);
ylabel('\bfMagnitude')

```

```

subplot(3,2,6);
plot(pipeline3)
ylabel('\bfMagnitude')
xlabel('\bfNumber of samples')
% Bit pruning CIC decimation filter
shift = round(N*(log2(actual_rate)));
cic_out = double(bitshift(int64(pipeline3),-shift));
cic_out_24 = (add_2((cic_out),0, 24));
% Output signal
disp('Plotting multiple spectrum by rearranging rows into columns')
figure
x_outfft = fftshift(fft(double(pipeline3), fftsize));
x_outtohb = fftshift(fft(double(cic_out_24), fftsize));
freq_out = freq_in/actual_rate;
plot(freq_out, dB(psdg([x_outfft/max(x_outfft) x_outtohb/max(x_outtohb)])));
hold on
stitle = sprintf('Output of the CIC filter with decimation rate of %g',actual_rate);
title(stitle)
xname = sprintf('Fsampling in = %g, Fsampling out = %g', fsample_in, fsample_in/actual_rate);
xlabel(xname)
ylabel('Magnitude in dB')
% ylim([-50 10])
legend('Actual output','Pruned output')
grid on
save('C:\Users\Nagarjun\Desktop\Mathworks\Matfiles\cic_out.mat','Fs_out', 'freq_out',
'cic_out_24')
fileID = fopen('C:\Users\Nagarjun\Desktop\Mathworks\Matfiles\cic2shb_TB.txt',
'w+');%%%%%%%%%%
for i= 1:nsamples/actual_rate-1
    fprintf(fileID, '%d\n',cic_out_24(i));
end
fclose(fileID);

```

Small (7-Tap) Half Band Filter

```
clc
clear all
close all
load('C:\Users\Nagarjun\Desktop\Mathworks\Matfiles\cic_out')
fftsize = 65536;
decim_rate = 2; % fixed decimation in usrp
Fs_in = Fs_out; % sampling rate input
Fs_out = Fs_in/decim_rate;% decimated sampling rate
samples_in = cic_out_24;% output from CIC 24bit precision
nsamples = length(samples_in);
freq_in = freq_out;
freq_out = (-0.5:1/fftsize:0.5 - 1/fftsize)*Fs_out;
bitsin_w = 24;
round_w= 17;
accum_w = 30;
bitsin = 24;
bitsout=17;
%% Rounding the input to 18 bits using truncation
round_in = int_round(samples_in,bitsin_w,round_w);
figure
subplot(2,1,1)
plot(samples_in)
title('samples in 24 bit')
xlabel('Time')
ylabel('Magnitude')
subplot(2,1,2)
plot(round_in)
title('round in 17 bit')
xlabel('Time')
ylabel('Magnitude')
figure
Spec_filtIn24 = fftshift(fft(samples_in, fftsize));
Spec_filtIn17 = fftshift(fft(round_in, fftsize));
plot(freq_in, dB(psdg([Spec_filtIn17/max(Spec_filtIn17)
Spec_filtIn24/max(Spec_filtIn24)])));
title('Input signal to small HB Filter')
```

```

xlabel('Frequency in Hertz')
ylabel('Magnitude in dB')
legend('actual input','rounded input')
%% generating the filter coefficients for halfband filter
shb_filt = fix(2^18 * halfgen4(0.75/8,2))
figure
subplot(2,1,1)
stem(shb_filt)
title('Normalized HalfBand filter Taps = 7')
xlabel('Time sample')
ylabel('value')
grid on
fft_usrp_filt = fftshift(fft(shb_filt, fftsize));
subplot(2,1,2)
plot(freq_in, dB(psdg(fft_usrp_filt/max(fft_usrp_filt))));
xlabel('Frequency')
ylabel('Power(dB)')
ylim([-80 10])
grid on
%% Shift register Implementation
Z = zeros(1, length(shb_filt));
col_sh = diag( ones(length(shb_filt)-1,1), 1);
for n = 1:1:length(round_in)
    Z = Z*col_sh;
    Z(1) = round_in(n);
    add_1(n) = Z(1)+Z(7);
    add_2(n) = Z(3)+Z(5);
    middle(n) = int32(Z(4)*2);
    m_reg(n) = bitshift(sign_ext(middle(n),18,2),10);
end
% sum and product implementation
% Decimating happens in the 2nd stage of the implementation taking advantage of HB Char's
sum_a = add_1(1:2:length(round_in));
sum_b = add_2(1:2:length(round_in));
middle_reg = [double(m_reg(1:2:length(round_in))) 0];
product_1 = int64(sum_a.*(-10690));
product_2 = int64(sum_b.*(75809));
product_a = (bitshift(product_1,-(36-accum_w)));
product_b = (bitshift(product_2,-(36-accum_w)));

```

```

product_a = [0 product_a]; % testing the phase delays
% Final accumulator. 30 bit
% NOTE: accum is of double datatype. carefull about the input sizes as
% accum will not overflow as 30 bit number does.
K = 1;
for i = 1:2:nsamples
    accum(i) = middle_reg(K)+product_a(K);
    accum(i+1) = accum(i) + product_b(K);
    K=K+1;
end
accum_round = int_round(accum(2:2:end), accum_w, 25);
filt_out = clip(accum_round,25,24);
save('C:\Users\Nagarjun\Desktop\Mathworks\Matfiles\hb0_out','filt_out','Fs_out')
%% plot results
figure
plot(filt_out)
title('samples out 24 bit samples')
xlabel('Time')
ylabel('Magnitude')
Spec_filtOut = fftshift(fft(filt_out, fftsize));
figure
plot(freq_out, dB(psdg(Spec_filtOut/max(Spec_filtOut))));
xlim([-Fs_out/2 Fs_out/2])
title('Output signal from small HB Filter')
xlabel('Frequency in Hertz')
ylabel('Magnitude in dB')
grid on
fileID = fopen('C:\Users\Nagarjun\Desktop\Mathworks\Matfiles\shb2\hb_TB.txt',
'w+');%%%%%%%%%%
for i= 1:nsamples/decim_rate
    fprintf(fileID, '%d\n',accum_round(i));
end
fclose(fileID);

```

Large (31-Tap) Half Band Filter

```
clc
clear all
close all
load('C:\Users\Nagarjun\Desktop\Mathworks\Matfiles\hb0_out');
data_in = filt_out;
clear('filt_out')
fs_in = Fs_out;
fftsize = 4096;
nsamples = length(data_in);
round_in = int_round(data_in, 24, 17);
figure
plot(round_in)
title('Rounded Input Signal')
xlabel('Time samples')
ylabel('Magnitude')
freq_in = (-0.5:1/fftsize:0.5-1/fftsize)*fs_in;
%% generating the filter coefficients for halfband filter according to USRP
myfilt = round(2^18 * halfgen4(.7/4,8));
Nord = length(myfilt);
myfilt_fft = fftshift(fft(myfilt,fftsize));
figure
subplot(2,1,1)
stem(myfilt)
title('\bfNormalized HalfBand filter Taps = 31')
xlabel('Time sample')
ylabel('value')
grid
subplot(2,1,2)
plot(freq_in,dB(psdg(myfilt_fft/max(myfilt_fft))))
% title('frequency response of the large filter')
ylabel('\itMagnitude in dB');
xlabel('\itFrequency')
grid
%% 31 tap HB has the 2 path polyphase implementation of the 31 tap halfband filter.
lambda = 2;
polyord = lambda*(ceil(Nord/lambda));
```

```

polytaps = polyord/lambda;
M = polytaps;
myfilt_v1 = [myfilt zeros(1, polyord-Nord)];
poly_filt = reshape(myfilt_v1,lambda,polytaps);
coeff1 = [-107 445 -1271 2959];
coeff2 = [-6107 11953 -24706 82359];
Z = zeros(lambda,polytaps);
Zshift = diag( ones(polytaps-1,1), 1);
numblocks = nsamples/lambda;
accum(1)=0;
for ii = 1:1:numblocks
    Z = Z*Zshift;
    Tindex = 1+((ii-1)*lambda:ii*lambda-1);
    Z(:,1) = (round_in(Tindex))';
    sum1 = [Z(1,1)+Z(1,16) Z(1,2)+Z(1,15) Z(1,3)+Z(1,14) Z(1,4)+Z(1,13)];
    sum2 = [Z(1,5)+Z(1,12) Z(1,6)+Z(1,11) Z(1,7)+Z(1,10) Z(1,8)+Z(1,9)];
    prod1 = sum1 .* coeff1; % 36 bit product
    prod2 = sum2 .* coeff2;
    sum_of_prod = (prod1+prod2); % 36 bit
    sum_of_prod = int64(prod1+prod2); % 36 bit
    round_sum = bitshift(sum_of_prod,-11); % round to 25 bit number for accumulator
    % round_sum = sum_of_prod; % uncomment to compare with Conventional polyphase
    implementation
    % actual place for middle is Z(2,8) but due to indexing issue it is Z(2,9)
    middle = bitshift(int32(Z(2,9)),6);% should have rounded to 25 bit but its okay since
    it is double is 2^53
    accum(ii) = sum(round_sum);
    final_sum(ii,:) = accum(ii)+ middle; %27 bit accumulator
    % Conventional polyphase implementation. Need to shift right by 11 bits
    % to match the outputs.
    % yvect(:,ii) = sum((Z) .* poly_filt,2);
    % filt_out(ii) = sum(yvect(:,ii)).';
end
% final_out = int_round()
% filt_out = int64(sum(yvect).');
figure
% subplot(1,2,1)
plot(final_sum)
title('31 TAP HB filt FPGA implementation Matched')

```

```

xlabel('Time samples')
ylabel('Magnitude')
% subplot(1,2,2)
% plot(filt_out)
% title('My polyphase output')
% xlabel('Time samples')
% ylabel('Magnitude')
fft_final_sum = fftshift(fft(double(final_sum), fftsize));
figure
plot(freq_in/2,dB(psdg(fft_final_sum/max(fft_final_sum))))
title('\bfFrequency spectrum')
xlabel('\bfFrequency')
ylabel('\bfMagnitude in dB')
grid

```

Half-Band filter generator

```

function A=halfgen4(up,N)
% up is the stopband width, as a fraction of input sampling rate
% N is the order of half-band filter to generate
% A is the full set of FIR coefficients, 4*N-1 long
npt=N*20;
wmax=2*pi*up;
x0=(0:npt-1)/npt;
yfit=1-x0.^2; % possibly bogus, but good enough to get started
wfit=yfit*wmax;
q=[1:2:(2*N-1)];
target=.5*ones(length(wfit),1)

```


Appendix B - VHDL Implementation

Cordic_z24.vhd

```
-----  
-----  
-- Company: Western Michigan University  
-- Engineer: Nagarjun Marappa  
--  
-- Create Date:      20:44:32 03/29/2014  
-- Design Name:  
-- Module Name:      Cordic_z24 - Behavioral  
--  
-----  
-----  
library IEEE;  
use IEEE.STD_LOGIC_1164.ALL;  
use IEEE.NUMERIC_STD.ALL;  
use IEEE.STD_LOGIC_SIGNED.ALL;  
  
entity Cordic_z24 is  
generic (zwidth : natural := 24;  
         bitwidth : natural := 25;  
         D_CARE_VAL : std_logic := 'X'  
        );  
Port ( CLK           : in   STD_LOGIC;  
       RST           : in   STD_LOGIC;  
       ddc_en        : in   STD_LOGIC;  
       Iin           : in   STD_LOGIC_VECTOR(bitwidth-1 downto 0);  
       Qin           : in   STD_LOGIC_VECTOR(bitwidth-1 downto 0);  
       Zin           : in   STD_LOGIC_VECTOR(zwidth-1 downto 0);  
       Iout          : out  STD_LOGIC_VECTOR(bitwidth-1 downto 0);  
       Qout          : out  STD_LOGIC_VECTOR(bitwidth-1 downto 0);  
       Zout          : out  STD_LOGIC_VECTOR(zwidth-1 downto 0)  
      );  
end Cordic_z24;  
  
architecture Behavioral of Cordic_z24 is  
  
  COMPONENT CORDIC_STAGE is  
  generic (zwidth : natural := 24;  
         bitwidth : natural := 26;  
         shift : natural := 1  
        );  
  Port ( CLK           : in   STD_LOGIC;  
       RST           : in   STD_LOGIC;  
       en            : in   STD_LOGIC;  
       Iin           : in   STD_LOGIC_VECTOR (bitwidth-1 downto 0);  
       Qin           : in   STD_LOGIC_VECTOR (bitwidth-1 downto 0);  
       zin           : in   STD_LOGIC_VECTOR (zwidth-1 downto 0);
```

```

        C_consts : in    STD_LOGIC_VECTOR (zwidth-1 downto 0);
        Iout     : out  STD_LOGIC_VECTOR (bitwidth-1 downto 0);
        Qout     : out  STD_LOGIC_VECTOR (bitwidth-1 downto 0);
        zout     : out  STD_LOGIC_VECTOR (zwidth-1 downto 0));
    end COMPONENT;

-- constants for 24 bit phase
constant C0 : STD_LOGIC_VECTOR(zwidth-1 downto 0) := x"200000";
constant C1 : STD_LOGIC_VECTOR(zwidth-1 downto 0) := x"12E405";
constant C2 : STD_LOGIC_VECTOR(zwidth-1 downto 0) := x"09FB38";
constant C3 : STD_LOGIC_VECTOR(zwidth-1 downto 0) := x"051112";
constant C4 : STD_LOGIC_VECTOR(zwidth-1 downto 0) := x"028B0D";
constant C5 : STD_LOGIC_VECTOR(zwidth-1 downto 0) := x"0145D8";
constant C6 : STD_LOGIC_VECTOR(zwidth-1 downto 0) := x"00A2F6";
constant C7 : STD_LOGIC_VECTOR(zwidth-1 downto 0) := x"00517C";
constant C8 : STD_LOGIC_VECTOR(zwidth-1 downto 0) := x"0028BE";
constant C9 : STD_LOGIC_VECTOR(zwidth-1 downto 0) := x"00145F";
constant C10 : STD_LOGIC_VECTOR(zwidth-1 downto 0) := x"000A30";
constant C11 : STD_LOGIC_VECTOR(zwidth-1 downto 0) := x"000518";
constant C12 : STD_LOGIC_VECTOR(zwidth-1 downto 0) := x"00028C";
constant C13 : STD_LOGIC_VECTOR(zwidth-1 downto 0) := x"000146";
constant C14 : STD_LOGIC_VECTOR(zwidth-1 downto 0) := x"0000A3";
constant C15 : STD_LOGIC_VECTOR(zwidth-1 downto 0) := x"000051";
constant C16 : STD_LOGIC_VECTOR(zwidth-1 downto 0) := x"000029";
constant C17 : STD_LOGIC_VECTOR(zwidth-1 downto 0) := x"000014";
constant C18 : STD_LOGIC_VECTOR(zwidth-1 downto 0) := x"00000A";
constant C19 : STD_LOGIC_VECTOR(zwidth-1 downto 0) := x"000005";
constant C20 : STD_LOGIC_VECTOR(zwidth-1 downto 0) := x"000003";
constant C21 : STD_LOGIC_VECTOR(zwidth-1 downto 0) := x"000001";
constant C22 : STD_LOGIC_VECTOR(zwidth-1 downto 0) := x"000001";
constant C23 : STD_LOGIC_VECTOR(zwidth-1 downto 0) := x"000000";

-- InPhase inter stage components
signal I0 : STD_LOGIC_VECTOR(bitwidth+1 downto 0);
signal I1 : STD_LOGIC_VECTOR(bitwidth+1 downto 0);
signal I2 : STD_LOGIC_VECTOR(bitwidth+1 downto 0);
signal I3 : STD_LOGIC_VECTOR(bitwidth+1 downto 0);
signal I4 : STD_LOGIC_VECTOR(bitwidth+1 downto 0);
signal I5 : STD_LOGIC_VECTOR(bitwidth+1 downto 0);
signal I6 : STD_LOGIC_VECTOR(bitwidth+1 downto 0);
signal I7 : STD_LOGIC_VECTOR(bitwidth+1 downto 0);
signal I8 : STD_LOGIC_VECTOR(bitwidth+1 downto 0);
signal I9 : STD_LOGIC_VECTOR(bitwidth+1 downto 0);
signal I10 : STD_LOGIC_VECTOR(bitwidth+1 downto 0);
signal I11 : STD_LOGIC_VECTOR(bitwidth+1 downto 0);
signal I12 : STD_LOGIC_VECTOR(bitwidth+1 downto 0);
signal I13 : STD_LOGIC_VECTOR(bitwidth+1 downto 0);
signal I14 : STD_LOGIC_VECTOR(bitwidth+1 downto 0);
signal I15 : STD_LOGIC_VECTOR(bitwidth+1 downto 0);
signal I16 : STD_LOGIC_VECTOR(bitwidth+1 downto 0);
signal I17 : STD_LOGIC_VECTOR(bitwidth+1 downto 0);
signal I18 : STD_LOGIC_VECTOR(bitwidth+1 downto 0);
signal I19 : STD_LOGIC_VECTOR(bitwidth+1 downto 0);
signal I20 : STD_LOGIC_VECTOR(bitwidth+1 downto 0);

attribute KEEP :string;

```

```

attribute KEEP of I0: signal is "TRUE";
attribute KEEP of I1: signal is "TRUE";
attribute KEEP of I2: signal is "TRUE";
attribute KEEP of I3: signal is "TRUE";
attribute KEEP of I4: signal is "TRUE";
attribute KEEP of I5: signal is "TRUE";
attribute KEEP of I6: signal is "TRUE";
attribute KEEP of I7: signal is "TRUE";
attribute KEEP of I8: signal is "TRUE";
attribute KEEP of I9: signal is "TRUE";
attribute KEEP of I10: signal is "TRUE";
attribute KEEP of I11: signal is "TRUE";
attribute KEEP of I12: signal is "TRUE";
attribute KEEP of I13: signal is "TRUE";
attribute KEEP of I14: signal is "TRUE";
attribute KEEP of I15: signal is "TRUE";
attribute KEEP of I16: signal is "TRUE";
attribute KEEP of I17: signal is "TRUE";
attribute KEEP of I18: signal is "TRUE";
attribute KEEP of I19: signal is "TRUE";
attribute KEEP of I20: signal is "TRUE";
-- QuadraturePhase inter stage components
signal Q0 : STD_LOGIC_VECTOR(bitwidth+1 downto 0);
signal Q1 : STD_LOGIC_VECTOR(bitwidth+1 downto 0);
signal Q2 : STD_LOGIC_VECTOR(bitwidth+1 downto 0);
signal Q3 : STD_LOGIC_VECTOR(bitwidth+1 downto 0);
signal Q4 : STD_LOGIC_VECTOR(bitwidth+1 downto 0);
signal Q5 : STD_LOGIC_VECTOR(bitwidth+1 downto 0);
signal Q6 : STD_LOGIC_VECTOR(bitwidth+1 downto 0);
signal Q7 : STD_LOGIC_VECTOR(bitwidth+1 downto 0);
signal Q8 : STD_LOGIC_VECTOR(bitwidth+1 downto 0);
signal Q9 : STD_LOGIC_VECTOR(bitwidth+1 downto 0);
signal Q10: STD_LOGIC_VECTOR(bitwidth+1 downto 0);
signal Q11: STD_LOGIC_VECTOR(bitwidth+1 downto 0);
signal Q12: STD_LOGIC_VECTOR(bitwidth+1 downto 0);
signal Q13: STD_LOGIC_VECTOR(bitwidth+1 downto 0);
signal Q14: STD_LOGIC_VECTOR(bitwidth+1 downto 0);
signal Q15: STD_LOGIC_VECTOR(bitwidth+1 downto 0);
signal Q16: STD_LOGIC_VECTOR(bitwidth+1 downto 0);
signal Q17: STD_LOGIC_VECTOR(bitwidth+1 downto 0);
signal Q18: STD_LOGIC_VECTOR(bitwidth+1 downto 0);
signal Q19: STD_LOGIC_VECTOR(bitwidth+1 downto 0);
signal Q20: STD_LOGIC_VECTOR(bitwidth+1 downto 0);

attribute KEEP of Q0: signal is "TRUE";
attribute KEEP of Q1: signal is "TRUE";
attribute KEEP of Q2: signal is "TRUE";
attribute KEEP of Q3: signal is "TRUE";
attribute KEEP of Q4: signal is "TRUE";
attribute KEEP of Q5: signal is "TRUE";
attribute KEEP of Q6: signal is "TRUE";
attribute KEEP of Q7: signal is "TRUE";
attribute KEEP of Q8: signal is "TRUE";
attribute KEEP of Q9: signal is "TRUE";

```

```

attribute KEEP of Q10: signal is "TRUE";
attribute KEEP of Q11: signal is "TRUE";
attribute KEEP of Q12: signal is "TRUE";
attribute KEEP of Q13: signal is "TRUE";
attribute KEEP of Q14: signal is "TRUE";
attribute KEEP of Q15: signal is "TRUE";
attribute KEEP of Q16: signal is "TRUE";
attribute KEEP of Q17: signal is "TRUE";
attribute KEEP of Q18: signal is "TRUE";
attribute KEEP of Q19: signal is "TRUE";
attribute KEEP of Q20: signal is "TRUE";
-- Inter Stage Phase Components
signal Z0 : STD_LOGIC_VECTOR(zwidth-1 downto 0);
signal Z1 : STD_LOGIC_VECTOR(zwidth-1 downto 0);
signal Z2 : STD_LOGIC_VECTOR(zwidth-1 downto 0);
signal Z3 : STD_LOGIC_VECTOR(zwidth-1 downto 0);
signal Z4 : STD_LOGIC_VECTOR(zwidth-1 downto 0);
signal Z5 : STD_LOGIC_VECTOR(zwidth-1 downto 0);
signal Z6 : STD_LOGIC_VECTOR(zwidth-1 downto 0);
signal Z7 : STD_LOGIC_VECTOR(zwidth-1 downto 0);
signal Z8 : STD_LOGIC_VECTOR(zwidth-1 downto 0);
signal Z9 : STD_LOGIC_VECTOR(zwidth-1 downto 0);
signal Z10: STD_LOGIC_VECTOR(zwidth-1 downto 0);
signal Z11: STD_LOGIC_VECTOR(zwidth-1 downto 0);
signal Z12: STD_LOGIC_VECTOR(zwidth-1 downto 0);
signal Z13: STD_LOGIC_VECTOR(zwidth-1 downto 0);
signal Z14: STD_LOGIC_VECTOR(zwidth-1 downto 0);
signal Z15: STD_LOGIC_VECTOR(zwidth-1 downto 0);
signal Z16: STD_LOGIC_VECTOR(zwidth-1 downto 0);
signal Z17: STD_LOGIC_VECTOR(zwidth-1 downto 0);
signal Z18: STD_LOGIC_VECTOR(zwidth-1 downto 0);
signal Z19: STD_LOGIC_VECTOR(zwidth-1 downto 0);
signal Z20: STD_LOGIC_VECTOR(zwidth-1 downto 0);

attribute KEEP of Z0: signal is "TRUE";
attribute KEEP of Z1: signal is "TRUE";
attribute KEEP of Z2: signal is "TRUE";
attribute KEEP of Z3: signal is "TRUE";
attribute KEEP of Z4: signal is "TRUE";
attribute KEEP of Z5: signal is "TRUE";
attribute KEEP of Z6: signal is "TRUE";
attribute KEEP of Z7: signal is "TRUE";
attribute KEEP of Z8: signal is "TRUE";
attribute KEEP of Z9: signal is "TRUE";
attribute KEEP of Z10: signal is "TRUE";
attribute KEEP of Z11: signal is "TRUE";
attribute KEEP of Z12: signal is "TRUE";
attribute KEEP of Z13: signal is "TRUE";
attribute KEEP of Z14: signal is "TRUE";
attribute KEEP of Z15: signal is "TRUE";
attribute KEEP of Z16: signal is "TRUE";
attribute KEEP of Z17: signal is "TRUE";
attribute KEEP of Z18: signal is "TRUE";
attribute KEEP of Z19: signal is "TRUE";
attribute KEEP of Z20: signal is "TRUE";

```

```

signal Iin_ext,Qin_ext: std_logic_vector(bitwidth+2 -1 downto 0);
attribute KEEP of Iin_ext,Qin_ext: signal is "TRUE";

begin
-- Sign extention to compensat the cordic gain 1.64xxxxxx
-- one more option for sign extention is using resize() function from
numeric_std library.
--works on signed and unsigned.
Iin_ext <= ((Iin(bitwidth-1)&Iin(bitwidth-1)) & Iin(bitwidth-1 downto
0));
Qin_ext <= ((Qin(bitwidth-1)&Qin(bitwidth-1)) & Qin(bitwidth-1 downto
0));
--phase_inc := phase_step;
--Iin_ext <= resize(Iin,26);
--Qin_ext <= resize(Qin,26);

Qudrant_process :process(CLK, RST,Iin_ext,Qin_ext,Zin)
begin
if rising_edge(CLK) then
    if RST = '1' then
        I0 <= (others => '0');
        Q0 <= (others => '0');
        Z0 <= (others => '0');
    else
--      case (Zin(Zin'high-1 downto Zin'high-2)) is -- error's out in
modelsim "case expression must be logically static"
        case (Zin(24-1 downto 24-2)) is
            when "00" => -- no pre-rotation
                I0 <= (Iin_ext);
                Q0 <= (Qin_ext);
                Z0 <= (Zin);
            when "01" => --interval between 90 to 180 degrees
                I0 <= -(Qin_ext);
                Q0 <= (Iin_ext);
                Z0 <= ("00" & Zin(zwidth-2-1 downto 0)); -- phase
rotation to +90 deg
            when "10" => --interval between -180 to -90 degrees
                I0 <= (Qin_ext);
                Q0 <= -(Iin_ext);
                Z0 <= ("11" & Zin(zwidth-2-1 downto 0)); -- Phase
rotatio to -90 deg
            when "11" => ---- no pre-rotation
                I0 <= (Iin_ext);
                Q0 <= (Qin_ext);
                Z0 <= (Zin);
            when others =>
                I0 <= (others => '0');
                Q0 <= (others => '0');
                Z0 <= (others => '0');
        end case;
    end if;
end if;
end process;

```

-- In this style of the portmap the order of the signals inside the braces are important

```
STAGE_0      : CORDIC_STAGE generic map(zwidth, bitwidth+2, 0) PORT
MAP(CLK,RST,ddc_en,I0,Q0,Z0,C0,I1,Q1,Z1);
STAGE_1      : CORDIC_STAGE generic map(zwidth, bitwidth+2, 1) PORT
MAP(CLK,RST,ddc_en,I1,Q1,Z1,C1,I2,Q2,Z2);
STAGE_2      : CORDIC_STAGE generic map(zwidth, bitwidth+2, 2) PORT
MAP(CLK,RST,ddc_en,I2,Q2,Z2,C2,I3,Q3,Z3);
STAGE_3      : CORDIC_STAGE generic map(zwidth, bitwidth+2, 3) PORT
MAP(CLK,RST,ddc_en,I3,Q3,Z3,C3,I4,Q4,Z4);
STAGE_4      : CORDIC_STAGE generic map(zwidth, bitwidth+2, 4) PORT
MAP(CLK,RST,ddc_en,I4,Q4,Z4,C4,I5,Q5,Z5);
STAGE_5      : CORDIC_STAGE generic map(zwidth, bitwidth+2, 5) PORT
MAP(CLK,RST,ddc_en,I5,Q5,Z5,C5,I6,Q6,Z6);
STAGE_6      : CORDIC_STAGE generic map(zwidth, bitwidth+2, 6) PORT
MAP(CLK,RST,ddc_en,I6,Q6,Z6,C6,I7,Q7,Z7);
STAGE_7      : CORDIC_STAGE generic map(zwidth, bitwidth+2, 7) PORT
MAP(CLK,RST,ddc_en,I7,Q7,Z7,C7,I8,Q8,Z8);
STAGE_8      : CORDIC_STAGE generic map(zwidth, bitwidth+2, 8) PORT
MAP(CLK,RST,ddc_en,I8,Q8,Z8,C8,I9,Q9,Z9);
STAGE_9      : CORDIC_STAGE generic map(zwidth, bitwidth+2, 9) PORT
MAP(CLK,RST,ddc_en,I9,Q9,Z9,C9,I10,Q10,Z10);
STAGE_10     : CORDIC_STAGE generic map(zwidth, bitwidth+2, 10) PORT
MAP(CLK,RST,ddc_en,I10,Q10,Z10,C10,I11,Q11,Z11);
STAGE_11     : CORDIC_STAGE generic map(zwidth, bitwidth+2, 11) PORT
MAP(CLK,RST,ddc_en,I11,Q11,Z11,C11,I12,Q12,Z12);
STAGE_12     : CORDIC_STAGE generic map(zwidth, bitwidth+2, 12) PORT
MAP(CLK,RST,ddc_en,I12,Q12,Z12,C12,I13,Q13,Z13);
STAGE_13     : CORDIC_STAGE generic map(zwidth, bitwidth+2, 13) PORT
MAP(CLK,RST,ddc_en,I13,Q13,Z13,C13,I14,Q14,Z14);
STAGE_14     : CORDIC_STAGE generic map(zwidth, bitwidth+2, 14) PORT
MAP(CLK,RST,ddc_en,I14,Q14,Z14,C14,I15,Q15,Z15);
STAGE_15     : CORDIC_STAGE generic map(zwidth, bitwidth+2, 15) PORT
MAP(CLK,RST,ddc_en,I15,Q15,Z15,C15,I16,Q16,Z16);
STAGE_16     : CORDIC_STAGE generic map(zwidth, bitwidth+2, 16) PORT
MAP(CLK,RST,ddc_en,I16,Q16,Z16,C16,I17,Q17,Z17);
STAGE_17     : CORDIC_STAGE generic map(zwidth, bitwidth+2, 17) PORT
MAP(CLK,RST,ddc_en,I17,Q17,Z17,C17,I18,Q18,Z18);
STAGE_18     : CORDIC_STAGE generic map(zwidth, bitwidth+2, 18) PORT
MAP(CLK,RST,ddc_en,I18,Q18,Z18,C18,I19,Q19,Z19);
STAGE_19     : CORDIC_STAGE generic map(zwidth, bitwidth+2, 19) PORT
MAP(CLK,RST,ddc_en,I19,Q19,Z19,C19,I20,Q20,Z20);

Iout <= I20(bitwidth+1 downto 2);
Qout <= Q20(bitwidth+1 downto 2);
Zout <= Z20;
end Behavioral;
```

CORDIC_STAGE.vhd

-- Company: Western Michigan University

```

-- Engineer: Nagarjun Marappa
--
-- Create Date:    17:07:42 03/17/2014
-- Design Name:
-- Module Name:    CORDIC_STAGE - Behavioral
-- Revised on the final implementation on 2/8/2015
-----
-----
library IEEE;
use IEEE.STD_LOGIC_1164.ALL;

use IEEE.std_logic_arith.ALL;
use IEEE.STD_LOGIC_UNSIGNED.all;

entity CORDIC_STAGE is
generic (zwidth : natural := 24;
          bitwidth : natural := 26;
          shift : natural := 1
          );
  Port ( CLK          : in    STD_LOGIC;
        RST          : in    STD_LOGIC;
        en           : in    STD_LOGIC;
        Iin         : in    STD_LOGIC_VECTOR (bitwidth-1 downto 0);
        Qin         : in    STD_LOGIC_VECTOR (bitwidth-1 downto 0);
        zin         : in    STD_LOGIC_VECTOR (zwidth-1 downto 0);
        C_consts    : in    STD_LOGIC_VECTOR (zwidth-1 downto 0);
        Iout        : out    STD_LOGIC_VECTOR (bitwidth-1 downto 0);
        Qout        : out    STD_LOGIC_VECTOR (bitwidth-1 downto 0);
        zout        : out    STD_LOGIC_VECTOR (zwidth-1 downto 0));
end CORDIC_STAGE;

architecture Behavioral of CORDIC_STAGE is

begin
main_process: process (CLK, Iin, Qin , zin, C_consts)
begin
if rising_edge (CLK) then
  if RST = '1' then
    Iout <= (others=>'0');
    Qout <= (others=>'0');
    zout <= (others=>'0');
  else
--    if en = '1' then
      if(zin(zwidth - 1) = '1') then
        Iout <= Iin + ((shift downto 0 => Qin(bitwidth-1)) &
Qin(bitwidth-2 downto shift));
        Qout <= Qin - ((shift downto 0 => Iin(bitwidth-1)) &
Iin(bitwidth-2 downto shift));
        zout <= zin + C_consts;
      else
        Iout <= Iin - ((shift downto 0 => Qin(bitwidth-1)) &
Qin(bitwidth-2 downto shift));
        Qout<= Qin + ((shift downto 0 => Iin(bitwidth-1)) &
Iin(bitwidth-2 downto shift));
        zout<= zin - C_consts;
      end if;
    end if;
  end if;
end process;
end Behavioral;

```

```

        end if;
    --     end if;
    end if;
end process;

end Behavioral;

```

cic_decim.vhd

```

-----
-----
-- Company: Western Michigan University
-- Engineer: Nagarjun Marappa
--
-- Create Date:    16:53:09 06/21/2014
-- Design Name:    Dr.Bazuin-SDR-LAB
-- Module Name:    ddc_chain - Behavioral
--
-----
-----
library IEEE;
use IEEE.STD_LOGIC_1164.ALL;
use IEEE.STD_LOGIC_SIGNED.ALL;

use IEEE.NUMERIC_STD.ALL;

entity cic_decim is
    generic(bits_in: natural := 24; -- natural range 0 to integer'HIGH
            log2_max_rate: natural := 7;
            K : natural := 3
            );
    port (CLK          : IN STD_LOGIC;
          RST          : IN STD_LOGIC;
          cic_en       : IN STD_LOGIC;
          strobe_in    : IN STD_LOGIC;
          strobe_out   : IN STD_LOGIC;
          rate         : IN STD_LOGIC_VECTOR(8-1 downto 0);
          signal_in    : IN STD_LOGIC_VECTOR(bits_in-1 downto 0);
          signal_out   : OUT STD_LOGIC_VECTOR(bits_in-1 downto 0)
          );
end cic_decim;

architecture Behavioral of cic_decim is

    component sign_extend is
        generic(bitsin: natural := 24;
                bitsout: natural := 25);
        port (CLK : in std_logic;
              RST : in std_logic;
              signal_in : in std_logic_vector(bitsin-1 downto 0);
              signal_out: out std_logic_vector(bitsout-1 downto 0)
              );
    end component;

```



```

component cic_decim_prun is
generic(bitsin: natural := 24;
        maxbitgain: natural := 21);
port (rate: in std_logic_vector(8-1 downto 0);
       signal_in : in std_logic_vector(bitsin+maxbitgain-1 downto
0);
       signal_out: out std_logic_vector(bitsin-1 downto 0)
       );
end component;

constant maxbitgain : natural := K*log2_max_rate;

type cic_reg is array (integer range <>) of
std_logic_vector(bits_in+maxbitgain-1 downto 0);
signal integrator      : cic_reg(K-1 downto 0);
signal pipeline       : cic_reg(K-1 downto 0);
signal differentiator: cic_reg(K-1 downto 0);

signal signal_in_ext   : std_logic_vector(bits_in+maxbitgain-1 downto
0);
signal signal_out_prun: std_logic_vector(bits_in-1 downto 0):= (others
=> '0');
signal sampler : std_logic_vector(bits_in+maxbitgain-1 downto 0):=
(others => '0');
-- NOTE: Samples needs to be initialized or else there will be unknown
signal out for some time period since
-- integrator would have finished computing

attribute KEEP: string;
attribute KEEP of signal_in_ext : signal is "TRUE";
attribute KEEP of integrator    : signal is "TRUE";
attribute KEEP of pipeline     : signal is "TRUE";
attribute KEEP of differentiator : signal is "TRUE";

begin

--signal_in_ext <=((maxbitgain-1 downto 0 => signal_in(bits_in-1)) &
signal_in);

integrating: process (CLK, RST, strobe_out)
begin
    if rising_edge(CLK) then
        if (RST = '1' or cic_en = '0') then
            for i in 0 to K-1 loop
                integrator(i) <= (others =>'0');
            end loop;
        else if (strobe_in = '1') then

            integrator(0) <= integrator(0)+ signal_in_ext;
            for i in 1 to K-1 loop
                integrator(i) <= integrator(i)+integrator(i-1);
            end loop;
        end if;
    end if;

```

```

    end if;
end process;

Comb_Filter: process (CLK, RST, strobe_out)
begin
    if rising_edge(CLK) then
        if(RST = '1' or cic_en = '0') then
            for i in 0 to K-1 loop
                pipeline(i) <= (others => '0');
                differentiator(i) <= (others => '0');
            end loop;
        else if (strobe_out = '1') then
            sampler <= integrator(K-1);
            differentiator(0) <= sampler;
            pipeline(0) <= sampler - differentiator(0);
            for i in 1 to K-1 loop
                differentiator(i) <= pipeline(i-1);
                pipeline(i) <= pipeline(i-1) -
differentiator(i);
            end loop;
        end if;
    end if;
end process;

--signal_out_buff <= differentiator(K-1);
--signal_out <= signal_out_buff(bits_in-1 downto 0);
signal_out <= signal_out_prun when RST = '0' else (others => '0');

sign_ext: sign_extend generic map(bitsin => bits_in,
                                bitsout=> bits_in+maxbitgain)
    port map(CLK => CLK,
            RST => RST,
            signal_in =>signal_in,
            signal_out=>signal_in_ext);

cic_prun: cic_decim_prun generic map(bitsin => bits_in,
                                maxbitgain => maxbitgain)
    port map(rate => rate,
            signal_in =>pipeline(K-1),
            signal_out=>signal_out_prun);

end Behavioral;

```

small_hb_top.vhd

```

-----
-----
-- Company: Western Michigan University
-- Engineer: Nagarjun Marappa
--
-- Create Date:    16:53:09 06/21/2014
-- Design Name:    Dr.Bazuin-SDR-LAB
-- Module Name:    ddc_chain - Behavioral
--

```

```

-----
-----
library IEEE;
use IEEE.STD_LOGIC_1164.ALL;
USE IEEE.STD_LOGIC_UNSIGNED.ALL;
use IEEE.STD_LOGIC_ARITH.ALL;

-- Uncomment the following library declaration if using
-- arithmetic functions with Signed or Unsigned values
--use IEEE.NUMERIC_STD.ALL;

-- Uncomment the following library declaration if instantiating
-- any Xilinx primitives in this code.
library UNISIM;
use UNISIM.VComponents.all;

entity Small_HB_top is
generic(
    INWIDTH : natural := 24;
    round_width : natural := 17;
    accum_width : natural := 30;
    D_CARE_VAL : std_logic:='X'
);
port (
    CLK          : in std_logic;
    RST          : in std_logic;
    enable       : in std_logic;
    bypass       : in std_logic;
    -- IN_RATE    : in std_logic_vector(7 downto 0);
    samples_in   : in std_logic_vector(INWIDTH-1 downto 0);
    samples_out  : out std_logic_vector(INWIDTH-1 downto 0);
    strobe_in    : in std_logic; -- remove CIC strober!!
    strobe_out   : out std_logic
);
end Small_HB_top;

architecture Behavioral of Small_HB_top is

component round_sd is
generic ( WIDTH_IN : natural := 24;
          WIDTH_OUT: natural := 17);
port(
    CLK          : in std_logic;
    RST          : in std_logic;
    strobe_in: in std_logic;
    data_in : in std_logic_vector(WIDTH_IN-1 downto 0);
    data_out : out std_logic_vector(WIDTH_OUT-1 downto 0);
    strobe_out: out std_logic
);
end component round_sd;

component clip is
generic( bitsin: natural:=INWIDTH+1;
        bitsout: natural := INWIDTH);
port( data_in : in std_logic_vector(bitsin-1 downto 0);

```

```

        data_out: out std_logic_vector(bitsout-1 downto 0)
    );
end component clip;
signal strobe_hb : std_logic;
signal round_data_in : std_logic_vector(round_width-1 downto 0);

--*****
-- | Filtering signals and constants | --
--*****
constant coeff_a : integer := -10690;--"111101011000111110"
constant coeff_b : integer := 75809;--"010010100000100001"
signal go, go_d1, go_d2, go_d3, go_d4: std_logic;
signal phase : std_logic;
signal Z1,Z2,Z3,Z4,Z5,Z6 : std_logic_vector(round_width-1 downto 0) :=
(others => '0');
signal sum_a, sum_b : std_logic_vector(round_width downto 0);-- :=
(others => '0');
signal extnd_in, extnd_Z2, extnd_Z4, extnd_Z6 :
std_logic_vector(round_width downto 0):= (others => '0');
signal middle : std_logic_vector(round_width downto 0);

signal coeff_reg      : std_logic_vector(round_width downto 0) := (others
=> '0');
signal sum_reg        : std_logic_vector(round_width downto 0) := (others
=> '0');
signal prod_reg       : std_logic_vector(accum_width-1 downto 0):= (others =>
'0');
signal middle_reg, middle_d1 : std_logic_vector(accum_width-1 downto
0):= (others => '0');
signal accum          : std_logic_vector(accum_width-1 downto 0);
signal product        : std_logic_vector(36-1 downto 0);
signal mult_CE        : std_logic;
signal samples_out_buff : std_logic_vector(INWIDTH-1 downto 0);

signal accum_rnd      : std_logic_vector(INWIDTH downto 0);
signal stb_rnd : std_logic;
attribute KEEP : string;
attribute KEEP of round_data_in: signal is "TRUE";
attribute KEEP of Z1,Z2,Z3,Z4,Z5,Z6: signal is "TRUE";
attribute KEEP of phase: signal is "TRUE";
attribute KEEP of go, go_d1, go_d2, go_d3, go_d4: signal is "TRUE";
attribute KEEP of sum_a,sum_b: signal is "TRUE";
attribute KEEP of extnd_in,extnd_Z2,extnd_Z4,extnd_Z6: signal is
"TRUE";
attribute KEEP of coeff_reg: signal is "TRUE";
attribute KEEP of sum_reg: signal is "TRUE";
attribute KEEP of middle,middle_d1,middle_reg: signal is "TRUE";
attribute KEEP of prod_reg: signal is "TRUE";
attribute KEEP of accum_rnd: signal is "TRUE";

type coeff_ram is array(1 downto 0) of std_logic_vector(17 downto 0);
signal coeff : coeff_ram :=
(
    0 => "111101011000111110", -- coeff_a
    1 => "010010100000100001",-- coeff_b

```

```

        others => (others=>'0')
    );

    attribute KEEP of coeff: signal is "TRUE";

begin
    process (CLK, RST)
    begin
        if rising_edge(CLK) then
            if RST = '1' or enable = '0' then
                phase <= '0';
            else
                if strobe_hb = '1' then
                    phase <= not(phase);
                end if;
            end if;
            -- go <= strobe_hb and phase;
        end if;
    end process;
    go <= strobe_hb and phase;
    --#####
    triggre: process(CLK, RST)
    begin
        if rising_edge(CLK) then
            if(RST = '1' or enable = '0')then
                go_d1 <= '0';
                go_d2 <= '0';
                go_d3 <= '0';
                go_d4 <= '0';
            else
                go_d1 <= go;
                go_d2 <= go_d1;
                go_d3 <= go_d2;
                go_d4 <= go_d3;
            end if;
        end if;
    end process triggre;
    --#####
    shift_reg: process(CLK, RST)
    begin
        if rising_edge(CLK) then
            if( RST = '1' or enable = '0')then
                Z1 <= (others => '0');
                Z2 <= (others => '0');
                Z3 <= (others => '0');
                Z4 <= (others => '0');
                Z5 <= (others => '0');
                Z6 <= (others => '0');
            else if (strobe_hb = '1') then
                Z1 <= round_data_in;
                Z2 <= Z1;
                Z3 <= Z2;
                Z4 <= Z3;
                Z5 <= Z4;
                Z6 <= Z5;
            end if;
        end if;
    end process shift_reg;
end;

```

```

                end if;
            end if;
        end if;
    end process shift_reg;
--#####
Sign_extend: process (CLK, RST)
begin
    if rising_edge(CLK) then
        if RST = '1' then
            extnd_in <= (others => '0');
            extnd_Z6 <= (others => '0');
            extnd_Z2 <= (others => '0');
            extnd_Z4 <= (others => '0');
        else
            extnd_in <= (round_data_in(round_width-1) &
round_data_in(round_width-1 downto 0));
            extnd_Z6 <= (Z6(round_width-1) & Z6(round_width-1 downto
0));
            extnd_Z2 <= (Z2(round_width-1) & Z2(round_width-1 downto
0));
            extnd_Z4 <= (Z4(round_width-1) & Z4(round_width-1 downto
0));
        end if;
    end if;
end process Sign_extend;
--
----#####
filter_reg : process(CLK, RST, go_d1)
begin
    if rising_edge(CLK) then
        if RST = '1' then
            sum_reg <= (others => '0');
            coeff_reg <= (others => '0');
        else if (go_d1 = '1') then
            sum_reg <= sum_b;
            coeff_reg <= "010010100000100000";
        else
            sum_reg <= sum_a;
            coeff_reg <= "111101011000111110";
        end if;
    end if;
end if;
end process;

----#####
-- 3/7/2015 -- timing adjustments for summing
sum_process: process(CLK,RST,go)
begin
    if rising_edge(CLK) then
        if RST = '1' then
            sum_a <= (others=>'0');
            sum_b <= (others=>'0');
            middle <=(others=>'0');
        else
            if go = '1' then

```

```

        sum_a <= extnd_in + extnd_Z6;
        sum_b <= extnd_Z2 + extnd_Z4;
        middle <= Z3 & '0';
    end if;
end if;
end if;
end process;

process(CLK, go_d1)
begin
if rising_edge(CLK) then
    if go_d1 = '1' then
        middle_reg <=
(middle(round_width)&middle(round_width)&middle&((round_width-
1+accum_width-36)-1 downto 0 => '0'));
    end if;
end if;
end process;

mult_CE <= go_d1 or go_d2;
--#####
accumulate: process(CLK, RST)
begin
    if rising_edge(CLK) then
        if (RST = '1' or enable = '0') then
            accum <= (others=>'0');
        else if go_d2 = '1' then
            accum <= middle_reg + prod_reg;
        else if go_d3 = '1' then
            accum <= accum + prod_reg;
        end if;
    end if;
end if;
end process accumulate;

Round_In: round_sd generic map(
    WIDTH_IN => INWIDTH,
    WIDTH_OUT => round_width)
port map(
    CLK => CLK,
    RST => RST,
    strobe_in => strobe_in,
    data_in => samples_in,
    data_out => round_data_in,
    strobe_out => strobe_hb
);
-- Multiplier Instantiation
Multiplier : MULT18X18S port map
(P => product,
 B => sum_reg,
 A => coeff_reg,
 C => CLK,
 CE=> mult_CE,
 R => RST

```

```

    );
    prod_reg <= product(36-1 downto 36-accum_width);

    Round_Accum: round_sd generic map(
        WIDTH_IN => accum_width,
        WIDTH_OUT => INWIDTH+1
    )
    port map(
        CLK => CLK,
        RST => RST,
        strobe_in => go_d4,
        data_in => accum,
        data_out => accum_rnd,
        strobe_out=> stb_rnd
    );

    clip_shb_out: clip generic map(
        bitsin => INWIDTH+1,
        bitsout => INWIDTH)
    port map(
        data_in => accum_rnd,
        data_out=> samples_out_buff
    );

    sync2clk: process(CLK, RST)
    begin
    if rising_edge(CLK) then
        if bypass = '0' then
            samples_out <= samples_out_buff;
            strobe_out <= stb_rnd;
        else
            samples_out <= samples_in;
            strobe_out <= strobe_in;
        end if;
    end if;
    end process sync2clk;
end Behavioral;

```

large_hb_top.vhd

```

-----
-----
-- Company: Western Michigan University
-- Engineer: Nagarjun Marappa
--
-- Create Date:    16:53:09 06/21/2014
-- Design Name:    Dr.Bazuin-SDR-LAB
-- Module Name:    ddc_chain - Behavioral
-----
-----

library IEEE;
use IEEE.STD_LOGIC_1164.ALL;

```



```

use IEEE.STD_LOGIC_UNSIGNED.ALL;
use IEEE.std_logic_arith.all;
use IEEE.std_logic_misc.all;
library UNISIM;
use UNISIM.VComponents.all;

entity large_hb is
generic(WIDTH: natural := 24
        );
port( CLK : in std_logic;
      RST : in std_logic;
      bypass: in std_logic;
      run: in std_logic;
      cpi : in std_logic_vector(8 downto 0);
      strobe_in: in std_logic;
      data_in : in std_logic_vector(WIDTH-1 downto 0);
      data_out: out std_logic_vector(WIDTH-1 downto 0);
      strobe_out: out std_logic
    );
end large_hb;

architecture Behavioral of large_hb is
  component round_sd is
    generic ( WIDTH_IN : natural := 24;
              WIDTH_OUT: natural := 17;
              DISABLE_SD: natural := 0);

    port(
      CLK          : in std_logic;
      RST          : in std_logic;
      strobe_in: in std_logic;
      data_in : in std_logic_vector(WIDTH_IN-1 downto 0);
      data_out : out std_logic_vector(WIDTH_OUT-1 downto 0);
      strobe_out: out std_logic
    );
  end component round_sd;
  -- SRL16E SHIFT REGISTER MODULE
  component srl_module is
    generic(WIDTH : natural:= 17);
    port( CLK : in std_logic;
          RST : in std_logic;
          enable: in std_logic;
          data_in : in std_logic_vector(WIDTH-1 downto 0);
          addr : in std_logic_vector(3 downto 0);
          Q_out : out std_logic_vector(WIDTH-1 downto 0)
        );
  end component srl_module;
  -- ACCUMULATOR 27 bit
  component acc is
    generic(IWIDTH: natural:= 25;
           OWIDTH: natural:= 27);
    port(
      CLK          : in std_logic;
      RST          : in std_logic;
      clear       : in std_logic;
      acc         : in std_logic;
    );
  end component acc;
end architecture Behavioral;

```

```

        data_in : in std_logic_vector(IWIDTH-1 downto 0);
        data_out : out std_logic_vector(OWIDTH-1 downto 0)
    );
end component;
-- SIGN EXTENTION
component sign_extend is
generic( bitsin: natural := 24;
        bitsout: natural := 25);
    Port(CLK : in std_logic;
        RST : in std_logic;
        signal_in : in STD_LOGIC_VECTOR (bitsin-1 downto 0);
        signal_out : out STD_LOGIC_VECTOR (bitsout-1 downto 0)
    );
end component sign_extend;
-- OUTPUT CLIP
component clip is
generic( bitsin: natural:=25;
        bitsout: natural := 24);
port( data_in : in std_logic_vector(bitsin-1 downto 0);
      data_out: out std_logic_vector(bitsout-1 downto 0)
    );
end component;

constant INTWIDTH: natural:= 17; --integer width
constant accwidth: natural:= WIDTH+3; --accumulator width
constant SHIFT_FACTOR: natural:= 6;

-- signals from/to input round module
signal rnd_data_in: std_logic_vector(INTWIDTH-1 downto 0);
signal stb_rnd: std_logic;

-- DELAY ELEMENTS ADDR/DATA OF UPPER POLYPHASE STRUCTURE
signal addr_odd_a, addr_odd_b, addr_odd_c, addr_odd_d :
std_logic_vector(4-1 downto 0);
signal data_odd_a, data_odd_b, data_odd_c, data_odd_d :
std_logic_vector(INTWIDTH-1 downto 0);
signal data_even : std_logic_vector(INTWIDTH-1 downto 0);
-- signal RATE : std_logic_vector(8-1 downto 0) := x"12";
signal odd: std_logic:= '0';
signal write_odd, write_even : std_logic:= '0';
signal addr_even : std_logic_vector(4-1 downto 0);
signal phase: std_logic_vector(2 downto 0):= "000";
signal phase_d1: std_logic_vector(2 downto 0):= "000";

-- LOGIC BLOCK ENABLE CONTROL SIGNALS
signal stb_out_pre : std_logic_vector(15 downto 0);
signal do_acc: std_logic := '0';
signal do_mult: std_logic := '1';
signal clear : std_logic:= '0';
signal coeff1, coeff2 : std_logic_vector(INTWIDTH downto 0):=
(others=>'0'); --18 bit
signal sum1, sum2 : std_logic_vector(INTWIDTH downto 0):= (others =>
'0'); --18 bit
signal prod1, prod2 : std_logic_vector(2*INTWIDTH+1 downto 0):= (others
=> '0'); --36 bit

```

```

signal sum_of_prod : std_logic_vector(2*INTWIDTH+1 downto 0) := (others
=> '0');
signal acc_out : std_logic_vector(ACCWIDTH-1 downto 0);
-- SIGNALS FOR EVEN PATH
signal data_even_signext: std_logic_vector(ACCWIDTH-1 downto 0);

signal final_sum : std_logic_vector(ACCWIDTH-1 downto 0);
signal final_sum_clip: std_logic_vector(WIDTH-1 downto 0);

signal selected_stb: std_logic;

attribute KEEP:string;
attribute KEEP of sum_of_prod : signal is "TRUE";
attribute KEEP of acc_out : signal is "TRUE";
attribute KEEP of final_sum : signal is "TRUE";

begin -- architecture

process(CLK, RST)
begin
if rising_edge(CLK) then
    if (RST = '1' or run = '0') then
        odd <= '0';
    else if (stb_rnd = '1') then
        odd <= not(odd);
    end if;
end if;
end if;
end process;

write_odd <= stb_rnd and odd;
write_even<= stb_rnd and not(odd);

phase_counter: process(CLK, RST)
begin
if rising_edge(CLK) then
    if (RST = '1' or run = '0') then
        phase <= "000";
    else if((stb_rnd and odd) = '1' ) then
        phase <= "001";
    else if(phase = "100") then
        phase <= "000";
    else if(phase /= "000") then
        phase <= phase + '1';
    end if;
end if;
end if;
end if;
end process phase_counter;

process(CLK)
begin
    if rising_edge(CLK) then
        phase_d1 <= phase;

```

```

    end if;
end process;

acc_ctrl: process (CLK, RST)
begin
if rising_edge(CLK) then
    if RST = '1' then
        stb_out_pre <= (others => '0');
    else
        stb_out_pre <= (stb_out_pre(14 downto 0) & (stb_rnd and odd));
    end if;
end if;
end process acc_ctrl;

-- moved or operation 1 bit to left compared to original to compensate
-- one clock cycle delay introduced from the process below\
-- Verilog reg data type would not require a clock cycle delay but VHDL
-- signals do.
--do_acc <= or_reduce(stb_out_pre(6 downto 3));
do_acc <= or_reduce(stb_out_pre(8 downto 5));
clear <= stb_out_pre(3);
-- addr_control logic
process (CLK,RST,phase)
begin
if (CLK'EVENT and CLK = '1') then
    if RST = '1' then
        addr_odd_a <= (others=>'0');
        addr_odd_b <= (others=>'0');
    else
        case(phase) is
            when "001" =>
                addr_odd_a <= x"0";
                addr_odd_b <= x"F";
            when "010" =>
                addr_odd_a <= x"1";
                addr_odd_b <= x"E";
            when "011" =>
                addr_odd_a <= x"2";
                addr_odd_b <= x"D";
            when "100" =>
                addr_odd_a <= x"3";
                addr_odd_b <= x"C";
            when others =>
                addr_odd_a <= x"0";
                addr_odd_b <= x"F";
        end case;
    end if;--rst
end if;--clk
end process;
process (CLK,RST,phase)
begin
if (CLK'EVENT and CLK = '1') then
    if RST = '1' then
        addr_odd_c <= (others=>'0');
        addr_odd_d <= (others=>'0');
    end if;
end if;
end process;

```

```

else
    case(phase) is
        when "001" =>
            addr_odd_c <= x"4";
            addr_odd_d <= x"B";
        when "010" =>
            addr_odd_c <= x"5";
            addr_odd_d <= x"A";
        when "011" =>
            addr_odd_c <= x"6";
            addr_odd_d <= x"9";
        when "100" =>
            addr_odd_c <= x"7";
            addr_odd_d <= x"8";
        when others =>
            addr_odd_c <= x"4";
            addr_odd_d <= x"B";
    end case;
end if;
end if;
end process;

-- data handling logic
coefficient1:process(CLK,RST,phase_d1)
begin
if(CLK'EVENT and CLK = '1') then
    if RST = '1' then
        coeff1 <= (others=>'0');
    else
        case phase_d1 is
            when "001" =>
                coeff1 <= conv_std_logic_vector(-107 , 18);
            when "010" =>
                coeff1 <= conv_std_logic_vector( 445 , 18);
            when "011" =>
                coeff1 <= conv_std_logic_vector(-1271, 18);
            when "100" =>
                coeff1 <= conv_std_logic_vector(2959 , 18);
            when others =>
                coeff1 <= conv_std_logic_vector(-107 , 18);
        end case;
    end if;
end if;
end process coefficient1;

coefficient2:process(CLK,RST,phase_d1)
begin
if(CLK'EVENT and CLK = '1') then
    if RST = '1' then
        coeff2 <= (others=>'0');
    else
        case phase_d1 is
            when "001" =>
                coeff2 <= conv_std_logic_vector(-6107 , 18);

```

```

        when "010" =>
            coeff2 <= conv_std_logic_vector(11963 , 18);
        when "011" =>
            coeff2 <= conv_std_logic_vector(-24706, 18);
        when "100" =>
            coeff2 <= conv_std_logic_vector(82359 , 18);
        when others =>
            coeff2 <= conv_std_logic_vector(-6107 , 18);
    end case;
end if;
end if;
end process coefficient2;

process(CLK, RST, cpi)
begin
    case(cpi) is
        when ('0' & x"02") =>
            addr_even <= x"9";
        when
            ('0' & x"03") | ('0' & x"04") | ('0' & x"05") | ('0' & x"06") | ('0' & x"07") =>
            addr_even <= x"8";
        when others =>
            addr_even <= x"7";
    end case;
end process;

round_in: round_sd generic map(
    WIDTH_IN => WIDTH,
    WIDTH_OUT => INTWIDTH)
port map(
    CLK => CLK,
    RST => RST,
    strobe_in => strobe_in,
    data_in => data_in,
    data_out => rnd_data_in,
    strobe_out => stb_rnd
);

--
=====
-- Polyphase 1st path filter
--
=====

srl_odd_a: srl_module generic map(INTWIDTH)port map(CLK, RST,
write_odd, rnd_data_in, addr_odd_a, data_odd_a);
srl_odd_b: srl_module generic map(INTWIDTH)port map(CLK, RST,
write_odd, rnd_data_in, addr_odd_b, data_odd_b);
srl_odd_c: srl_module generic map(INTWIDTH)port map(CLK, RST,
write_odd, rnd_data_in, addr_odd_c, data_odd_c);
srl_odd_d: srl_module generic map(INTWIDTH)port map(CLK, RST,
write_odd, rnd_data_in, addr_odd_d, data_odd_d);

accumulator: process(CLK)
begin

```

```

        if rising_edge(CLK) then
            sum1 <= (data_odd_a(INTWIDTH-1) &
data_odd_a)+(data_odd_b(INTWIDTH-1) & data_odd_b);
            sum2 <= (data_odd_c(INTWIDTH-1) &
data_odd_c)+(data_odd_d(INTWIDTH-1) & data_odd_d);
        end if;
    end process accumulator;

do_mult <= '1'; -- multipliers are always enabled
mult1: MULT18X18S port map(
    C    => CLK,
    CE => do_mult,
    R    => RST,
    P    => prod1,
    A    => coeff1,
    B    => sum1
);
mult2: MULT18X18S port map(
    C    => CLK,
    CE => do_mult,
    R    => RST,
    P    => prod2,
    A    => coeff2,
    B    => sum2
);

prod_summer: process(CLK)
begin
    if rising_edge(CLK) then
        sum_of_prod <= prod1 + prod2;
    end if;
end process prod_summer;

final_accum : acc generic map(
    IWIDTH => ACCWIDTH-2,
    OWIDTH => ACCWIDTH
)
port map(
    CLK => CLK,
    RST => RST,
    clear => clear,
    acc => do_acc,
    data_in => sum_of_prod(35 downto 38-ACCWIDTH),
    data_out => acc_out
);

--
=====
-- Polyphase 2nd path filter
--
=====
srl_even : srl_module generic map(INTWIDTH)port map(CLK, RST,
write_even, rnd_data_in, addr_even, data_even);

```

```

data_eve_ext:
    sign_extend generic map(
        bitsin => INTWIDTH,
        bitsout=> ACCWIDTH-SHIFT_FACTOR)
    port map(
        CLK => CLK,
        RST => RST,
        signal_in => data_even,
        signal_out=> data_even_signext(ACCWIDTH-1 downto SHIFT_FACTOR)
    );
data_even_signext(SHIFT_FACTOR-1 downto 0) <= (others => '0');

process (CLK, RST)
begin
    if rising_edge(CLK) then
        if RST = '1' then
            final_sum <= (others=> '0');
        else
            final_sum <= acc_out + data_even_signext;
        end if;
    end if;
end process;

output_clip:
clip generic map(
    bitsin => ACCWIDTH,
    bitsout=> WIDTH)
    port map(
        data_in => final_sum,
        data_out=> final_sum_clip
    );

selected_stb    <= stb_out_pre(10) when bypass = '0' else
                strobe_in;

OutPut: process (CLK, RST)
begin
    if rising_edge(CLK) then
        strobe_out <= selected_stb;
        if RST = '1' then
            data_out <= (others => '0');
        elsif selected_stb = '1' then
            data_out <= final_sum_clip;
        --
        end if;
    end if;
end process OutPut;

end Behavioral;

```


Appendix C - Pattern Generator Code

wb_slv_cram.vhd

```
-----  
-----  
-- Company: Western Michigan University  
-- Engineer: Nagarjun Marappa  
--  
-- Create Date:      15:12:56 11/04/2013  
-- Design Name:  
-- Module Name:      wb_slv_cram - Behavioral  
--  
-----  
-----  
library IEEE;  
use IEEE.STD_LOGIC_1164.ALL;  
use IEEE.numeric_std.all;  
  
library work;  
use work.zpu_memory.all;  
  
entity wb_slv_cram is  
  generic(  
    WORD_SIZE   : natural:=32;  -- 32 bits data path  
    MDATA_SIZE  : natural:=16;  -- 32 bits data path  
    D_CARE_VAL  : std_logic:= 'X'; -- Fill value  
    CLK_FREQ    : positive:=50; -- 50 MHz clock  
    ADDR_W      : natural:=25;  -- M space = 32 MB, 16MB CRAM, 32 kB  
    DRAM, I/O space  
    CRAM_ADDR_W : natural:=24); -- CRAM space=128 Mb, 16MB  
  
  Port ( clk_i : in  STD_LOGIC;  
        rst_i  : in  STD_LOGIC;  
        wbs3_dat_o : OUT unsigned(WORD_SIZE-1 downto 0);  
        wbs3_ack_o : OUT std_logic;  
        wbs3_dat_i : IN  unsigned(WORD_SIZE-1 downto 0);  
        wbs3_we_i  : IN  std_logic;  
        wbs3_sel_i : IN  std_logic_vector(3 downto 0);  
        wbs3_adr_i : IN  unsigned(ADDR_W-1 downto 2);  
        wbs3_cyc_i : IN  std_logic;  
        wbs3_stb_i : IN  std_logic;  
  
        CramOE   : out std_logic;  
        CramWR   : out std_logic;  
        CramClk  : out std_logic;  
        CramAdv  : out std_logic;  
        CramWait : in  std_logic;  
        CramCS   : out std_logic;
```

```

        CramLB   : out std_logic;
        CramUB   : out std_logic;
        CramCRE  : out std_logic;

        MemAdr_o : out unsigned(CRAM_ADDR_W-1 downto 1);
        MemDB_i  : in  unsigned(MDATA_SIZE-1 downto 0);
        MemDB_o  : out unsigned(MDATA_SIZE-1 downto 0);
        MemDB_dir : out std_logic
    );

end wb_slv_cram;

architecture Behavioral of wb_slv_cram is
    constant BYTE_BITS : integer:=WORD_SIZE/16; -- # of bits in a word
    that addresses bytes

    COMPONENT cram_interface
    generic(
        WORD_SIZE   : natural:=32; -- 32 bits data path
        MDATA_SIZE  : natural:=16; -- 16 bits data to cram
        BYTE_BITS   : integer:=2;  -- Bits used to address bytes
        D_CARE_VAL  : std_logic:='X'; -- Fill value
        CLK_FREQ    : positive:=50; -- 50 MHz clock
        CRAM_ADDR_W : natural:=24); -- 24 bits RAM space=16MB -
128Mb
    PORT (
        clk_i : IN std_logic;
        rst_i : IN std_logic;
        we_i  : IN std_logic;
        en_i  : IN std_logic;
        addr_i : IN unsigned(CRAM_ADDR_W-1 downto BYTE_BITS);
        write_i : IN unsigned(WORD_SIZE-1 downto 0);
        MemDB_i : IN unsigned(MDATA_SIZE-1 downto 0);
        read_o  : OUT unsigned(WORD_SIZE-1 downto 0);
        busy_o  : OUT std_logic;
        CramOE  : OUT std_logic;
        CramWR  : OUT std_logic;
        CramClk : OUT std_logic;
        CramAdv : OUT std_logic;
        CramWait : IN std_logic;
        CramCS  : OUT std_logic;
        CramLB  : OUT std_logic;
        CramUB  : OUT std_logic;
        CramCRE : OUT std_logic;
        MemAdr_o : OUT unsigned(CRAM_ADDR_W-1 downto 1);
        MemDB_o  : OUT unsigned(MDATA_SIZE-1 downto 0);
        MemDB_dir : OUT std_logic
    );
    END COMPONENT;

    -- Memory (SinglePort_RAM)
    signal ram_busy      : std_logic;
    signal ram_we        : std_logic;
    signal ram_en        : std_logic;
    -- signal slv_cycle    : std_logic;

```

```

signal busy_ff      : std_logic;
signal busy_cond    : std_logic;

attribute KEEP : string;
attribute KEEP of ram_busy : signal is "TRUE";
attribute KEEP of ram_we   : signal is "TRUE";
attribute KEEP of busy_ff   : signal is "TRUE";
attribute KEEP of busy_cond: signal is "TRUE";

```

begin

```

cram_if: cram_interface
  generic map(
    WORD_SIZE => WORD_SIZE,
    MDATA_SIZE => MDATA_SIZE,
    BYTE_BITS => BYTE_BITS,
    CLK_FREQ => CLK_FREQ,
    CRAM_ADDR_W => CRAM_ADDR_W)

  port map(
    clk_i => clk_i,
    rst_i => rst_i,
    we_i => ram_we,
    en_i => ram_en,
    addr_i => wbs3_adr_i(CRAM_ADDR_W-1 downto 2),
    write_i => wbs3_dat_i,
    read_o => wbs3_dat_o,
    busy_o => ram_busy,

    CramOE => CramOE,
    CramWR => CramWR,
    CramClk => CramClk,
    CramAdv => CramAdv,
    CramWait => CramWait,
    CramCS => CramCS,
    CramLB => CramLB,
    CramUB => CramUB,
    CramCRE => CramCRE,

    MemAdr_o => MemAdr_o(CRAM_ADDR_W-1 downto 1),
    MemDB_i => MemDB_i,
    MemDB_o => MemDB_o,
    MemDB_dir => MemDB_dir
  );

ram_we <= wbs3_we_i and wbs3_stb_i;
ram_en <= wbs3_stb_i;

slave3_cycle:
process (clk_i)
begin
  if rising_edge(clk_i) then
    if rst_i = '1' then
      busy_ff <= '1';
    else -- reset_i='0'

```

```

        if wbs3_stb_i = '1' then
            busy_ff <= '0';
        else
            busy_ff <= '1';
        end if;
    end if; -- reset_i='0'
end if;
end process slave3_cycle;

busy_cond <= (busy_ff and wbs3_stb_i) or ram_busy;
wbs3_ack_o <= wbs3_stb_i and not(busy_cond);

```

```
end Behavioral;
```

cram_interface.vhd

```

-----
-----
-- Company: Western Michigan University
-- Engineer: Dr. Bradley J. Bazuin
--
-- Create Date:      09:42:12 11/06/2013
-- Design Name:
-- Module Name:      cram_interface - Behavioral
-----
-----
library IEEE;
use IEEE.STD_LOGIC_1164.ALL;
use IEEE.numeric_std.all;

-- Uncomment the following library declaration if using
-- arithmetic functions with Signed or Unsigned values
--use IEEE.NUMERIC_STD.ALL;

-- Uncomment the following library declaration if instantiating
-- any Xilinx primitives in this code.
--library UNISIM;
--use UNISIM.VComponents.all;

entity cram_interface is
    generic(
        WORD_SIZE   : natural:=32; -- 32 bits data path
        MDATA_SIZE  : natural:=16; -- 16 bits data to cram
        BYTE_BITS   : integer:=2;  -- Bits used to address bytes
        D_CARE_VAL  : std_logic:='X'; -- Fill value
        CLK_FREQ    : positive:=50; -- 50 MHz clock
        CRAM_ADDR_W : natural:=24); -- 24 bits RAM space=16MB -
128Mb

    Port (
        clk_i      : in  std_logic;
        rst_i      : in  STD_LOGIC;

```

```

we_i      : in  std_logic;
en_i      : in  std_logic;
addr_i    : in  unsigned(CRAM_ADDR_W-1 downto BYTE_BITS);
write_i   : in  unsigned(WORD_SIZE-1 downto 0);
read_o    : out unsigned(WORD_SIZE-1 downto 0);
  busy_o  : out std_logic;

CramOE    : out std_logic;
CramWR    : out std_logic;
CramClk   : out std_logic;
CramAdv   : out std_logic;
  CramWait : in  std_logic;
CramCS    : out std_logic;
CramLB    : out std_logic;
CramUB    : out std_logic;
  CramCRE  : out std_logic;

MemAdr_o  : out  unsigned(CRAM_ADDR_W-1 downto 1);
  MemDB_i  : in   unsigned(MDATA_SIZE-1 downto 0);
  MemDB_o  : out  unsigned(MDATA_SIZE-1 downto 0);
  MemDB_dir : out  std_logic
);
end cram_interface;

architecture Behavioral of cram_interface is

  -- Cellular RAM Signals
  signal ramOE      : std_logic;
  signal ramWR      : std_logic;
  signal ramCLK     : std_logic;
  signal ramAdv     : std_logic;
  signal ramWait    : std_logic;
  signal ramCS      : std_logic;
  signal ramLB      : std_logic;
  signal ramUB      : std_logic;
  signal ramCRE     : std_logic;

  signal data_read  : unsigned (WORD_SIZE-1 downto 0);

  signal ls_adr     : std_logic;
  signal bus_busy   : std_logic;

  -- Memory interface state descriptions
  type mif_state_t is (st_idle, st_0, st_1, st_2, st_3, st_end);
  signal mif_state : mif_state_t:=st_idle;

begin

  mem_cycle:
  process (clk_i)
  begin
    if rising_edge (clk_i) then
      if rst_i = '1' then
        ls_adr <= '0';
      end if;
    end if;
  end process;
end architecture Behavioral;

```

```

bus_busy <= '0';

read_o <= (others => D_CARE_VAL);

ramAdv <= '1';
ramCS <= '1';
ramWR <= '1';
ramOE <= '1';
ramLB <= '1';
ramUB <= '1';
ramCLK <= '0'; -- never needs to change
ramCRE <= '0'; -- never needs to change
MemAdr_o <= (others => D_CARE_VAL);
MemDB_o <= (others => D_CARE_VAL);
MemDB_dir <= '1';
mif_state <= st_idle;
else
  case mif_state is
    when st_idle =>
      if en_i = '1' then
        ramAdv <= '0';
        ramCS <= '0';

        ramLB <= '0';
        ramUB <= '0';

        ls_adr <= '0';
        bus_busy <= '1';

        MemAdr_o <= addr_i & '0';
        mif_state <= st_0;
      else
        read_o <= (others => D_CARE_VAL);
        ramAdv <= '1';
        ramCS <= '1';
        ramWR <= '1';
        ramOE <= '1';
        ramLB <= '1';
        ramUB <= '1';
        MemAdr_o <= (others => D_CARE_VAL);
        MemDB_o <= (others => D_CARE_VAL);
        MemDB_dir <= '1';
      end if;
    when st_0 => -- 0-20 ns
      if en_i = '1' then
        if we_i = '1' then
          ramWR <= '0';
        else
          ramOE <= '0';
        end if;
        mif_state <= st_1;
      else
        mif_state <= st_idle;
      end if;
  end case;
end if;

```

```

when st_1 =>          -- 20-40 ns
  if en_i = '1' then
    if we_i = '0' then -- prepare to read from
cram
      ramOE <= '0';
    else
      MemDB_dir <= '0';
      if ls_adr = '0' then
        MemDB_o <= write_i(MDATA_SIZE-1
down to 0);

      else
        MemDB_o <= write_i(WORD_SIZE-1
down to MDATA_SIZE);

      end if;
    end if;
    mif_state <= st_2;
  else
    mif_state <= st_idle;
  end if;
when st_2 =>          -- 40-60 ns
  if en_i = '1' then
    mif_state <= st_3;
  else
    mif_state <= st_idle;
  end if;
when st_3 =>          -- 60-80 ns
  if en_i = '1' then
    ramAdv <= '1';
    ramCS <= '1';
    ramWR <= '1';
    ramOE <= '1';
    ramLB <= '1';
    ramUB <= '1';
    ramWR <= '1';
    MemAdr_o <= (others => D_CARE_VAL);
    MemDB_o <= (others => D_CARE_VAL);
    MemDB_dir <= '1';
    if we_i = '0' then -- read the cram value
      if ls_adr = '0' then
        read_o(MDATA_SIZE-1 down to 0)<=
MemDB_i;

      else
        read_o(WORD_SIZE-1 down to
MDATA_SIZE)<= MemDB_i;

      end if;
    end if;
    if ls_adr = '1' then
      bus_busy <= '0';
    end if;
    mif_state <= st_end;
  else
    mif_state <= st_idle;
  end if;
when st_end =>       -- 80-100 ns
  if en_i = '1' then

```

```

        if ls_adr = '0' then
            ls_adr <= '1';
            ramAdv <= '0';
            ramCS <= '0';

            ramLB <= '0';
            ramUB <= '0';

            MemAdr_o <= addr_i & '1';

            mif_state <= st_0;
        else
            ls_adr <= '0';
            mif_state <= st_idle;
        end if;
    else
        mif_state <= st_idle;
    end if;

    when others =>
        mif_state <= st_idle;
    end case; -- mif_state
end if; -- else reset_i='1'
end if; -- rising_edge(clk_i)

end process mem_cycle;

CramOE <= ramOE;
CramWR <= ramWR;
CramClk <= '0';
CramAdv <= ramAdv;
CramCS <= ramCS;
CramLB <= ramLB;
CramUB <= ramUB;
CramCRE <= '0';

ramWait <= CramWait;

busy_o <= bus_busy;

end Behavioral;

```

fifo_if.vhd

```

-----
-----
-- Company: Western Michigan University
-- Engineer: Nagarjun Marappa
--
-- Create Date:    15:53:21 11/29/2014
-- Design Name:
-- Module Name:    wb slv fifo - Behavioral
-----
-----

```



```

library IEEE;
use IEEE.STD_LOGIC_1164.ALL;
use IEEE.NUMERIC_STD.ALL;
use ieee.std_logic_unsigned.all;

library UNISIM;
use UNISIM.VComponents.all;

entity fifo_if is
Generic(WORD_SIZE: natural:= 32;
        ADDR_W : natural:= 25;
        FIFO_W : natural:= 32);
port(
    clk_i : in std_logic;
    rst_i : in std_logic;
    wbs4_dat_i : in unsigned(WORD_SIZE-1 downto 0);
    wbs4_we_i : in std_logic;
    wbs4_sel_i: in std_logic_vector(3 downto 0);
    wbs4_adr_i: in unsigned(ADDR_W-1 downto 2);
    wbs4_cyc_i: in std_logic;
    wbs4_stb_i: in std_logic;
    wbs4_dat_o : out unsigned(WORD_SIZE-1 downto 0);
    -- fifo signals
    fifo_data_out: out std_logic_vector(16-1 downto 0);
    fifo_rd_clk: out std_logic;
    dsp_rst:out std_logic;
    ddc_en : out std_logic;
    half_full: out std_logic;
    fifo_wr_en_buff : out std_logic;
    sclk : out std_logic
);
end fifo_if;

architecture Behavioral of fifo_if is
COMPONENT fifo_stage_o
PORT (
    rst : IN STD_LOGIC;
    wr_clk : IN STD_LOGIC;
    rd_clk : IN STD_LOGIC;
    din : IN STD_LOGIC_VECTOR(31 DOWNTO 0);
    wr_en : IN STD_LOGIC;
    rd_en : IN STD_LOGIC;
    dout : OUT STD_LOGIC_VECTOR(15 DOWNTO 0);
    full : OUT STD_LOGIC;
    almost_full : OUT STD_LOGIC;
    wr_ack : OUT STD_LOGIC;
    empty : OUT STD_LOGIC;
    prog_full : OUT STD_LOGIC
);
END COMPONENT;

signal fifo_data_reg: std_logic_vector(WORD_SIZE-1 downto 0):= (others
=> '0');
constant fifo_data_addr : unsigned(3 downto 0):= "0010";

```

```

signal fifo_ctrl1: std_logic_vector(7 downto 0):= (others => '0');
constant fifo_ctrl1_adr : unsigned(3 downto 0):= "0001";

signal wr_clk, rd_clk: std_logic := '0';
signal fifo_wr_en: std_logic:= '0';
signal fifo_rd_en:std_logic := '0';
signal fifo_din: std_logic_vector(32-1 downto 0);
signal fifo_dout: std_logic_vector(16-1 downto 0);

signal rd_busy : std_logic;
signal wr_ack : std_logic;
signal prog_full : std_logic;
signal full : std_logic;
signal empty : std_logic;
signal almost_full: std_logic;

signal my_start: std_logic:= '1';
signal ddc_en_buff: std_logic:= '0';

signal phase_out : std_logic;
signal rd_count: std_logic_vector(15 downto 0):=(others => '0');
signal dsp_rst_d1: std_logic:= '1';
signal sclk_d1 : std_logic:= '0';

type fifo_states is (idle_state, wr_state, rd_state, wait_write,
wait_read);
signal state : fifo_states;

attribute KEEP: string;
attribute KEEP of fifo_din      : signal is "TRUE";
attribute KEEP of fifo_dout : signal is "TRUE";
attribute KEEP of full        : signal is "TRUE";
attribute KEEP of prog_full  : signal is "TRUE";
attribute KEEP of empty      : signal is "TRUE";
attribute KEEP of my_start    : signal is "TRUE";
attribute KEEP of rd_count    : signal is "TRUE";
attribute KEEP of fifo_wr_en  : signal is "TRUE";
attribute KEEP of fifo_rd_en  : signal is "TRUE";
attribute KEEP of almost_full : signal is "TRUE";

begin

auto_process: process(clk_i,rst_i,rd_clk)
begin
if rising_edge(clk_i) then
    if rst_i = '1' then
        fifo_wr_en <= '0';
        wbs4_dat_o <= (others => '0');
        fifo_din <= (others => '0');
        fifo_data_reg <= (others => '0');
        state <= idle_state;
    else
        case state is

```

```

when idle_state =>
    rd_busy <= '0';
    if(wbs4_stb_i = '1' and wbs4_cyc_i = '1') then
        if wbs4_we_i = '1' then
            state <= wr_state;
        else
            state <= rd_state;
        end if;
    else
        state <= idle_state;
    end if;
when wr_state =>
    fifo_wr_en <= '1';
    if((wbs4_adr_i(5 downto 2)) = fifo_data_addr) then
        fifo_din <= std_logic_vector(wbs4_dat_i(32-1
downto 0));
    else
        fifo_din <= fifo_din;
    end if;
    state <= wait_write;
    when wait_write => -- Actual writing to fifo takes place in
this state.
        fifo_wr_en <= '0';
        if wr_ack = '1' then
            state <= idle_state;
        else
            state <= wait_write;
        end if;
when rd_state =>
    rd_busy <= '1';
    if((wbs4_adr_i(5 downto 2)) = fifo_ctrl1_addr) then
        wbs4_dat_o <= x"000000" & unsigned(fifo_ctrl1);
    end if;
    state <= wait_read;
when wait_read =>
    rd_busy <= '0';
    state <= idle_state;
when others =>
    state <= idle_state;
end case;
end if;
end if;
end process;

rd_clk_thingy:
process(clk_i, rst_i, rd_count)
begin
if rising_edge(clk_i) then
    if rst_i = '1' then
        rd_count <= (others => '0');
        rd_clk <= '0';
    else
        if rd_count = x"007D" then --3F
            rd_clk <= not(rd_clk);
            rd_count <= (others => '0');
        end if;
    end if;
end process;

```

```

        else
            rd_count <= rd_count + '1';
        end if;
    end if;
end if;
end process rd_clk_thingy;

process(rd_clk)
begin
    if falling_edge(rd_clk) then
--        if dsp_rst_d1 = '1' then
--            sclk_d1 <= '0';
--        else
            sclk_d1 <= not(sclk_d1);
--        end if;
    end if;
end process;
sclk<=sclk_d1;

rd_en_thingy:
process (clk_i,full,rst_i,my_start)
begin
if rising_edge(clk_i) then
    if (rst_i = '1') then
        my_start <= '1';
    else
        if almost_full = '1' then
            my_start <= '0';
        else
            my_start <= my_start;
        end if;
    end if;
end if;
fifo_rd_en <= not(my_start);
end process rd_en_thingy;
--#####
-- it takes approx one clk cycle for placing data on
-- fifo_dout so delay DDC enable for 1 rd_clk cycle
--#####
ddc_enable: process(rd_clk, rst_i, fifo_rd_en)
begin
    if rising_edge(rd_clk) then
        if fifo_rd_en = '1' then
            ddc_en_buff <= '1';
        else
            ddc_en_buff <= '0';
        end if;
    end if;
end process ddc_enable;
ddc_en <= fifo_rd_en;

--#####
-- dsp board reset logic
--#####
dsp_reset: block

```

```

signal counter : std_logic_vector(15 downto 0) := x"0000";
signal init : std_logic := '0';
begin
    process(rst_i, clk_i)
    begin
        if rising_edge(clk_i) then
            if rst_i = '1' then
                dsp_rst_d1 <= '1';
                counter <= (others => '0');
            else
                if counter = x"1388" then
                    dsp_rst_d1 <= '0';
                else
                    counter <= counter + '1';
                end if;
            end if;
        end if;
        dsp_rst <= dsp_rst_d1;
    end process;

end block dsp_reset;

    fifo_rd_clk <= rd_clk;
    fifo_data_out <= fifo_dout;
    fifo_wr_en_buff <= fifo_wr_en;
    half_full <= full;

    -- busy_out <= rd_busy or wr_ack;

    -- OutPut signals
    fifo_ctrl1(0) <= '0';
    fifo_ctrl1(1) <= full;
    fifo_ctrl1(2) <= empty;
    fifo_ctrl1(3) <= not(prog_full);
    fifo_ctrl1(7 downto 4) <= (others => '0');

    output_fifo: fifo_stage_o PORT MAP (
        rst => rst_i,
        wr_clk => clk_i,
        rd_clk => rd_clk,
        din => fifo_din,
        wr_en => fifo_wr_en,
        rd_en => fifo_rd_en,
        dout => fifo_dout,
        full => full,
        almost_full => almost_full,
        wr_ack => wr_ack,
        empty => empty,
        prog_full => prog_full
    );

end Behavioral;

```



```

#define fifo_full 0x00000002

volatile unsigned long i=1, j=0;

/* void go_fill_fifo(void)
{
    volatile unsigned long j=0;
    for(j=0;j<20;j++)
    {
        FIFO_DATA1 = i;
        i = i+1;
    }
} */

int main(int argc, char **argv)
{
    unsigned long fifo_reg, fifo_ctrl, temp = 0x0000FFFF;
    unsigned long int i=0,j=0;
    //unsigned long int walk_1 = 0x00010001, walk_0 = 0xFFFFEFFF,
    cram_data;
    //unsigned int k, test_cnt = 0x00;
    volatile unsigned long int *ptr = 0x00100000, fifo_burst =
0x00000000;
    //SEG7_WRITE = test_cnt;
    /* // Initial CRAM
    for(j = CRAM_BOT; j<= CRAM_TOP; j=j+4)
    {
        *ptr = 0x0000FFFF;
        ptr++;
    } */
    // Initial FIFO fill-up
    temp = 0x00000000;
    ptr = CRAM_BOT;
    fifo_burst = CRAM_BOT;
    while(i<FIFO_SIZE-1)
    {
        FIFO_DATA1 = *ptr;
        ptr++;
        i = i+1;
        /* if (i > 0){
            i = i-1;
            ptr++;
        }
        else
            i = 31; */
    }
    while(1)
    {
        while (ptr<=(CRAM_BOT+65535))
        {
            fifo_reg = FIFO_CTRL1;

```

```

if(fifo_reg == 0x00000008 || fifo_reg == 0x0000000C)
{
    for(i = fifo_burst; i<= fifo_burst+200; i=i+4)
    {
        FIFO_DATA1 = *ptr;
        ptr++;
        //FIFO_DATA1 = cram_data;
    }
    fifo_burst = i;
}
//iprintf("%u",temp);
}
ptr = CRAM_BOT;
fifo_burst = CRAM_BOT;
}
}

```

Compiling process

Requirements:

1. Cygwin 32-bit environment with binutils, cmake, gcc, g++, gdb, and make.
2. ZPUGCC toolchain (download from <http://opensource.zylin.com/zpudownload.html>)

Procedure:

- a) Copy The ZPUGCC to a convenient location. You'll have to setup the environment variables to point to this location.

Note: The GCC compiler may not like a path which has spaces in its names. Avoid this situation if possible.

- b) Open the cygwin terminal. If the path to the bin folder of the ZPUGCC toolchain is *C:/zpu gcc/toolchain/bin*, then type **export PATH=\$PATH:C:/zpu gcc/toolchain/bin**

- c) Alternatively you can set the environment variables in windows 7 as shown below (My computer-->Properties-->Advanced System Settings-->Environment Variables.

An entry for PATH should already be present under system Variables.

Append *C:/zpu gcc/toolchain/bin* to the existing using ; for separator.

- d) As a check type **echo \$PATH** in the cygwin terminal to print the value for the PATH variable. You can also type **zpu-elf-gcc --help** to check if the installation was successful.
- e) To compile, go to cygwin and **cd** to the location of the helloworld example. To compile type
- f) **zpu-elf-gcc -O3 -save-temps -phi "`pwd'/hello.c" -o hello.elf -Wl,--relax -Wl,--gc-sections -g** If the compiling was successful then an elf file should be generated successfully. **ls -s** is the command to list the files in the current directory.
- g) Sometimes the elf file is too big for the BRAM in our FPGA. To strip the elf file use **zpu-elf-strip hello.elf**
- h) To convert the *.elf file into *.bin file use **zpu-elf-objcopy -O binary hello.elf hello.bin**
- i) Finally to get the BRAM contents use **./zpuromgen hello.bin > hello_bram.txt**
The *.txt file contains the program data that needs to get loaded into BRAM. After copying, implement the design again in ISE and download the bit file to the board.